สำนักหอสมุดกลาง พระจอมเกล้าลาดกระบัง

A STUDY OF ELECTRICAL PROPERTIES DEVELOPMENT OF p-n JUNCTION DIODE USING X-RAY IRRADIATION

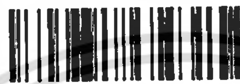
E076513

POOPOL RUJANAPICH

เลขหมู่..........
เลขทะเบียน 76513
วัน เดือน ปี 25 ส.ค. 2557
.b..........
.i..........

A THESIS SUBMITTED IN PARTIAL FULFILLMENT
OF THE REQUIREMENT FOR THE DEGREE OF
DOCTOR OF ENGINEERING IN ELECTRICAL ENGINEERING
FACULTY OF ENGINEERING
KING MONGKUT'S INSTITUTE OF TECHNOLOGY LADKRABANG
2013

KMITL 2013 –EN-D-018-161

This material is reserved for educational use only, not allowed for commercial use.
Forbidden to modify the content, and cite the document when use.

COPYRIGHT 2013

FACULTY OF ENGINEERING

KING MONGKUT'S INSTITUTE OF TECHNOLOGY LADKRABANG

This material is reserved for educational use only, not allowed for commercial use.

Forbidden to modify the content, and cite the document when use.

หัวข้อวิทยานิพนธ์ การศึกษาการพัฒนาคุณภาพทางไฟฟ้าของ พี-เอ็นจังก์ชันไดโอด ด้วยรังสีเอ็กซ์

นักศึกษา นาย พอพล รุจนพิชญ์

รหัสประจำตัว 51060034

ปริญญา วิศวกรรมศาสตรดุษฎีบัณฑิต

พ.ศ. 2556

อาจารย์ผู้ควบคุมวิทยานิพนธ์ รศ.ดร. วิสุทธิ์ ฐิติรุ่งเรือง

บทคัดย่อ

ปัจจุบันการเพิ่มประสิทธิภาพของอุปกรณ์ไฟฟ้าด้วยเทคโนโลยีหลากหลายที่ได้รับการรับรองและเชื่อถือมีความสำคัญอย่างยิ่งในทางการวิจัยและพัฒนารวมถึงการต่อยอดทางธุรกิจในการเพิ่มมูลค่าของอุปกรณ์ไฟฟ้าต่างๆ โดยเฉพาะอย่างยิ่งในช่วงไม่กี่ปีที่ผ่านมามีการพัฒนาอย่างมากและรวดเร็วในการปรับปรุงประสิทธิภาพของอุปกรณ์ไดโอดโดยการปรับความสมดุลระหว่างการสูญเสียที่เกิดในขณะที่อุปกรณ์อยู่ในสถานะเปิด (on-state) กับการสูญเสียที่เกิดในขณะที่อุปกรณ์เปลี่ยนไปสู่สถานะปิด (turn off switching) ซึ่งในปัจจุบันสวิทชิ่งไดโอด (Switching Diode) ที่ใช้งานโดยทั่วไปได้รับการพัฒนาการเพิ่มความเร็วในการสวิทชิ่ง (Switching speed) โดยการควบคุมอายุของพาหะ (carrier lifetime) โดยการเจืออะตอมสารเจือประเภททองคำหรือทองคำขาว อย่างไรก็ตามการออกแบบวงจรด้วยอุปกรณ์ดังกล่าวจะต้องพิถีพิทันในเลือกอุปกรณ์ดังกล่าวเพื่อความเหมาะสมสูงสุดในการใช้งาน นอกจากเทคนิคการเจืออะตอมสารเจือประเภททองคำหรือทองคำขาวแล้วเทคนิคการควบคุมอายุของพาหะเพื่อเพิ่มประสิทธิภาพของอุปกรณ์ไฟฟ้าโดยการฉายรังสีก็เป็นที่ยอมรับอย่างแพร่หลายในปัจจุบันซึ่งกระบวนการดังกล่าวจะช่วยให้สามารถลด reverse recovery charge ได้อย่างมีประสิทธิภาพ โดยรังสีอิเล็กตรอนจะทำให้เกิด defects ที่สม่ำเสมอในอุปกรณ์ซึ่งจะทำหน้าที่เป็น Recombination center ที่จะทำให้กระแส Reverse recovery ลดลงและเข้าถึง blocking state ได้เร็วขึ้น

วัตถุประสงค์หลักในการศึกษาวิทยานิพนธ์ฉบับนี้คือการสร้างแนวความคิดใหม่ในการใช้การฉายรังสีเอกซ์เพื่อปรับปรุงประสิทธิภาพของพี-เอ็นจังก์ชันไดโอดและวัตถุประสงค์ต่อไปก็คือการสร้างวิธีการใหม่ในการกู้คืนอุปกรณ์ที่มีคุณสมบัติทางไฟฟ้าต่ำกว่ามาตรฐานในกระบวนการผลิต ซึ่งตามมาตรฐานการผลิตในปัจจุบันนั้น

This material is reserved for educational use only, not allowed for commercial use.
Forbidden to modify the content, and cite the document when use.

คือการปรับปรุงประสิทธิภาพในการผลิตและลดของเสียอิเล็กทรอนิกส์ด้วยต้นทุนการดำเนินงานต่ำ ในการศึกษา ผู้วิจัยได้ทำการตรวจสอบผลของการฉายรังสีซอฟต์เอกซ์เรย์ (Soft X-ray) ต่อสมบัติทางไฟฟ้าของพี-เอ็นจังก์ชั่นไดโอด โดยเฉพาะอย่างยิ่งภายใต้เงื่อนไขการไบอัสตรงที่ 1.0 โวลต์และที่อุณหภูมิ 303 K ทำให้กระแสไบอัสตรงของอุปกรณ์ที่ผ่านการฉายรังสีซอฟต์เอกซ์เรย์มีค่าสูงกว่าค่ากระแสไบอัสตรงก่อนการฉายรังสีถึง 100 เท่า นอกจากนั้นเรายังเพิ่มการตรวจสอบผลลัพท์นี้ด้วยการประเมินคุณสมบัติต่อไปนี้ภายใต้เงื่อนไขการไบอัสตรง: ideality factor, saturation current และ series resistance และยัง ประเมินคุณสมบัติต่อไปนี้ภายใต้เงื่อนไขการไบอัสย้อนกลับ: carrier-generation lifetime และ activation energy โดยเฉพาะอย่างยิ่งค่า Barrier Schottly (SBH) ของอุปกรณ์ที่ผ่านการฉายรังสีซอฟต์เอกซ์เรย์จะมีค่าต่ำกว่าอุปกรณ์ที่ไม่ได้รับการฉายรังสีประมาณร้อยละห้า ผลลัพธ์ข้างต้นให้เห็นว่ากระบวนการฉายรังสีซอฟต์เอกซ์เรย์ สามารถใช้ควบคุม series resistance ของพี-เอ็นจังก์ชั่นไดโอดได้โดยไม่ก่อให้เกิดความเสียหายอย่างมีนัยสำคัญต่ออุปกรณ์ อย่างไรก็ตาม เงื่อนไขที่เหมาะสมในกระบวนการสร้างอาจต้องมีการพัฒนาขึ้นโดยเฉพาะสำหรับอุปกรณ์แต่ละชนิดที่มีความต้องการที่แตกต่างกัน

This material is reserved for educational use only, not allowed for commercial use.
Forbidden to modify the content, and cite the document when use.

Thesis Title A STUDY OF ELECTRICAL PROPERTIES DEVELOPMENT OF p-n JUNCTION DIODE USING X-RAY IRRADIATION

Student Mr. Poopol Rujanapich

Student ID 51060034

Degree Doctor of Engineering

Year 2013

Thesis Advisor Assoc.Prof.Dr. Wisut Titiroongruang

ABSTRACT

Recently, there are numbers of technological procedures that proven to purposely optimize the power device characteristics. Especially, in the past few years, significant progresses in the development of fast diodes have been achieved optimizing the trade-off between on-state losses and turn off switching losses. Conventional fast switching diodes are using gold or platinum doping to control carrier lifetime. However, the circuit designer has to be careful on choosing the device that will be expected to use on the different application. Rather than the techniques using impurities gold and platinum, the irradiation techniques to control carrier lifetime is nowadays accepted for power device characteristics optimization. The reverse recovery charge can be efficiently reduced by electron irradiation, since the defect centers introduced uniformly by electron irradiation are acting as recombination centers. As such the reverse recovery current decreases and the blocking state is reached faster.

The first objective of this study is creating the brand new idea of utilize the X-ray irradiation process to improve or modify the electrical performance of new p-n junction products. The second objective is to create the new way to recover products that already fail from the electrical specification by using the facilities and equipments that already exist. The end result of this study is to improve production output and reduce electronics waste with the

This material is reserved for educational use only, not allowed for commercial use.

Forbidden to modify the content, and cite the document when use.

minimum cost of operation. We investigated the effect of soft X-ray irradiation on the electrical properties of p–n junction diodes. Of particular significance is that, under a forward bias of 1.0 V at 303 K, the forward current is approximately two orders of magnitude higher for X-ray irradiation than for non-X-ray irradiated samples. We further investigated this effect by evaluating the following properties under forward-bias conditions: ideality factor, saturation current, and series resistance, and under reverse-bias conditions, carrier-generation lifetime, and activation energy. Under the forward bias condition, the Schottly Barrier Height (SBH) is approximately five percent lower for X-ray irradiated device than for non-irradiated device. These results suggest that soft X-ray process reduce series resistance of p–n junction diodes under forward-bias conditions without significant damage to the device. However, optimum process conditions may need to be specifically developed for each particular device.

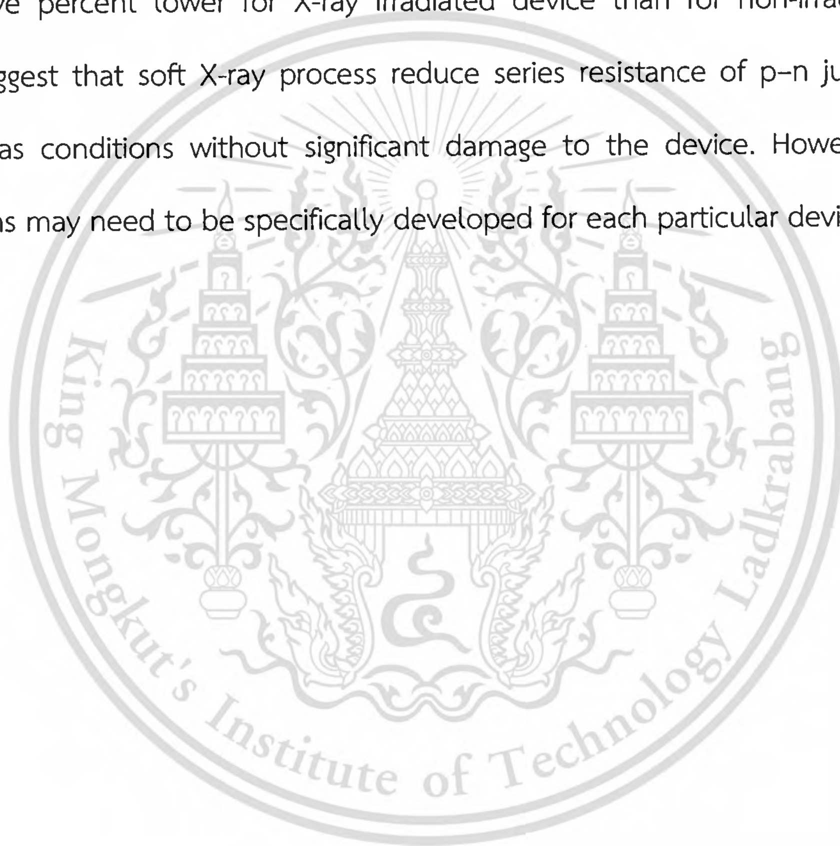

This material is reserved for educational use only, not allowed for commercial use.
Forbidden to modify the content, and cite the document when use.

Acknowledgment

This doctor thesis has been done with kindness advices and support of Assoc.Prof.Dr. Wisut Titiroongruang of King Mongkut's Institute of Technology Ladkrabang.

Thanks to Assoc.Prof.Dr.Somkiat Supadech, Asst.Prof.Dr. Surasak Niemchroen of King Mongkut's Institute of Technology Ladkrabang for their kind support and advices of this thesis concept and Dr. Amporn Poyai is director of Thai Microelectronics Center (TMEC) for their strong and kindness support and suggestion for device fabrication and data analysis.

Thanks to Dr. Ekalak chaowicharat, Dr. Putapon Pengpat and Dr. Nipapan Klunngien from TMEC for support *I-V* and *C-V* measurement.

Thanks to Mr. Prasong Thusaranon for support X-ray radiation generator at King Mongkut's University Technology North Bangkok (KMUTNB).

Special thanks to Dr. Itsara Srithanachai and Dr. Jirawat Prabket for their support and suggestion and analysis of the electrical properties of p-n junction diode as well as Miss. Surada Ueamanapong and Miss. Yuwadee Sundarasaradula for their help of measurement the results.

Finally, thanks to my parents and family for their love, support and encouragement.

And for the benefits of this thesis, I would like contribute to all ex-members of Electronics research Center, Department of Electronics engineering, Faculty of engineering, King Mongkut's Institute of Technology Ladkrabang, Thailand. Place that I gain fundamental elements of my successes.

Poopol Rujanapich

This material is reserved for educational use only, not allowed for commercial use.

Forbidden to modify the content, and cite the document when use.

Contents

Page

บทคัดย่อ.....I

Abstract.....III

Acknowledge.....V

Content.....VI

Content of table.....IX

Content of picture.....X

Abbreviation.....XIII

List of symbol.....XV

Chapter 1: Introduction.....1

1.1 Background.....1

1.2 Significance of the study.....3

1.3 Literature works.....3

1.4 Research hypotheses.....7

1.5 Research objectives.....7

1.6 Summary and layout of thesis.....7

Chapter 2: Theory.....9

2.1 p–n Junction Diode Theory.....9

2.1.1 Properties of a p-n junction.....9

2.1.2 Equilibrium (zero bias).....10

2.1.3 Forward bias.....12

2.1.4 Reverse bias.....14

2.2 Capacitance-voltage characteristics (C-V).....15

This material is reserved for educational use only, not allowed for commercial use.

Forbidden to modify the content, and cite the document when use.

2.3 Diode Equation....16

2.4 Shockley diode model....19

2.5 Ideality factor....19

2.6 Activation Energy....20

2.7 Series Resistance....21

2.8 Carrier generation and recombination....22

2.8.1 Generation and recombination processes....24

2.8.2 Carrier-generation Lifetime....28

2.9 Radiation Effects and Damage....29

2.9.1 Ionizing Radiations....29

2.9.2 Heavy Charged Particles....31

2.9.3 Light Charged Particles....31

2.9.4 Neutral Radiations....32

2.9.5 General Radiation Effects....33

2.9.6 Impurity Production....34

2.9.7 Atomic Displacement (Damage)....34

2.9.8 Ionization....37

2.9.9 Energy Deposition....39

2.9.10 Specific Radiation Effects....39

Chapter 3: Device fabrication and Experiment....45

3.1 Design and Fabrication P-N diode....45

3.2. Experiment....50

Chapter 4: Results and Discussion....61

4.1 Study of Electrical properties of p-n diode....61

4.2 Capacitance-voltage characteristics (C–V) of p-n junction diode....63

This material is reserved for educational use only, not allowed for commercial use.
Forbidden to modify the content, and cite the document when use.

4.3 Current-voltage characteristics (I-V) study of p-n junction diode..............................66
before and after X-ray irradiated
4.3.1 Forward bias study of p-n junction diode after X-ray irradiation.............67
4.3.1.1 Forward-bias voltages of <0.5 V..70
4.3.1.2 Forward-bias activation Energy (E_T) study of p-n junction........73
Diode after X-ray irradiation
4.3.1.3 Forward-bias voltages of ≥0.5 V..74
4.3.1.4 Series Resistance study of p-n junction diode after..................75
X-ray irradiation
4.3.1.5 SBH study of p-n junction diode after X-ray irradiation............77
4.3.2 Reverse bias...80
4.3.2.1 Leakage current (I_0) study of study of p-n junction diode........80
after X-ray irradiation
4.3.2.2 Carrier-generation lifetime (τ_g) study of study of.......................81
p-n junction diode after X-ray irradiation
4.3.2.3 Reverse-bias activation Energy (E_T) study of p-n junction........83
diode after X-ray irradiation
5 Conclusion...86

This material is reserved for educational use only, not allowed for commercial use.
Forbidden to modify the content, and cite the document when use.

Content of Table

Page

Table 2.1 Comparison of Ionizing Radiation 30

Table 2.2 Radiation Damage to Materials.. 33

Table 3.1 Dose rate of X-ray radiation.. 52

Table 4.1 X-ray radiation conditions.. 66

Table 4.2 Basic conduction processes.. 68

This material is reserved for educational use only, not allowed for commercial use.
Forbidden to modify the content, and cite the document when use.

Content of picture

Page

Fig. 1.1 Variation of the reverse branch of the current-voltage characteristic for.............................4
on the type D1602V diodes

Fig. 1.2 I-V before and after irradiation by X-ray at 2 x 10^{-1} rad...5

Fig. 1.3 Reverse branch of the IV characteristics of the D205 silicon diode.....................................6
(1) before, (2) X-ray 15 min, (3) 50 min, (4) 100 min, and (5) 140 min

Fig. 2.1 p–n junction diode...9

Fig. 2.2 A p–n junction in thermal equilibrium with zero bias voltage applied.............................10

Fig. 2.3 A p–n junction in thermal equilibrium, charge density, the electric field........................12
and the voltage with zero bias voltage applied

Fig. 2.4 A silicon p–n junction in forward bias..13

Fig. 2.5 A silicon p–n junction in reverse bias...14

Fig. 2.6 I—V plot of p—n junction diode...21

Fig. 2.7 I—R_S plot of p—n junction diode...22

Fig 2.8 Electronic band structure of a semiconductor material..23

Fig. 2.9 Individual energy levels VS recombination processes..25

Fig. 2.10 Individual energy levels VS generation processes..26

Fig. 2.11 Ionization mechanism caused by an electron/hole...27

Fig. 2.12 Radiation paths in tissue...30

Fig. 2.13 Displacement damage..35

Fig. 2.14 Displacement cascade damage from movement of silicon atom after............................36
primary collision

Fig. 2.15 Ionic bond of salt before and after irradiation..38

This material is reserved for educational use only, not allowed for commercial use.
Forbidden to modify the content, and cite the document when use.

Fig. 2.16 Electron population in an insulator....42
Fig. 2.17 Photoconduction in which a photon raises the energy of a valence....43
electron to the conduction band and leave behind a hole in the valence band
Fig. 3.1 Plan of experiment for study the effect of X-ray irradiation....45
Fig. 3.2 Process flow of P-N diode fabrication base on silicon....46
Fig. 3.3 p-n junction diode after fabrication....50
Fig. 3.4 X-ray irradiation on front side of p-n junction diode....51
Fig. 3.5 IV probe station HP4156B (a) monitor and control center, (b) the....53
cascada microtech model M150, (c,d) probe station and chunk
and (d) probe control
Fig. 3.6 X-ray machine C-arm Siemens Siremobil compact 650 135....56
(a) C-arm, (b) X-ray point, (c,d) controller and (e) X-ray test device
Fig. 3.7 X-ray irradiation machine at Chulalongkorn University (a,b) head of....58
X-ray irradiation, (c) X-ray head spec, and (d) controller
Fig. 4.1 Leakage current versus bias voltage of the p-n junction diode....64
Fig. 4.2 Capacitance-voltage (C-V) characteristics of p-n junction diode....65
Fig. 4.3 Leakage current versus depletion width of the p-n junction diode....65
Fig. 4.4 Plots of forward I–V characteristics for a p—n junction diode....69
before and after X-ray annealing, measured at 303 K
Fig. 4.5 Plots of saturation current vs X-ray quantity for a p—n junction....71
diodes before and after X-ray annealing under various conditions,
measured at different temperatures
Fig. 4.6 Plots of ideality factor vs X-ray quantity for a p—n junction diode....72
before and after X-ray annealing, measured at 303 K
Fig. 4.7 Plots of $\ln(I_0)$ vs 1/kT for a p—n junction diodes before and after....73

This material is reserved for educational use only, not allowed for commercial use.
Forbidden to modify the content, and cite the document when use.

X-ray annealing under various conditions, measured at 303 K
Fig. 4.8 Plots of forward I vs V (log–log scale) for a p—n junction diodes..74
before and after X-ray annealing under various conditions, measured at 303 K
Fig. 4.9 Plots of series resistance vs bias voltage for p—n junction diodes....................................75
before and after X-ray annealing under various conditions, measured at 303 K
Fig. 4.10 Plots of sheet resistance of Boron doped Si and Aluminum layer...................................77
before and after X-ray annealing
Fig. 4.11 Plots of SHB vs X-ray quantity before and after X-ray annealing.....................................79
Fig. 4.12 Plots of leakage current vs depletion width for p—n junction..81
diodes before and after X-ray annealing under various conditions,
measured at 303 K
Fig. 4.13 Plots of carrier-generation lifetime vs depletion width for..82
p—n junction diodes before and after X-ray annealing
under various conditions, measured at 303 K
Fig. 4.14 Arrhenius plots of $I_g/T^{1.7}$ vs 1/kT for p—n junction diodes...83
after X-ray annealing (dose 2.01 X 10^8 R under various reverse biases
Fig. 4.15 Activation energy of p-n junction diode after X-ray annealing...84
under various conditions

This material is reserved for educational use only, not allowed for commercial use.
Forbidden to modify the content, and cite the document when use.

Abbreviation

Abbreviation word	Full word
AC	Alternating Current
amu	Atomic Mass Unit
C	Carbon
$^{\circ}C$	Celsius
CO_2	Carbon dioxide
CMOS	Complementary Metal-Oxide Semiconductor
const.	Constant
DC	Direct Current
dpa	Displacements per atom
eV	Electron Volt
Ge	Germanium
H_2O	Water
K	Kelvin
keV	Kilo-Electron Volt
LED	Light Emitting Diode
log	Logarithm
mA	Milliamperes
MeV	Mega-Electron Volt
min	Minute
NaCl	Sodium chloride
NIEL	non-ionizing energy loss

King Mongkut's Institute of Technology Ladkrabang

This material is reserved for educational use only, not allowed for commercial use.

Forbidden to modify the content, and cite the document when use.

Abbreviation (cont.)

Abbreviation word	Full word
PECVD	Plasma enhance chemical vapor deposition
SBH	Schottky Barrier Height
SD	Schottky diode
sec	Second
Si	Silicon
TMEC	Thai Microelectronics Center
yr	Year

This material is reserved for educational use only, not allowed for commercial use.

Forbidden to modify the content, and cite the document when use.

List of Symbols

A	is	Richardson constant
C_j	is	Junction capacitance
D_n	is	Diffusion coefficient of electrons
D_p	is	Diffusion coefficient of holes
E_g	is	Energy gap
E_T	is	Activation Energy
ε	is	Permittivity
ε_{Si}	is	Dielectric permittivity of silicon
I_0	is	Saturation current
I_d	is	Diffusion current
IR_S	is	Voltage drop across series resistance of device
J	is	Current density
k	is	Boltzmann constant
L_n	is	Electron diffusion length
L_p	is	Hole diffusion length
η	is	Diode ideality factor
n_i	is	Intrinsic carrier concentration
μ	is	Carrier mobility
Δp	is	Minority carrier concentration at the edge of the depletion region
ρ	is	Resistivity
ρ_i	is	Charge density
q	is	Magnitude of the electron charge

This material is reserved for educational use only, not allowed for commercial use.
Forbidden to modify the content, and cite the document when use.

List of Symbols (cont.)

R	is	The rate at which the failure mechanism occurs
R_s	is	Series resistance
S_n	is	Losses energy via nuclear energy loss
S_e	is	Losses energy via electronic energy loss
T	is	Temperature of the semiconductor
τ_g	is	Carrier-generation lifetime
τ_r	is	Recombination lifetime
V_{bi}	is	Built-in voltage
V_D	is	Voltage across the terminal of diode
V_f	is	Forward bias voltage
V_T	is	Thermal voltage (kT/q)
W	is	Depletion width
φ	is	Electric potential
σ	is	Conductivity
Φ_{B0}	is	Zero bias barrier height

This material is reserved for educational use only, not allowed for commercial use.
Forbidden to modify the content, and cite the document when use.

Chapter 1

Introduction

1.1 Background

Recently, there are numbers of technological procedures that proven to purposely optimize the power device characteristics. Especially, in the past few years, significant progresses in the development of fast diodes have been achieved optimizing the trade-off between on-state losses and turn off switching losses. Fast diode is important as the operating frequency of AC/DC-converters, inverters, DC choppers and switch mode power supplies tends to increase to achieve more compact circuit lay-outs and reduced noise levels. Conventional fast switching diodes are using gold or platinum doping to control carrier lifetime. The recombination level introduced by gold diffusion is different from that by platinum diffusion. The superior conduction characteristics are observed in gold-doped devices. For example, for equal forward voltage, gold-doped device will have faster switching time than platinum-doped device. However, the leakage current of platinum doped devices will be much lower than for gold-doped devices. Since gold-doped devices created a larger leakage current (especially the high temperature leakage current is significantly high.) so the parasitic heating of the gold-doped rectifier occurs highly than platinum doped rectifier. A continuous heating will, finally, cause thermal run away. But the gold- doped devices will introduce a softer recovery waveform than platinum. From the trade-off comparison the circuit designer has to be careful on choosing the device that will be expected to use on the different application. [1]-[9]

Rather than the techniques using impurities gold and platinum, the irradiation techniques to control carrier lifetime is nowadays accepted for power device characteristics optimization. [10] – [13] The reverse recovery charge can be efficiently reduced by electron

This material is reserved for educational use only, not allowed for commercial use.
Forbidden to modify the content, and cite the document when use.

irradiation, since the defect centers introduced uniformly by electron irradiation are acting as recombination centers for the free charge carriers and, consequently, accelerate the removal of the charge carrier plasma. [14] As a consequence the reverse recovery current decreases and the blocking state is reached faster. Partial annealing of the defect centers will results in a less effective reduction of the reverse recovery charge.

In contrast to electron irradiation, proton irradiation leads to a non-uniform defect profile with a maximum defect concentration close to the penetration depth of the protons. [14] The non-uniform defect profile causes a pronounced modification of the vertical charge carrier distribution. Consequently, the reverse recovery behavior does not only depend on the fluence of the irradiation and the annealing conditions but also on the penetration depth as well. For example, the reduction of the reverse recovery charge is most efficient when the defect peak is located close below the gate oxide.

The second important effect induced by irradiation concerns is the modifications of the effective doping concentration. [14] The irradiation process can cause significant donor formation under properly chosen annealing conditions. The peak concentration and the donor charge integrated along the vertical direction can be controlled over a wide range by the choice of the annealing temperature and the proton fluence.

King Mongkut's Institute of Technology Ladkrabang

Comparing the carrier lifetime adjustment by irradiation with the adjustment by impurities such as gold and platinum doped, the irradiation techniques offer the possibility to reduce the carrier life time at the end of the fabrication process and to create spatially varying lifetime profiles.

Apart from controlling the local carrier lifetime, light-ion radiation can also be applied to modify the doping profile of silicon devices. This is especially important for power devices, which usually have a very high resistivity of the starting material to provide high blocking voltages. Proton-irradiated and subsequently annealed silicon shows the formation of shallow

This material is reserved for educational use only, not allowed for commercial use.
Forbidden to modify the content, and cite the document when use.

donors that are related to hydrogen defect complexes. Possible applications are the integration of an overvoltage protection function into thyristors or the implementation of a field-stop layer in high-voltage devices. It is even possible to use both effects, local reduction of carrier lifetime and increasing the doping concentration, simultaneously by applying single proton irradiations, as has been shown for local lifetime controlled IGBT with a punch-trough structure. [15]

1.2 Significance of the study

The advance high power radiator was used for most of today irradiation techniques, which is resulting in high cost of operation. [4] To adopt similar concept with much lower cost of operation, the study of the impact of the low energy x-ray irradiation to the electrical properties of p-n junction diode is developing using the low energy of x-ray sources from 40 keV to 70 keV. The low energy x-ray source that used in this technique is not only provides benefit of lower cost of operation but also open the opportunities for users to access either in most of their laboratories or even in the most hospitals. The benefits of this study are not only creating the brand new idea to improve and modify the electrical performance of new p-n junction products but also creates the new opportunities to recover products that already fail from the electrical specification, which finally improved production output and reduce electronics waste.

1.3 Literature works

The X-ray radiation technique were studied from 1962-1969 (reference on website). The electrical properties were degradation after irradiation by X-ray. The literature work of X-ray radiation effect on the characteristics of semiconductor device were shown as follows

1.3.1 M. A. Krivov and S. V. Malyanov- *Effect of Roentgen radiation on germanium and germanium P-N junctions*. [16]

This material is reserved for educational use only, not allowed for commercial use.
Forbidden to modify the content, and cite the document when use.

This paper have been studied the action of X-ray on germanium devices. The latter paper showed that the reverse branch of the current-voltage characteristic of the point-contact diodes undergoes significant changes under the action of X-ray. The effect of soft X-rays on laboratory and commercial germanium p-n junction was studied in our earlier paper. This investigation indicated that both the forward and reverse branches of the current-voltage characteristic may be change by X-ray action.

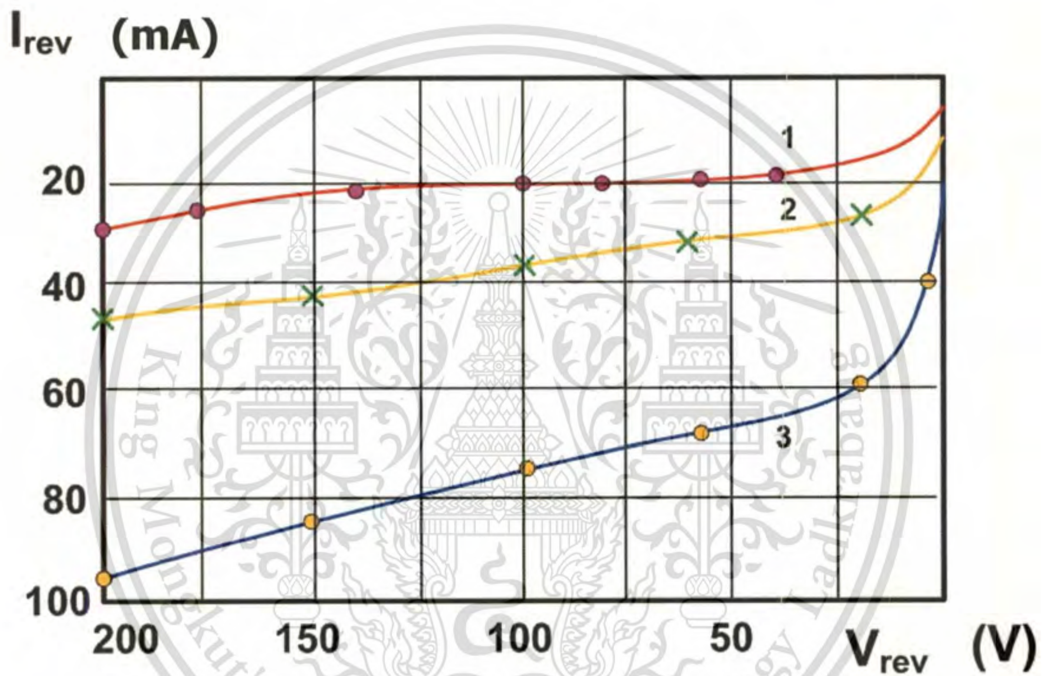

Fig. 1.1 Variation of the reverse branch of the current-voltage characteristic for on the type D1602V diodes: 1) before irradiation, 2) $D_n = 3.7 \times 10^{-1}$ rad, 3) $D_n = 9 \times 10^{-1}$ rad.

This material is reserved for educational use only, not allowed for commercial use.
Forbidden to modify the content, and cite the document when use.

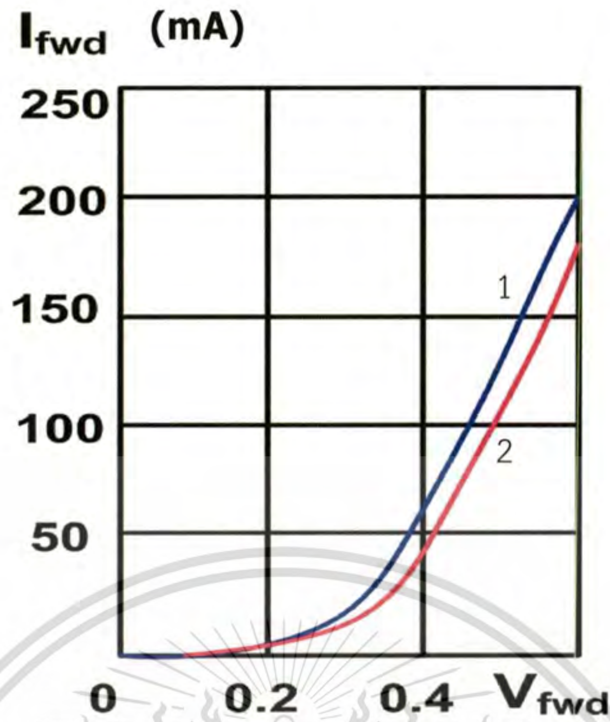

Fig. 1.2 Forward current-voltage characteristic for D72h diode: 1) before irradiation, 2) D_n = 2 x 10^{-1} rad

This paper is concerned with the effect of X-rays on the p-n junction of commercial germanium diodes, types D7Zh and D1602V, and also on laboratory germanium p-n junctions, all experiments were conducted in a dark room, and the junctions were placed in a black paper package. The experiment showed that the reverse branch of the current-voltage characteristic undergoes marked change under X-ray radiation. The photoelectric increment of the reverse current is independent of the resistivity of the base and is determined by the parameters of the incident radiation. The variation of the reverse branch of the current-voltage characteristic for on the type D1602V diodes is shown in fig. 1.1.

The forward was decrease after irradiation by X-ray at 2 x 10^{-1} rad. Here, also, the change in current will be determined by the change in minority carrier concentration. The results of this paper show that X-ray will decrease the forward current of germanium p-n device.

This material is reserved for educational use only, not allowed for commercial use.
Forbidden to modify the content, and cite the document when use.

1.3.2 M. A. Krivov, S. V. Malyanov, and V. I. Gaman- *The effect of X-rays on silicon and silicon P-N junction.* [17]

In this contribution we consider the effect of X-ray beams with energies of 45-90 KeV on the static current-voltage characteristics and the rectification coefficient of industrial silicon diode type D205.

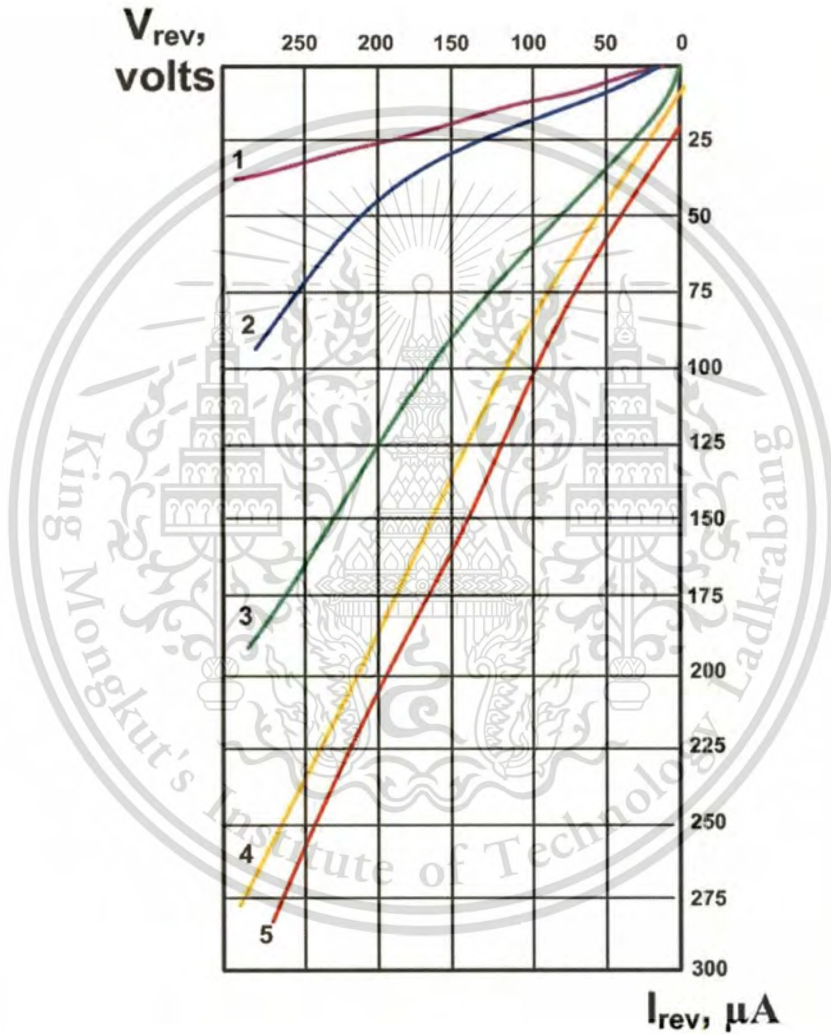

Fig. 1.3 Reverse branch of the IV characteristics of the D205 silicon diode (1) before, (2) X-ray 15 min, (3) 50 min, (4) 100 min, and (5) 140 min

The experimental curves were taken both directly during the action of the X-ray beams, and at room temperature after stopping the radiation. The heating of the specimens during

This material is reserved for educational use only, not allowed for commercial use.
Forbidden to modify the content, and cite the document when use.

radiation did not exceed 5 ^{o}C. It was shown that when germanium diodes are exposed to X-ray beams the reverse current through the p-n junction approaches saturation with prolonged radiation. A similar effect is also observed in silicon diodes shown in fig. 1.3. Form fig. 1.3 shows that the leakage current after irradiation various time of exposure were increased. Therefore, the performance of p-n diode was decrease after X-ray irradiation.

1.4 Research hypotheses

The X-ray radiation can be changing the characteristics of semiconductor devices. From the literature review were studied the effect of X-ray radiation at low dose. Therefore, this thesis will be study the effect of X-ray radiation on the electrical properties of p-n diode and found the optimize dose of X-ray to enhancement the p-n diode performance. Investigate and analyze the effect of X-ray on the mechanism of p-n junction diode such as carrier lifetime, activation energy, series resistance, built in voltage, and carrier concentration.

1.5 Research objectives

1) To create the brand new idea to improve or modify the electrical performance of new p-n junction products and creates the new way to recover products that already fail from the electrical specification by using the facilities and equipments that already exist.

2) To improve production output and reduce electronics waste with the minimum operating cost of electronics manufacturing.

1.6 Summary and layout of thesis

Chapter 1 Introduction, this chapter mentions the history and significance of the research, aim, objective, hypothesis, and literature review the effect of radiation on the characteristics of semiconductor device and the benefits from this thesis.

King Mongkut's Institute of Technology Ladkrabang

This material is reserved for educational use only, not allowed for commercial use.

Forbidden to modify the content, and cite the document when use.

Chapter 2 Theory, this chapter explains the p-n junction diode properties such as I-V and C-V characteristics. And also describe the incidence process of radiation such as neutron, beta, alpha and X-ray.

Chapter 3 Design and fabrication, this chapter discusses the design and fabrication process of the p-n junction diode by using CMOS technology at Thai Microelectronics Center (TMEC), and X-ray generator to use in this thesis.

Chapter 4 Results and discussions, this chapter shows the result and analyze the effect of X-ray irradiation on the electrical properties of p-n diode. The electrical of p-n diode which are current-voltage (I-V) and capacitance-voltage (C-V) characteristics and analysis the parameters of the device such as carrier lifetime, carrier concentration, activation energy, series resistance, built in voltage and ideality factor.

Chapter 5 Conclusions, this chapter summarizes the results of experiments on the effect of X-ray irradiation and concluded the optimize X-ray dose for enhance of the p-n junction diode.

King Mongkut's Institute of Technology Ladkrabang

This material is reserved for educational use only, not allowed for commercial use.
Forbidden to modify the content, and cite the document when use.

Chapter 2
Theory

2.1 p–n Junction Diode Theory

A p–n junction is a junction formed by joining p-type and n-type semiconductors together in close contact (see figure 2.1), which first recovered by American physicist Russell Ohl of Bell Laboratories. P–n junctions are often created in a single crystal of semiconductor by doping.

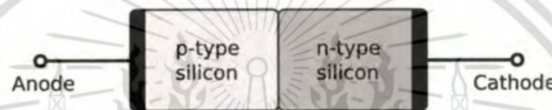

Fig. 2.1 p–n junction diode

Regularly p–n junctions are fabricated from a single crystal with different dopant concentrations diffused across it. Creating from two separate pieces of semiconductor material will introduces a grain boundary between the metals which reduces its efficiency by scattering the electrons and holes.

2.1.1 Properties of a p-n junction

A p-doped and n-doped semiconductor is relatively conductive but the junction between them is a nonconductor. This nonconducting layer usually called the depletion zone, which occurs because of the electrical charge carriers in doped n-type and p-type silicon (electrons and holes, respectively) attract and eliminate each other in a process called recombination.

This material is reserved for educational use only, not allowed for commercial use.
Forbidden to modify the content, and cite the document when use.

p–n junctions are normally used as diodes, which allow a flow of electricity in one direction but not in the other (opposite) direction. This property is explained in terms of forward bias and reverse bias.

2.1.2 Equilibrium (zero bias)

An equilibrium condition is reached in a p–n junction, without an external applied voltage. The potential difference is formed across the junction called built-in potential V_{bi}. In an equilibrium p–n junction, electrons near the p–n interface tend to diffuse into the p region and leave positively charged ions (donors) in the n region. Similarly, holes near the p–n interface begin to diffuse into the n-type region leaving fixed ions (acceptors) with negative charge. Then the regions nearby the p–n interfaces lose their neutrality and become charged and forming the space charge region or depletion layer (see figure 2.2).

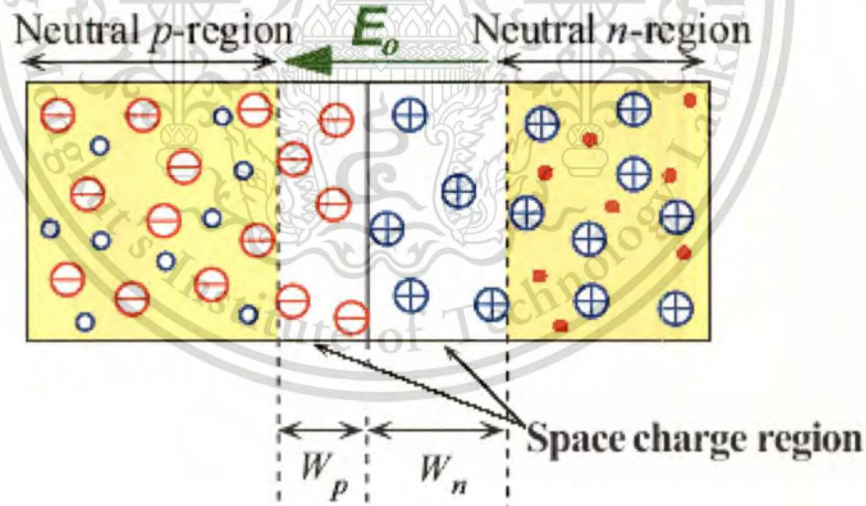

Fig. 2.2 A p–n junction in thermal equilibrium with zero bias voltage applied

This material is reserved for educational use only, not allowed for commercial use.
Forbidden to modify the content, and cite the document when use.

The electric field is shown on the bottom, created by the space charge region opposes the diffusion process for both electrons and holes. There is a diffusion process that tends to generate more space charge and the electric field generated by the space charge that tends to counteract the diffusion. The carrier concentration profile at equilibrium is shown as blue and red lines in fig. 2.2.

The zone with a net charge provided by the fixed ions (donors or acceptors) called space charge region, which have been left uncovered by majority carrier diffusion. In equilibrium condition, the charge density is approximated by the displayed step function. In fact, the region is completely depleted of majority carriers (leaving a charge density equal to the net doping level), and the edge between the space charge region and the neutral region is quite sharp (see fig. 2.3). The space charge region has the same charge on both sides of the p–n interfaces, thus it extends farther on the less doped side (the n side in fig. 2.2 and fig 2.3).

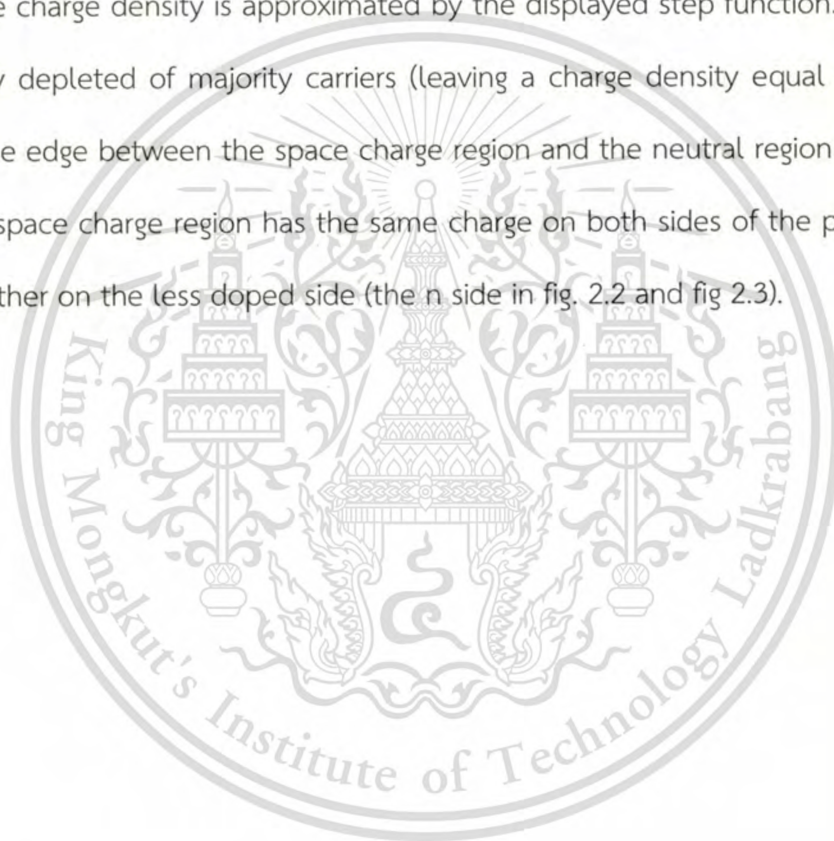

This material is reserved for educational use only, not allowed for commercial use.
Forbidden to modify the content, and cite the document when use.

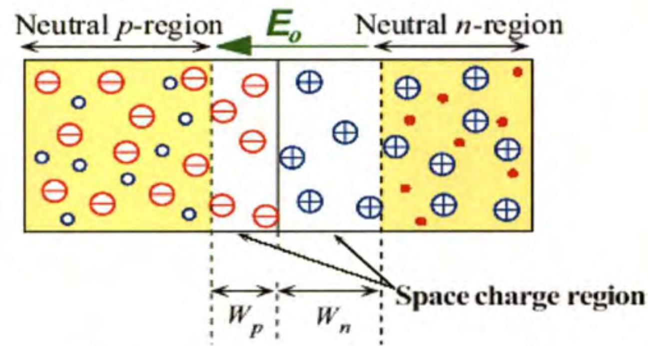

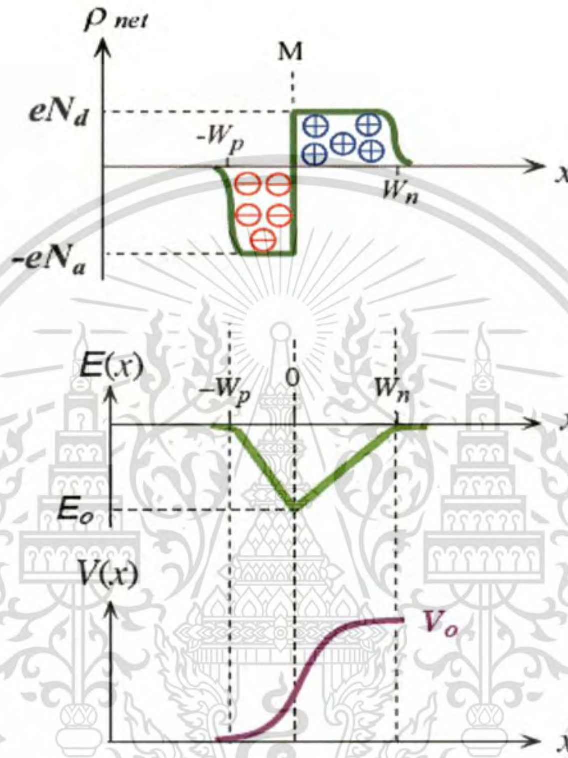

Fig. 2.3 A p–n junction in thermal equilibrium, charge density, the electric field and the voltage with zero bias voltage applied

2.1.3 Forward bias

P—n junction diode, p-type is connected to the positive terminal of a battery and the n-type is connected to the negative terminal, called forward bias (see figure 2.4). This usually makes the p–n junction conduct.

This material is reserved for educational use only, not allowed for commercial use.
Forbidden to modify the content, and cite the document when use.

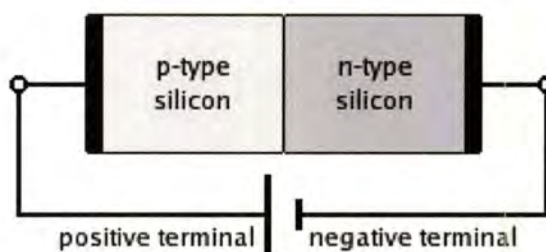

Fig. 2.4 A silicon p–n junction in forward bias

In forward bias condition, holes in the p-type region and electrons in the n-type region are pushed towards the junction, therefore, the width of the depletion zone is reduced. The positive charge applied to the p-type push away the holes, while the negative charge applied to the n-type push away the electrons, the distance between them decreases and lowers the barrier in potential. While increasing forward-bias voltage, the depletion zone becomes thin enough that the zone's electric field can't counteract charge carrier motion across the p–n junction, consequently reducing electrical resistance. The electrons which cross the p–n junction into the p-type material (or holes which cross into the n-type material) will diffuse in the near-neutral region. Therefore, the amount of minority diffusion in the near-neutral zones determines the amount of current that may flow through the diode.

The forward bias pushing electrons from the n side toward the P side but they do not continue to flow through the p-type material indefinitely, because it is energetically favorable for them to recombine with holes. The average length an electron travels through the p-type material before recombining is called the diffusion length, and it is typically on the order of microns.

Although the electrons penetrate only a short distance into the p-type material, the electric current continues uninterrupted, because holes (the majority carriers) begin to flow in the opposite direction. The total current (the sum of the electron and hole currents) is constant

This material is reserved for educational use only, not allowed for commercial use.
Forbidden to modify the content, and cite the document when use.

in space, because any variation would cause charge buildup over time (this is Kirchhoff's current law).

The macroscopic picture of the current flow through the diode involves electrons flowing through the n-type region toward the junction, holes flowing through the p-type region in the opposite direction toward the junction, and the two species of carriers constantly recombining in the vicinity of the junction. The electrons and holes travel in opposite directions, but they also have opposite charges, so the overall current is in the same direction on both sides of the diode.

2.1.4 Reverse bias

P-type is connected to negative terminal of the battery and the n-type is connected to the positive terminal, called reverse bias (see figure 2.5). In this condition the voltage at the cathode is higher than that at the anode and no current will flow until the diode breaks down. The connections are illustrated in the following diagram:

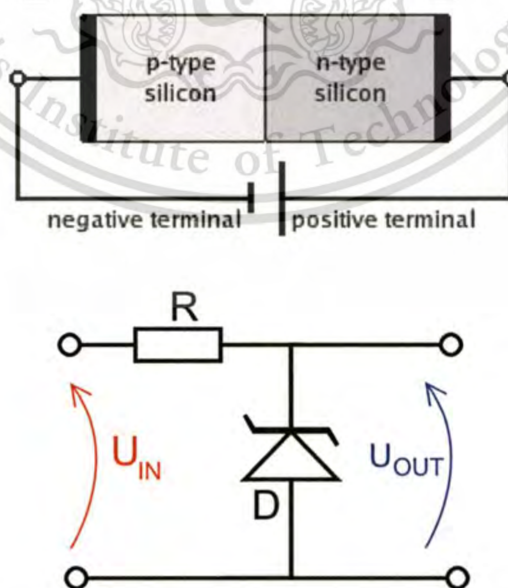

Fig. 2.5 A silicon p–n junction in reverse bias

This material is reserved for educational use only, not allowed for commercial use.
Forbidden to modify the content, and cite the document when use.

The p-type is connected to the negative terminal and n-type is connected to the positive terminal of the power supply, the holes in the p-type and the electrons are pulled away from the junction, causing the width of the depletion zone to increase. Therefore the depletion region widens and does so increasingly with increasing reverse-bias voltage. This increases the voltage barrier causing a high resistance to the flow of charge carriers.

The depletion zone electric field increases as the reverse-bias voltage increases. Once the electric field intensity increases beyond a critical level, the p–n junction depletion zone breaks-down and current begins to flow, usually by either the zener or avalanche breakdown processes. Both of these breakdown processes are non-destructive and are reversible, so long as the amount of current flowing does not reach levels that cause the semiconductor material to overheat and cause thermal damage.

2.2 Capacitance-voltage characteristics (C-V)

The depletion layer between the n- and p-sides of a p–n-diode serves as an insulating region that separates the two diode contacts. In reverse bias the width of the depletion layer is widened with increasing reverse bias and the capacitance is accordingly decreased.

Normally, the capacitance is measured by monitoring the response of the junction to a small-signal voltage superimposed upon the dc voltage. The corresponding junction capacitance (C_j) is given by

$$C_j = B\varepsilon_{si}/W \qquad (2.1)$$

where B is the area of device, ε_{si} is the silicon permittivity and W is the depletion width.

The junction capacitance is calculated using the expression for the parallel plate capacitance. When applied small voltage variations one finds that charge is only added and

This material is reserved for educational use only, not allowed for commercial use.
Forbidden to modify the content, and cite the document when use.

removed at the edge of the depletion region. Therefore, the capacitance depends on the dielectric constant of plate

$$C_j = \varepsilon_s/W = \{ [(q\varepsilon_s)/2(\phi_i - V_a)] [N_a N_d / (N_a + N_d)] \}^{1/2} \quad (2.2)$$

The capacitance-voltage characteristics can be calculation many parameters such as carrier concentration, depletion width and built in voltage.

2.3 Diode Equation:

For a p-n junction Poisson's equation is

$$\Delta\varphi = -(\rho_i/\varepsilon) = (q/\varepsilon)((n_0 - p_0) + (N_A - N_D)) \quad (2.3)$$

where φ is the electric potential, ρ_i is the charge density, ε is permittivity and q is the magnitude of the electron charge.

Since the total charge on either side of the depletion region must cancel out it is

$$d_p N_A = d_n N_D \quad (2.4)$$

From Eg. (2.4) and by deploying basic calculus it can be shown that the total width of the depletion region is

$$d = d_p + d_n = \{(2\varepsilon/q)((N_A + N_D)/N_A N_D)(V_{bi} - V)\}^{1/2} \quad (2.5)$$

Furthermore, by implementing the Einstein relation and assuming the semiconductor is nondegenerate (i.e. the product $p_0 n_0$ is independent of the Fermi energy) it follows that

$$V_{bi} = (kT/q) \ln\{(N_A N_D)/p_0 n_0\} \quad (2.6)$$

This material is reserved for educational use only, not allowed for commercial use.
Forbidden to modify the content, and cite the document when use.

where T is the temperature of the semiconductor and k is Boltzmann constant.

Refer to Eq. (2.6) the built-in voltage is also given by

$$V_{bi} = (kT/q)\ ln\{(N_A N_D)/n_i^2\} \quad (2.7)$$

By applying the law of mass action $n_i^2 = n_{n0} \times p_{n0}$ we get

$$V_{bi} = (kT/q)\ ln\{(n_{n0} p_{n0})/n_i^2\} \quad (2.8)$$

Rearranging

$$p_{po} = p_{n0}\ exp\{(qV_{bi})/kT\} \quad (2.9)$$

For non-equilibrium situation, when there's forward bias voltage V_f

$$p_{p(o)} = p_{n(0)}\ exp\{q(V_{bi} - V_f)/kT\} \quad (2.10)$$

or

$$p_{po} = p_{n0}\ exp(qV/kT) \quad (2.11)$$

where $V = V_{bi} - V_f$ assuming low injection level, i.e. $p_p \approx p_{p0}$ Eq.(2.9)/Eq.(2.10) by doing this we get minority carrier concentration at the edge of the depletion region (Δp) therefore

$$\Delta p = p_{n0}\ exp\{(qV/kT) - 1\} \quad (2.12)$$

Using the continuity equation, we get an expression for the current density

This material is reserved for educational use only, not allowed for commercial use.
76513
Forbidden to modify the content, and cite the document when use.

$$J_{p(x)} = q(D_p/L_p)\delta_{p(x)} \qquad (2.13)$$

since $\Delta p = \delta_{p(x-0)}$ so $\delta_{p(x-0)} = p_{n0}\, exp\{(qV/kT) - 1\}$

$$J_{p(x)} = q(D_p p_{n0}/L_p) exp\{(qV/kT) - 1\} \qquad (2.14)$$

Same with electrons, hence

$$J_{total} = J_p + J_n = J_s\, exp\{(qV/kT) - 1\} \qquad (2.15)$$

However, if we multiply the above expression by the cross-section area, we get the current I.

$$I = I_0\,(e^{qV/kT} - 1) \qquad (2.16)$$

Where I is the net current flowing through the diode, I_0 is the saturation current, V is Voltage across the terminal of diode, q is charge on an electron, k is "Boltzmann's constant", T is absolute temperature (K).

$$I = I_0(e^{(qv/\eta kT)} -1) \qquad (2.17)$$

η is the diode ideality factor. In case of "ideal" diode, no defect is present, the total diode current would be a diffusion current and n would be 1. In case of "non-ideal" diode, more defects drive n up to 2.

King Mongkut's Institute of Technology Ladkrabang

This material is reserved for educational use only, not allowed for commercial use.
Forbidden to modify the content, and cite the document when use.

2.4 Shockley diode model

The Shockley diode equation relates the diode current I of a p-n junction diode to the diode voltage V_D. This relationship is the diode I-V characteristic given in Eq. (2.17):

When $V_D = \eta V_T$ the formula can be simplified to:

$$I \approx I_0 \cdot e^{V_D/(\eta V_T)} \quad (2.18)$$

This is only an approximation of a more complex I-V characteristic. It is no applicable for ultrashallow junctions, which require better analytical models. V_D

2.5 Ideality factor

The ideality factor, or slope parameter (n) can be calculate from modify of the Schottky diode I – V equation:

$$I(V) = I_0\{exp(qV/\eta kT) - 1\} \quad (2.19)$$

As mention earlier, the ideality factor is a number around 1.0, typically between 1.1 and 1.2 for real diodes. As the ideality factor increases, the non-linearity behavior of the diode decreases changing the gradient of its I – V plot.

At very low currents there is very little voltage drop across any series resistance, within the structure, therefore any change in voltage per decade of current remains constant. Manipulation of the above equation results in an expression for the ideality factor of a diode:

$$\eta = (q/kT)\,\Delta V\,log(e) \quad (2.20)$$

This material is reserved for educational use only, not allowed for commercial use.
Forbidden to modify the content, and cite the document when use.

Where ΔV is the change in voltage across the junction per decade of current and e is the constant: 2.71828 .

2.6 Activation Energy

Activation Energy (E_T), in semiconductor is defined as the minimum amount of energy required to trigger a temperature-accelerated failure mechanism.

A discussion on activation energy is never complete without mentioning the Arrhenius Equation, which gives the basic relationship between the rate at which a failure mechanism occurs, the temperature, and the activation energy of the failure mechanism. The Arrhenius Equation is as follows:

$$R = Ae^{-E_T/(kT)} \tag{2.21}$$

where R is the rate at which the failure mechanism occurs, A is a constant, E_T is the activation energy of the failure mechanism, k is Boltzmann's constant ($8.6e^{-5}$ eV/K), and T is the absolute temperature at which the mechanism occurs.

E_T is expressed in electron volts (eV). If one were to collect the median lifetime (time it takes for 50% of a set of samples to fail) data of different sets of samples accelerated to fail by the same, specific failure mechanism at different temperatures, the natural logarithms (ln) of these median lifetimes can be plotted against 1/T (T is the temperature in deg K) to yield a straight line whose slope is equal to E_T/k.

The value of activation energy indicates the relative tendency of a failure mechanism to be accelerated by temperature, i.e., the lower the E_T, the easier it is to trigger a failure mechanism with temperature. A negative E_T means that the failure mechanism is accelerated by decreasing

This material is reserved for educational use only, not allowed for commercial use.
Forbidden to modify the content, and cite the document when use.

the temperature. Hot carrier injection is an example of a failure mechanism with a negative activation energy.

2.7 Series Resistance

The series resistance (R_s) within a Schottky diode structure is mainly formed from highly doped semiconductor regions at semiconductor – metal interfaces. This causes the deviation of the I – V characteristics from a straight line at high currents (>0.1mA), as seen in fig. 2.6. This is because at higher currents the voltage drop across the ohmic becomes significant compared to the voltage drop at the Schottky contact.

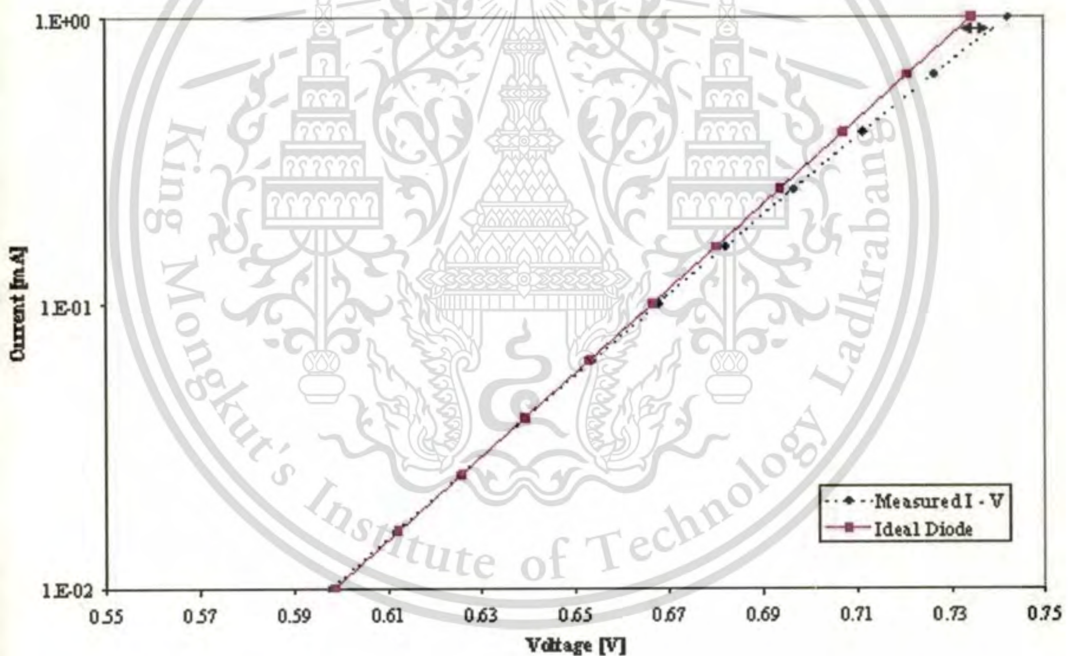

Fig. 2.6 I—V plot of p—n junction diode

If at current I_D the deviation in voltage from an ideal diode to the measured voltage is ΔV_D (marked by the arrow in fig. 2.6) the series resistance is:

This material is reserved for educational use only, not allowed for commercial use.
Forbidden to modify the content, and cite the document when use.

$$R_S = \Delta V_D / I_D \tag{2.22}$$

As increasing currents, the series resistance decreases as a function current, see the fig. 2.7.

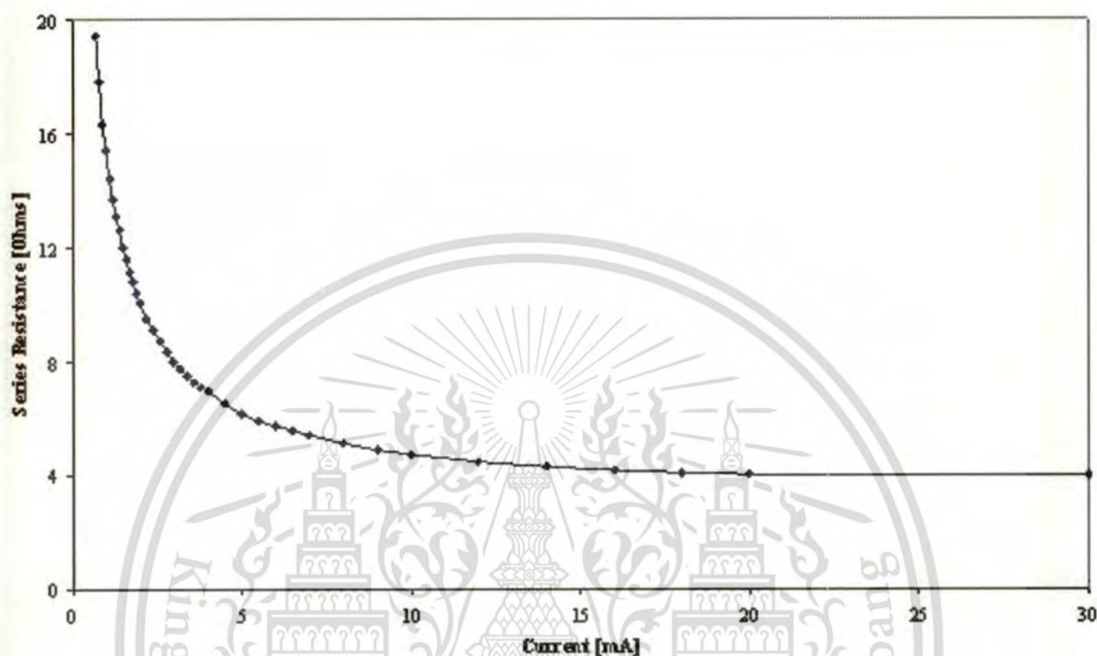

Fig. 2.7 I—R_S plot of p—n junction diode

In fig. 2.7, the calculations of series resistance are made at 1mA, as this is part of the standard parameter method for calculating a Schottky diode's I - V characteristics.

2.8 Carrier generation and recombination

In the solid state physics of semiconductors, carrier generation and recombination are processes by which mobile charge carriers (electrons and electron holes) are created and eliminated. The electron–hole pair is the fundamental unit of generation and recombination, corresponding to an electron transitioning between the valence band and the conduction band.

This material is reserved for educational use only, not allowed for commercial use.
Forbidden to modify the content, and cite the document when use.

Band structure

Semiconductor materials have electronic band structure determined by the crystal properties of the material. The actual energy distribution among the electrons is described by the Fermi energy and the temperature of the electrons. At absolute zero temperature, all of the electrons have energy below the Fermi energy; but at non-zero temperatures the energy levels are randomized and some electrons have energy above the Fermi level.

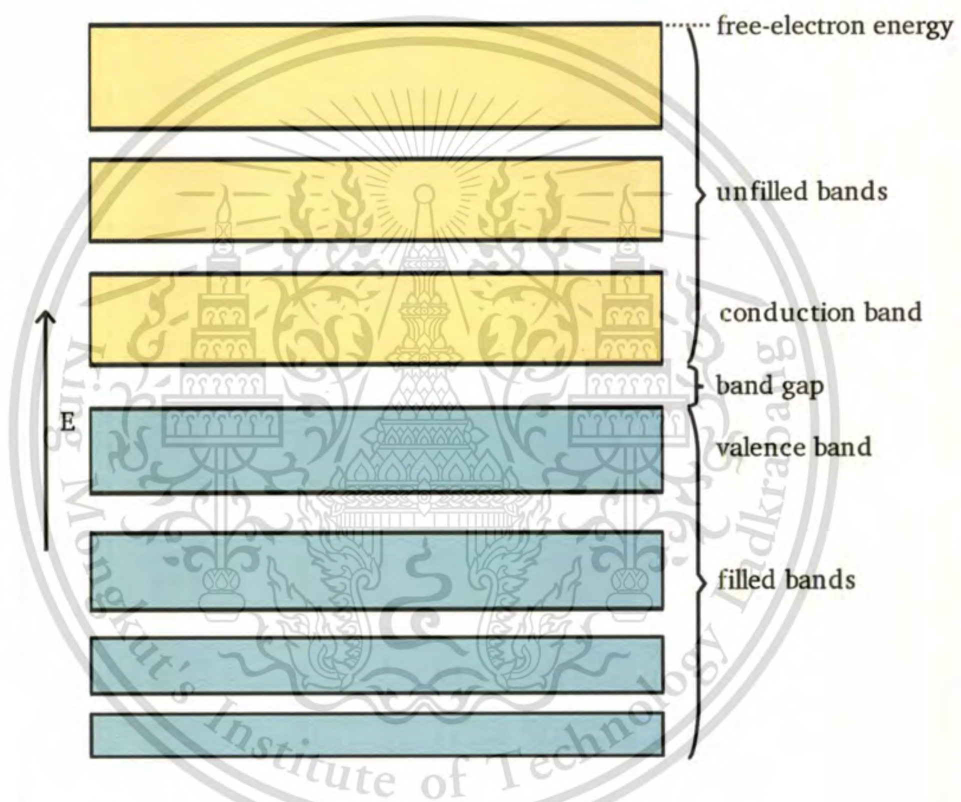

Fig 2.8 Electronic band structure of a semiconductor material

In semiconductors the Fermi energy lies in the middle of a *forbidden band* or band gap between two *allowed bands* called the *valence band* and the *conduction band*. The valence band, immediately below the forbidden band, is normally very nearly completely occupied. The conduction band, above the Fermi level, is normally nearly completely empty. Because the valence band is so nearly full, its electrons are not mobile, and cannot flow as electrical current.

This material is reserved for educational use only, not allowed for commercial use.
Forbidden to modify the content, and cite the document when use.

However, if an electron in the valence band acquires enough energy to reach the conduction band, it can flow freely among the nearly empty conduction band energy states. Furthermore it will also leave behind an electron hole that can flow as current exactly like a physical charged particle. Carrier *generation* describes processes by which electrons gain energy and move from the valence band to the conduction band, producing two mobile carriers; while *recombination* describes processes by which a conduction band electron loses energy and re-occupies the energy state of an electron hole in the valence band.

In a material at thermal equilibrium generation and recombination are balanced, so that the net charge carrier density remains constant. The equilibrium carrier density that results from the balance of these interactions is predicted by thermodynamics. The resulting probability of occupation of energy states in each energy band is given by Fermi-Dirac statistics.

2.8.1 Generation and recombination processes

Recombination of electrons and holes is a process by which both carriers defeat each other and eventually disappear in the process: electrons occupy - through one or multiple steps - the empty state associated with a hole. The energy difference between the initial and final state of the electron is released in the process. This leads to one possible classification of the recombination processes. In the case of radiative recombination, this energy is emitted in the form of a photon. In the case of non-radiative recombination, it is passed on to one or more phonons and in the case of Auger recombination it is given off in the form of kinetic energy to another electron. Another classification scheme considers the individual energy levels and particles involved. These different processes are presented fig. 2.9:

This material is reserved for educational use only, not allowed for commercial use.
Forbidden to modify the content, and cite the document when use.

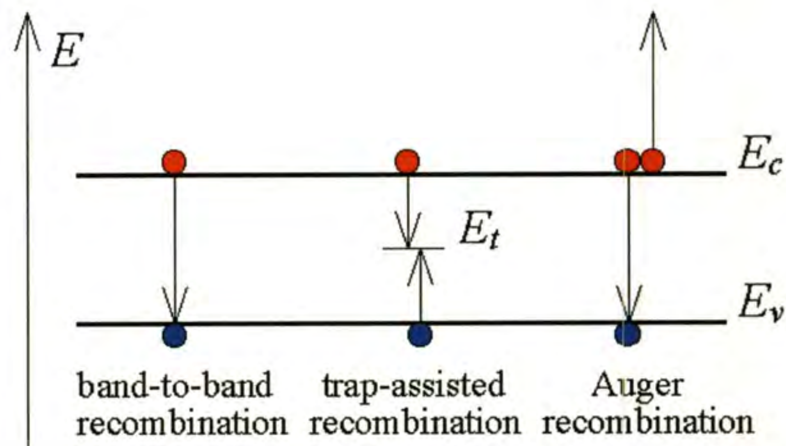

Fig. 2.9 Individual energy levels vs recombination processes

a) Band-to-band recombination occurs when an electron moves from its conduction band state into the empty valence band state associated with the hole. This band-to-band transition is typically also a radiative transition in direct bandgap semiconductors.

b) Trap-assisted recombination or *Shockley-Read-Hall (SRH) recombination* occurs when an electron falls into a "trap", an energy level within the bandgap caused by the presence of a foreign atom or a structural defect. Once the trap is filled it cannot accept another electron. The electron occupying the trap, in a second step, moves into an empty valence band state, thereby completing the recombination process. One can envision this process as a two-step transition of an electron from the conduction band to the valence band or as the annihilation of the electron and hole, which meet each other in the trap.

c) Auger recombination is a process in which an electron and a hole recombine in a band-to-band transition, but now the resulting energy is given off to another electron or hole. The involvement of a third particle affects the recombination rate so that we need to treat Auger recombination differently from band-to-band recombination.

This material is reserved for educational use only, not allowed for commercial use.
Forbidden to modify the content, and cite the document when use.

Each of these recombination mechanisms can be reversed leading to carrier generation rather than recombination. A single expression will be used to describe recombination as well as generation for each of the above mechanisms.

In addition, there are generation mechanisms, which do not have an associated recombination mechanism, such as generation of carriers by light absorption or by a high-energy electron/particle beam. These processes are referred to as ionization processes. Impact ionization, which is the generation mechanism associated with Auger recombination, also belongs to this category. The generation mechanisms are presented in fig. 2.10 :

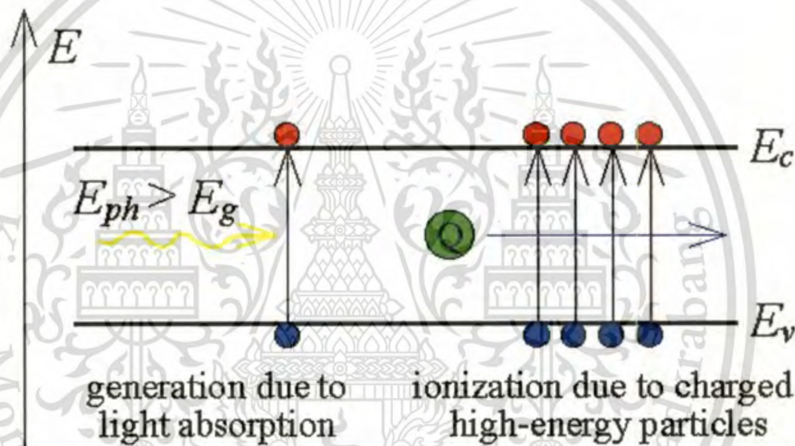

Fig. 2.10 Individual energy levels VS generation processes

Carrier generation due to light absorption occurs if the photon energy is large enough to raise an electron from the valence band into an empty conduction band state, thereby generating one electron-hole pair. The photon energy needs to be larger than the bandgap energy to satisfy this condition. The photon is absorbed in this process and the excess energy, E_{ph} - E_g, is added to the electron and the hole in the form of kinetic energy.

Carrier generation or ionization due to a high-energy beam consisting of charged particles is similar except that the available energy can be much larger than the bandgap energy so that

This material is reserved for educational use only, not allowed for commercial use.
Forbidden to modify the content, and cite the document when use.

multiple electron-hole pairs can be formed. The high-energy particle gradually loses its energy and eventually stops.

Finally, there is a generation process called impact ionization, the generation mechanism that is the counterpart of Auger recombination. Impact ionization is caused by an electron/hole with an energy, which is much larger/smaller than the conduction/valence band edge. The detailed mechanism is presented in fig. 2.11:

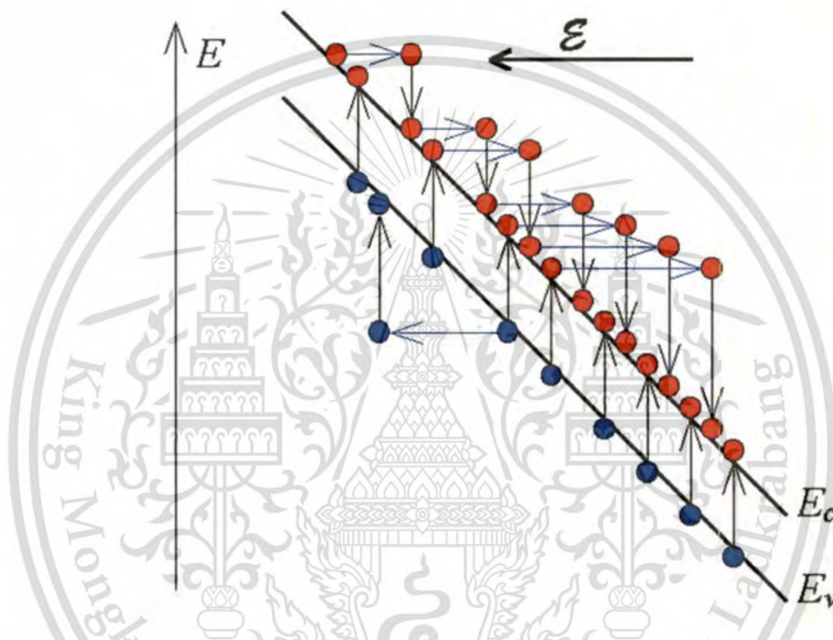

Fig. 2.11 Ionization mechanism caused by an electron/hole

The excess energy is given off to generate an electron-hole pair through a band-to-band transition. This generation process causes avalanche multiplication in semiconductor diodes under high reverse bias: As one carrier accelerates in the electric field it gains energy. The kinetic energy is given off to an electron in the valence band, thereby creating an electron-hole pair. The resulting two electrons can create two more electrons which generate four more causing an avalanche multiplication effect. Electrons as well as holes contribute to avalanche multiplication.

This material is reserved for educational use only, not allowed for commercial use.
Forbidden to modify the content, and cite the document when use.

The energy released due to recombination can be either thermal, thereby heating up the semiconductor (thermal recombination or non-radiative recombination, one of the sources of waste heat in semiconductors), or released as photons (optical recombination, used in LEDs and semiconductor lasers).

In indirect band gap semiconductors, the carrier lifetime strongly depends on the concentration of recombination centers. Gold atoms act as highly efficient recombination centers, silicon for some high switching speed diodes and transistors is therefore alloyed with a small amount of gold. Many other atoms, e.g. iron or nickel, have similar effect however today, involve the use of irradiation.

2.8.2 Carrier-generation Lifetime

Refer to the reverse bias condition, Saturation current I_0 is a combination of diffusion current I_d and generation current I_g in the depletion region, as shown in Eq. (2.23):

$$I_0 = I_d + Bqn_iW/\tau_g \tag{2.23}$$

where B is the p–n junction area, n_i is the intrinsic carrier concentration, τ_g is the carrier-generation lifetime, and W is the depletion-region width. The latter can be calculated from Eq. (2.24):

$$W = B\varepsilon_{Si}/C \tag{2.24}$$

where ε_{Si} is the dielectric permittivity of silicon and C is capacitance, which can be obtained from a plot of capacitance–voltage (C–V) characteristics.

This material is reserved for educational use only, not allowed for commercial use.
Forbidden to modify the content, and cite the document when use.

The equation for carrier-generation lifetime (Eq. 2.25, below) is exactly in the form of Eq. (2.23) reversed slope.

$$\tau_g = Bqn_iW/(I_0 - I_d) \tag{2.25}$$

This parameter is used as a monitoring method for the device degradation since it can be refer to amount of defects or lattice disorders in the p-n junction effective area which lead to a breakdown condition of the device.

2.9 RADIATION EFFECTS AND DAMAGE

2.9.1 Ionizing Radiations

The radiations of concern here include charged particles such as electrons (beta particles), protons, alphas and fission fragment ions, and the neutral radiations including photons (gamma and X rays) and neutrons.

Table 2.1 compares some key characteristics of the radiations. For a kinetic energy of 1 MeV, the electron is relativistic (0.94c). For the same energy, the heavier particles are slower, stopped easier and deposit their entire energy over a shorter distance. The passage of radiation through tissue is depicted in Fig. 2.12.

King Mongkut's Institute of Technology Ladkrabang

This material is reserved for educational use only, not allowed for commercial use.

Forbidden to modify the content, and cite the document when use.

Table 2.1 Comparison of Ionizing Radiation

Characteristic	Radiation (E_K = 1 MeV)				
	Alpha (α)	Proton (*p*)	Beta (β) or Electron (*e*)	Photon (γ or X ray)	Neutron (*n*)
Symbol	${}^{4}_{2}\alpha$ *or* He^{2+}	${}^{1}_{1}p$ *or* H^{1+}	${}^{0}_{-1}e$ *or* β	${}^{0}_{0}\gamma$	${}^{1}_{0}n$
Charge	+2	+1	−1	neutral	neutral
Ionization	Direct	Direct	Direct	Indirect	Indirect
Mass (amu)	4.001506	1.007276	0.00054858	—	1.008665
Velocity (cm/sec)	6.944×10^{8}	1.38×10^{9}	2.82×10^{10}	$c=2.998\times10^{10}$	1.38×10^{9}
Speed of Light	2.3%	4.6%	94.1%	100%	4.6%
Range in Air	0.56 cm	1.81 cm	319 cm	82,000 cm*	39,250 cm*

* range based on a 99.9% reduction

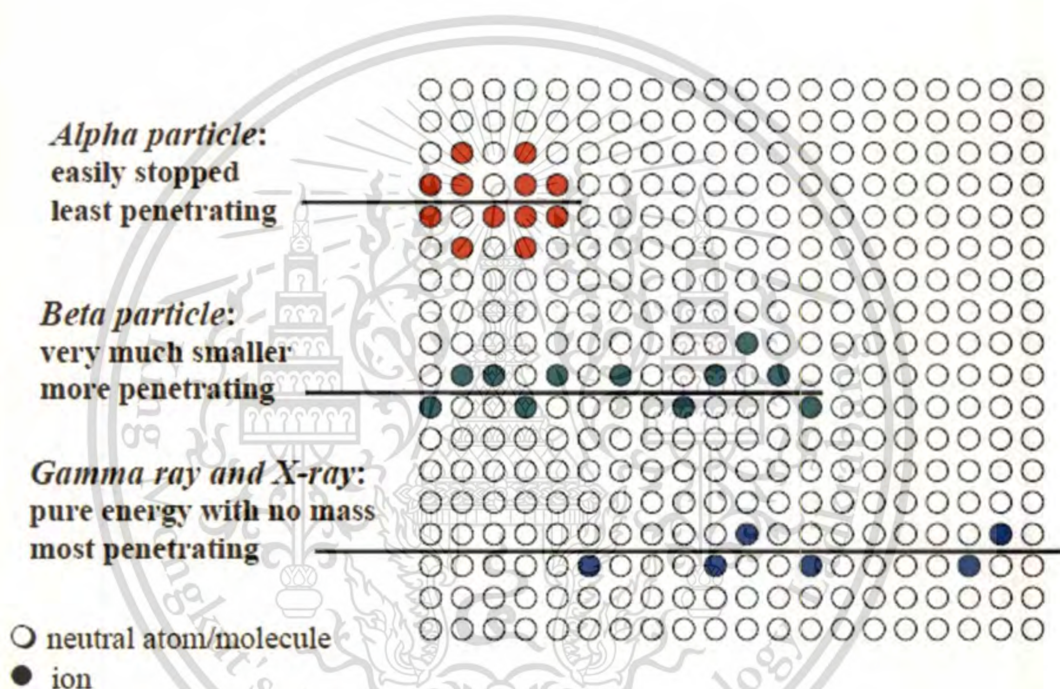

Fig. 2.12 Radiation paths in tissue

The behavior of charged particles (α, β, p) passing through matter is fundamentally different from that of the neutral radiations (n, γ). In particular, the charged particles strongly interact with the orbital electrons of the material through which the particles move. As such, we classify charged particles as directly ionizing. Further, the charged particle interactions can be subdivided into two cases based on mass: (1) heavy charged particles such as alphas and protons, and (2) light electrons (both positrons and negatrons).

This material is reserved for educational use only, not allowed for commercial use.
Forbidden to modify the content, and cite the document when use.

2.9.2 Heavy Charged Particles

Initially, a heavy moving particle loses energy in small steps through interactions with the electrons in the material through which it passes. Once the heavy particle loses enough energy such that it no longer has sufficient energy to excite an electron, then the particle loses energy by nuclear collisions. As the particle slows, it captures electron(s) to form a neutral atom (e.g., a proton becomes hydrogen, and an alpha forms helium). The heavy particles slow down almost entirely due to Coulombic interactions with the atomic electrons. Because of the large number of these interactions, the slowing down is nearly continuous.

Because of their large size, ions are not easily deflected by atomic electrons and so they travel straight line paths. In contrast with the exponential decrease of neutrons and gamma rays, the heavy particle has a well-defined range of only a few centimeters in air, even for quite energetic particles.

2.9.3 Light Charged Particles

When beta particles and electrons pass through matter, several possible processes occur, including:

2.9.3.1 Ionization in which the energy loss mechanism is similar to that for heavy charged particles,

2.9.3.2 Bremsstrahlung, which is the creation of X-rays from electron deceleration, and

2.9.3.3 Elastic scattering from nuclear and electronic interactions.

Scattering is more important in the case of beta particles than with heavy charged particles. This means that the path of an electron is zigzagged, and its range is greater, but its path is not well defined.

King Mongkut's Institute of Technology Ladkrabang

This material is reserved for educational use only, not allowed for commercial use.

Forbidden to modify the content, and cite the document when use.

2.9.4 Neutral Radiations

The uncharged radiations can liberate directly ionizing particles or initiate a nuclear transformation. The fundamental interactions of neutrons are scattering and absorption, which includes both capture and fission. Neutron capture frequently produces radioactive nuclei, which in turn emit radiation(s). The three fundamental interactions by photons and their approximate energy range of interest are

2.9.4.1 The photoelectric effect (low energy: $E < 200$ keV) in which the photon transfers all of its energy to an orbital electron, which is ejected with kinetic energy equal to the incident photon energy less the binding energy (ionization energy) needed to remove the electron ($E_e = E_\gamma - BE_e$). The bottom line is that all the photon energy is absorbed into the incident material.

2.9.4.2 Compton scattering (intermediate energies: 200 keV to 1.5 MeV) which is an elastic scattering of the photon by an atomic electron, which is excited in the process. Here the photon is reduced in energy and deflected from its original direction.

2.9.4.3 Pair production (high energy: $E > 1.5$ MeV) in which the photon disappears and an electron (negatron)-positron pair is formed. Since the rest mass energy of an electron/positron is 0.511 MeV, pair production requires a photon of at least 1.02 MeV to occur. The remainder of the photon energy is received as kinetic energy by the negatron-positron pair. Eventually the positron combines with an electron, and two photons (annihilation radiation) are produced, each having an energy of 0.511 MeV.

We have noted how the mass-less photon predominantly interacts with the atomic electrons, whereas the neutron interacts with the nucleus. Although both of these neutral radiations are classified as indirectly ionizing, each can cause the direct liberation of charged particles.

This material is reserved for educational use only, not allowed for commercial use.
Forbidden to modify the content, and cite the document when use.

2.9.5 General Radiation Effects

The general types of radiation effects on materials can be categorized into

2.9.5.1 Impurity Production, that is, transmutation of nuclei into other nuclei which themselves may be radioactive; this mechanism is caused by neutrons through fission and activation (capture). Impurities can also be deposited from the creation of hydrogen or helium when a proton or an alpha particle, respectively, becomes neutralized in the material of passage.

2.9.5.2 Atom Displacement from their normal position in the structure of the material; displacement atoms may leave lattice vacancies and lodge in interstitial locations or cause interchange of dissimilar atoms in the lattice structure.

2.9.5.3 Ionization, that is, the removal of electrons from atoms in the material and the formation of ion pairs in the path of the charged particles.

Neutrons are particularly efficient at causing the first two effects above. A comparison and contrast of the radiations and their effects is presented in Table 2.2.

Table 2.2 Radiation Damage to Materials

<table>
<tr><th>Radiation</th><th>Impurity Production</th><th>Atom Displacement</th><th>Ionization</th><th>Energy Release</th></tr>
<tr><td>Thermal (eV) neutron</td><td rowspan="2">Directly by absorption reactions (mostly thermal neutrons), also may lead to more radiations</td><td>Yes, indirectly</td><td rowspan="2">Indirectly</td><td rowspan="2">Indirectly</td></tr>
<tr><td>Fast (MeV) neutron</td><td rowspan="2">Multiple displacements via scattering reactions; can cause displacement of "knock-on" atoms</td></tr>
<tr><td>Fission fragment</td><td>Become impurities themselves</td><td>These highly charged ions cause considerable ionization, and they emit β and γ</td><td>Considerable heat deposition over a very short range</td></tr>
<tr><td>Alpha</td><td>He buildup can cause pressurization problems</td><td>Yes, may cause atom displacement</td><td>Causes sizable ionization</td><td>Yes, over a very short range</td></tr>
<tr><td>Proton</td><td>H buildup can also cause pressurization</td><td>Yes</td><td>Directly</td><td>Yes, over a short range</td></tr>
<tr><td>Beta</td><td>n/a</td><td>Some displacement</td><td>Directly</td><td>Localized heat deposition</td></tr>
<tr><td>Photon (γ and X ray)</td><td>n/a</td><td>Rare displacements (via Compton effect)</td><td>Indirectly</td><td>Gamma heating over large distance</td></tr>
</table>

This material is reserved for educational use only, not allowed for commercial use.
Forbidden to modify the content, and cite the document when use.

2.9.6 Impurity Production

In this discussion, impurity production refers to radiation-caused impurities, not any impurities that may have pre-existed in a material. Impurities in a crystal constitute structural imperfections which can alter electrical and mechanical properties. As Table 2.2 indicates, electrons and photons do not directly cause impurity production. One might consider that these radiations can indirectly cause impurity production through chemical bond breakage.

More important to impurity production are the effects of neutron and ion irradiation. Incident ions will eventually slow and capture the necessary electrons to render them neutral. As stated earlier, the protons will become hydrogen and alpha particles will become helium. In both of these cases, the neutral atom is a gas at room temperature, and hence, will exert 'pressure' on its neighboring atoms. In solids, this internal pressurization has been observed to cause swelling in the material.

Neutron and ion irradiation can also form radioactive species. Neutron capture by a nucleus does not necessarily change the chemical element present, but does change the isotope present. The new isotope may be radioactive and decay by one of several schemes, which can change the chemical element present. Of course, the decay process emits additional radiation into the material. In contrast, ion absorption by a nucleus immediately changes the chemical element present; however, the exact reaction products must be determined before a full conclusion is reached.

2.9.7 Atomic Displacement (Damage)

Atomic displacement can occur ballistically through kinetic energy transfer, or radiolytically by the conversion of radiation-induced excitation into atom motion (i.e., recoil). As a charged particle passes through matter, the particle energy dissipates by exciting orbital electrons and by elastic collisions with the material nuclei. An elastic collision can eject an atom from its normal lattice position. The ejected atom is known as a primary knock-on, which,

This material is reserved for educational use only, not allowed for commercial use.

Forbidden to modify the content, and cite the document when use.

in turn, may cause a cascade of atomic displacements before eventually coming to rest. In Figure 2.20, the displaced atom becomes an interstitial, and the position the atom formerly occupied becomes a vacancy. Together the interstitial and vacancy are referred to as a Frenkel pair. Some displaced atoms can lead to secondary displacements. For example, the displaced atom may collide with and replace another atom in the material.

Displacement damage is the result of nuclear interactions, typically scattering, which cause lattice defects. Displacement damage is due cumulative long-term non-ionizing damage from the ionizing radiations. The collision between an incoming particle and a lattice atom subsequently displaces the atom from its original lattice position as shown in Figure 2.13. In space, the particles producing displacement damage include protons of all energies, electrons with energies above 150 keV, and neutrons.

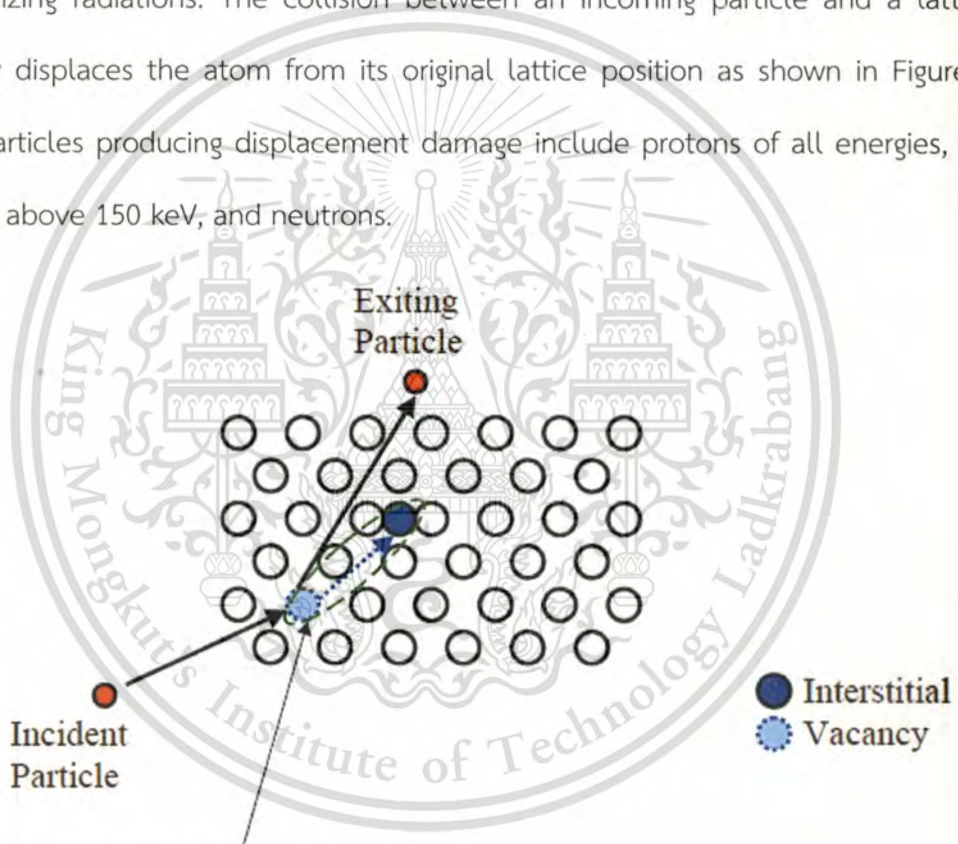

Fig. 2.13 Displacement damage

A single incident particle can cause a cascade of collisions to occur to a portion of the affected material (e.g., Si) lattice atoms. These collisions are produced by both incident “heavy” particles (p, n, ions) and secondary particles. Defects (vacancies, interstitials, Frenkel pairs,

This material is reserved for educational use only, not allowed for commercial use.
Forbidden to modify the content, and cite the document when use.

dislocations) are produced along the tracks of the secondary particles and in clusters at the end of these tracks as shown in fig. 2.14.

Displacement damage can be quantified using the non-ionizing energy loss (NIEL). The NIEL is energy lost to non-ionizing events per unit length, MeV/cm or MeV·cm^2/g. The NIEL is based upon fact that displacement damage effects are proportional to the non-ionizing particle's energy loss and the nuclear recoils produced.

The production of vacancies and interstitials involves a transfer of particle kinetic energy to potential energy stored in the crystal lattice. Both vacancies and interstitials, especially the latter, are mobile at sufficiently high temperature and annealing facilitates their recombination. At the higher temperature, the vibration of the atoms in the lattice increases, thereby providing a mechanism by which an interstitial atom can migrate to a vacancy; and hence, fix both defects.

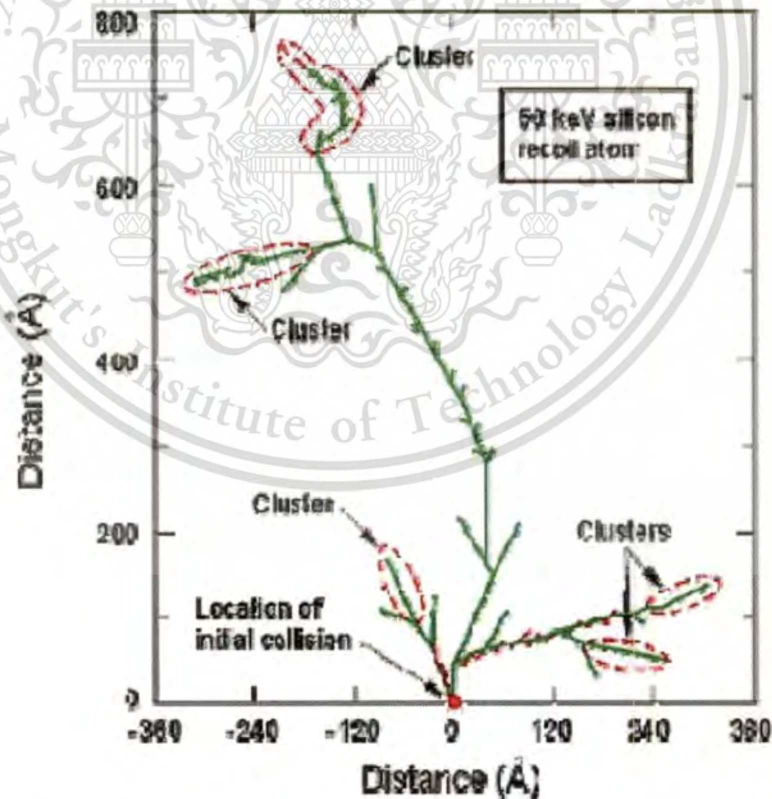

Fig. 2.14 Displacement cascade damage from movement of silicon atom after primary collision

This material is reserved for educational use only, not allowed for commercial use.
Forbidden to modify the content, and cite the document when use.

2.9.8 Ionization

Ionization is the process of removing or adding an electron to a neutral atom, thereby creating an ion. The term is also often used in connection with the removal of an electron from a partially ionized atom. A closely related process is excitation, in which the energy level of an electron is raised; however, excitation occurs at an energy less than that required for ionization. Table I shows that those radiations which are charged (α, β, p) can directly ionize matter; however, those radiations which are neutral (n, γ) are said to indirectly cause ionization.
Ionizing radiation tends to be increasingly damaging in the following order of molecular formation (largely due to the ability of ionization to disrupt the bonds):

a) metallic bond (least damaged)

b) ionic bond

c) covalent bond (most damaged)

Since biological tissue is characterized by substantial covalent bonding, it is generally more susceptible to radiation damage than metallic-bonded structural components.

2.9.8.1 Metallic bonds

Metallic bonding consists of positive ions with free valence electrons, which hold the ions together. Ionizing radiation increases the kinetic energy of the electrons or excites the electron to a higher energy level, but they shortly return to their normal energy level. In either case, there is no permanent damage from ionization, only temporary internal heat production. Note: this is not to say that metals are not damaged by ionizing radiation as we examined earlier the fact that displacement damage can occur in materials.

King Mongkut's Institute of Technology Ladkrabang

This material is reserved for educational use only, not allowed for commercial use.

Forbidden to modify the content, and cite the document when use.

2.9.8.2 Ionic bonds

Ionic bonds are weaker than metallic bonds from an ionizing radiation point of view. Recall that for an ionic bond, electrons are transferred from one element to another element; hence the ionic compound (e.g., NaCl) is composed of positive (cation) and negative (anion) ions which attract one another. Overall, the electrostatic attractive and repulsive forces between the ions lead to well-ordered, three-dimensional arrangements of the ions in crystalline substances. Radiation causes only temporary ionization of the lattice atoms, which soon become neutral. Discoloration (e.g., in glass) may occur due to free electrons being trapped at lattice perfections.

Illustrative Example: Let us use salt (NaCl) as an example. Sodium transfers its loosely bound valence electron to chlorine, such that Na+Cl– is formed, as shown in Fig. 2.15(a). Ionization of the sodium cation would result in a doubly charged Na ion, and the Na_2+ would continue to be attracted to the Cl– anion. Conversely, ionization of the Cl– anion would result in the chlorine atom returning to a neutral state, and the Na+ cation is no longer attracted to the chlorine atom, and hence, the ionic bond is broken, as illustrated in Fig. 2.15(b).

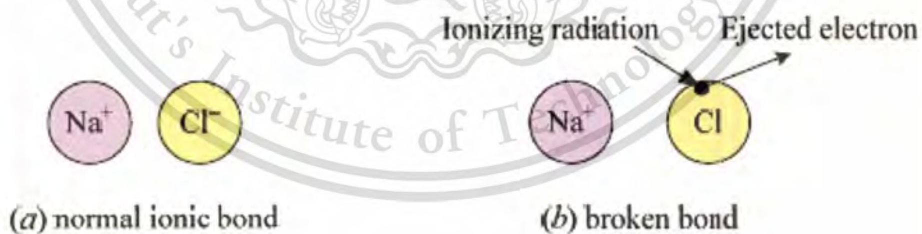

Fig. 2.15 Ionic bond of salt before and after irradiation

2.9.8.3 Covalent bonds

For a covalent bond such as found in water (H_2O), the outer electrons in a molecule are no longer uniquely associated with a particular atom, but rather are shared between all the

This material is reserved for educational use only, not allowed for commercial use.
Forbidden to modify the content, and cite the document when use.

atoms in the molecule. Covalent compounds (e.g., H_2O, CO_2, C, Si, and Ge) share electrons among the joined atoms, with the binding force being the attraction of each atom to the jointly held electrons. Covalent bonds are typical of the gases, liquids and organic materials. The resultant covalent molecules do not attract one another to any degree. Covalent bond energies are in the low eV range. Radiation of sufficient energy to overcome the covalent bond can permanently separate the molecule into its constituent atoms or radicals. Hence, the chemical composition of the material is fundamentally changed.

2.9.9 Energy Deposition

All of the radiations cause energy (and charge) deposition within the absorbing material through the ionization process. In water and organics, most of the absorbed ionization energy breaks chemical bonds. In metals, almost all of the absorbed energy from ionization appears as heat. It is the kinetic energy deposition that generally manifests itself as thermal heating of the material. The corresponding temperature rise can change a number of material properties.

2.9.10 Specific Radiation Effects

Radiation can cause changes to a variety of material properties including chemical, electrical, magnetic, mechanical, optical, and so on. In this section, we look at two examples of these effects. Materials such as insulators, dielectrics, plastics, lubricants and rubber are but a few of the materials that are ionization sensitive.

2.9.10.1 Mechanical Effects

The effects of radiation on the mechanical (and metallurgical) properties include changes to strength and ductility. Mechanical properties are directly related to microstructural characteristics of a given material. In general, nuclear radiation tends to destroy the well-defined lattice structure of crystalline materials. These imperfections ultimately alter the basic

This material is reserved for educational use only, not allowed for commercial use.

Forbidden to modify the content, and cite the document when use.

material properties such as hardness, ductility, etc. The radiation damage is primarily due to point defects being created in the crystalline structure. As an example, if a fast neutron causes displacement damage, then the ordered structure of the material has been weakened and the material properties changed due to the irregularities and vacancies. In a process known as amorphization or metamictization, radiation may convert crystalline material to an amorphous structure.

Microstructural change then affects macroscopic properties. Consider a neutron-caused atomic displacement in a crystalline solid. The radiation has therefore caused point defects in the lattice. Various mechanical properties are affected by the way in which one plane of atoms slips over the adjacent plane. The dislocations inhibit slip processes, that is, more energy is required to initiate slipping. Consequently, the material resistance to penetration (hardness) and the stress required to initiate failure (strength) increase, but there is a concomitant decrease in the energy needed for failure by fracture (toughness) and permanent strain (ductility).

Metals: Metals represent an appropriate material for which to examine mechanical effects of radiation. The changes produced by radiation are comparatively small in metals. The relaxation time for self-annealing in metals is short. The radiation effects are similar to those produced by cold working; specifically, the hardness and the creep rate are increased, and the electrical and thermal conductivities are decreased. In addition, ordered alloys become disordered. Metals with their shared valence electrons are affected very little by ionization. Neutron damage to metals is more pronounced for higher energy neutrons. Under fast neutron irradiation, all steels experience radiation-induced hardening and embrittlement. Steels bombarded by fast neutrons also experience swelling (volume increase) and radiation-induced creep. Typically, radiation causes the hardness and strength to increase with a concurrent decrease in the ductility and toughness. Annealing will soften and toughen materials.

Steels used in nuclear reactors are exposed to significant neutron fluence. Irradiation damage is sometimes quantified in terms of the number of displacements per atom (dpa).

This material is reserved for educational use only, not allowed for commercial use.
Forbidden to modify the content, and cite the document when use.

Klueh states that typical displacement rates in steel are 0.03, 30 and 60 dpa/yr, respectively, for light-water, fast and fusion reactor applications [3]. It is phenomenal to consider that each steel atom being used in a fast reactor is displaced 30 times in a single year!

2.9.10.2 Electrical Effects

Radiation can change electrical properties such as the conductivity of a material. Primary radiation damage mechanisms from indirectly ionizing radiation (neutrons and photons) are of two types: atomic displacements resulting in lattice defects, and changes at the molecular level. The former is the key damage mechanism in metals, the latter in nonmetals. A combination of both mechanisms is important for electrical components such as semiconductors and insulators. We separate our discussion of electrical properties into those on metallic conductors and those on semiconductors and insulators.

a) Metallic conductors: First, we examine radiation effects on metallic conductors. We have already seen that ionization does little to the metals, rather atomic displacement is the radiation damage mechanism of importance. The conductivity (σ) and resistivity (ρ) of a metal can be expressed as

$$\sigma = 1/\rho = q\, m\, \mu \qquad (2.26)$$

where q is the fundamental charge unit, m is the number of charge carriers and μ is the carrier mobility. The mobility is the ratio of the drift velocity and electric field (v E).

Valence electrons travel through a metal as standing waves. The introduction of a point defect (imperfection) in the material can cause electrons to be deflected. Such a disordered structure has a shorter mean free path for electron movement. The electron drift velocity is correspondingly reduced which subsequently causes a decrease in the carrier mobility. As can

This material is reserved for educational use only, not allowed for commercial use.
Forbidden to modify the content, and cite the document when use.

be seen from Eq. (2.26), a decrease in μ causes conductivity of metals to decrease (and resistivity to increase). Hence, any radiation that introduces irregularities into the crystal structure of a metal causes an increase in the electrical resistivity since the lattice imperfections decrease the mobility of the charge carriers (electrons). Again, ionization does little to change the conductivity of a metallic conductor.

b) Semiconductors and Insulators: To investigate the effects of radiation on semiconductor and insulator electrical properties, we begin our discussion by recalling the basic electronic difference between metals, and semiconductors and insulators.

The outermost electrons, which are not associated with any particular atom, have energy levels that fall into two bands: a valence (filled) band and a conduction band. In all materials, a region of forbidden energies separates these two bands. In an insulator, electrons occupy all the energy levels in the valence band and the conduction band is empty. However, in a conductor, not only is the valence band full, but the conduction band also has electron(s). Electrons in the conduction band are relatively free to move throughout the material under the influence of an electric field, and create an electric current.

The forbidden energy gap between the valence and conduction bands is small in semiconductors whereas the gap is large for insulators. Thermal agitation of valence electrons in semiconductors is sufficient to allow the electrons to jump the gap and move into the conduction band.

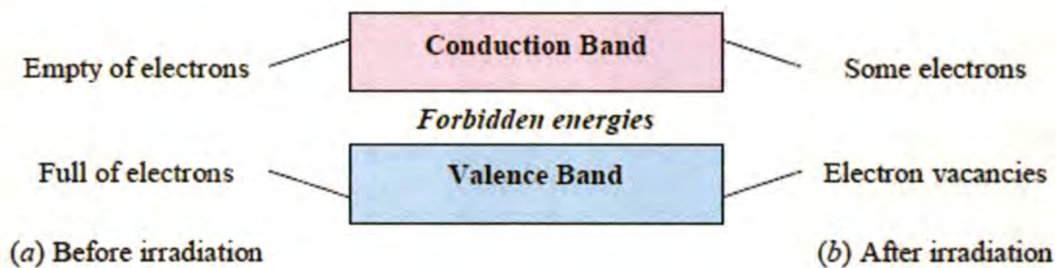

Fig. 2.16 Electron population in an insulator

This material is reserved for educational use only, not allowed for commercial use.
Forbidden to modify the content, and cite the document when use.

Consider the passage of radiation through some material. Ionizing radiations can carry more substantial excitation energy than thermal agitation, such that large numbers of valence electrons in both semiconductors and insulators can be readily excited to the conduction band. The radiation produces a large number of excited atoms along its track. After the traversal of the radiation, vacancies may be left in the valence band and there will be some electrons in the conduction band (see fig. 2.16). Since the direct recombination of the conduction band electron with the vacancy is a highly forbidden process, the electron is free to drift through the material. Thus, this irradiation event has created electron-hole pairs—an electron in the conduction band and a hole in the valence band.

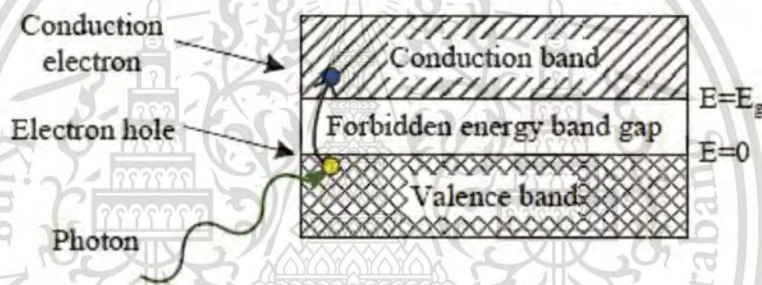

Fig. 2.17 Photoconduction in which a photon raises the energy of a valence electron to the conduction band and leave behind a hole in the valence band

Photoconduction occurs when an electron is excited across the forbidden energy gap between the valence and conduction bands, as depicted in fig. 2.17. Radiation of sufficient energy (for example, photons in the ultraviolet-to-gamma range) can increase the number of intrinsic carriers (electrons and holes) by several orders of magnitude. Since photoconduction increases intrinsic carrier concentration, both electrons and holes, the resistivity of semiconductors is decreased according to

This material is reserved for educational use only, not allowed for commercial use.
Forbidden to modify the content, and cite the document when use.

$$\sigma = 1/\rho = q\,(n_n\,\mu_n + n_p\,\mu_p) \qquad (2.27)$$

where the subscript n denotes the negative electron carriers and p signifies the positive hole carriers.

The excitation of valence electrons into the conduction band can significantly increase the electrical conductivity of both insulators and semiconductors, this phenomena is known as radiation-induced conductivity. Recombination occurs when the electron drops from the conduction band back down to the valence band. The first-order time constant for recombination to occur is known as the relaxation time.

Impurities in a crystal constitute structural imperfections which create trapping sites for holes and electrons that are diffusing. Damage also arises in insulators and semiconductors as a result of atomic displacements, whereby point defects serve as charge-carrier donors and traps. Transient effects in these materials are analogous to molecular effects. Irradiation creates secondary-electron charge carriers, and thus affects electrical properties. The longer relaxation time in semiconductors as compared to metals leads to damage that is more permanent. Semiconductors, such as germanium, can have their conductivity altered by irradiation.

This material is reserved for educational use only, not allowed for commercial use.
Forbidden to modify the content, and cite the document when use.

Chapter 3

Device fabrication and Experiment

The p-n junction diode was fabricated by using CMOS technology at Thai Microelectronics Center (TMEC). The diode after fabricate are study the electrical properties such as current-voltage (I-V) and capacitance-voltage (C-V) characteristics. Fig. 3.1 shows the experiment plan to study the effect of low-high dose of X-ray irradiation on the electrical properties of p-n junction diode.

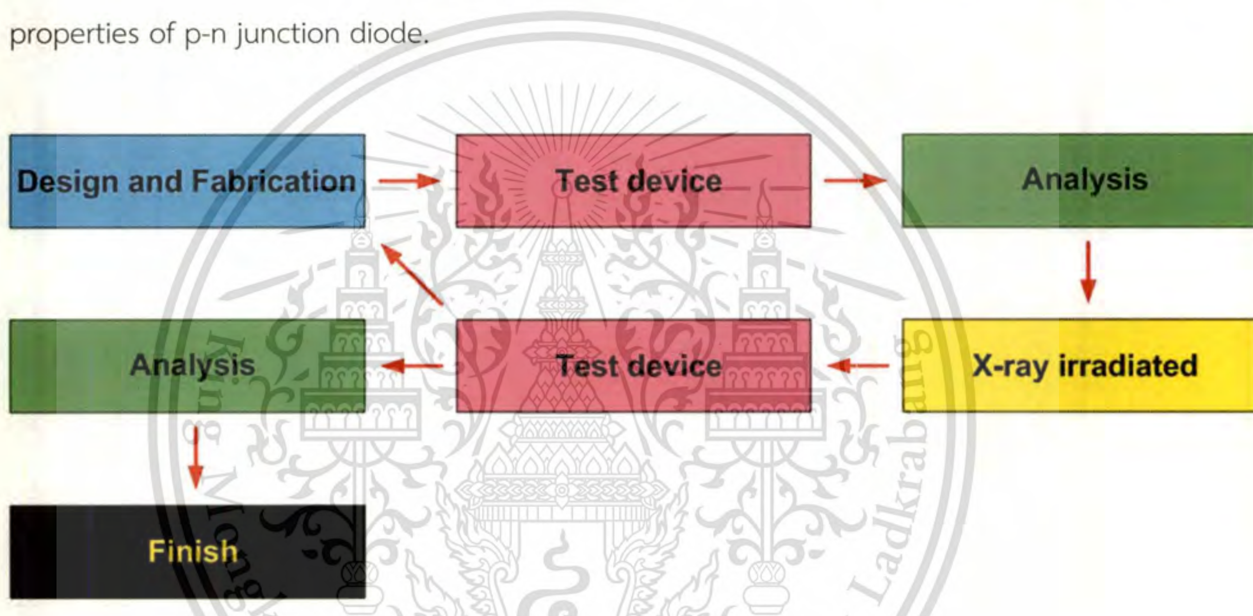

Fig. 3.1 Plan of experiment for study the effect of X-ray irradiation.

3.1 Design and Fabrication p-n diode

Experimentally, the shallow p-n junction diode flow process with CMOS technology was facilitated by TMEC. The p-n junction diodes were fabricated by using the 325 3M thick 60-90 Ω-cm (100) n-type silicon substrate. The diode process module consisted of (i) deposition of silicon dioxide on the substrate, (ii) dry-etching of active area, (iii) implantation of boron at energy of 120 keV and dose of 1×10^{16} atoms/cm^{-2} on the front side wafers (the implantation been followed by a thermal annealing at 1050 $^{\circ}$C for 60 min, resulting in a

This material is reserved for educational use only, not allowed for commercial use.
Forbidden to modify the content, and cite the document when use.

junction depth of about 2 μm), (iv) E-beam evaporation of Pt on the back side (v) thermal annealing for 6 hours, (vi) 1 μm thick Al deposition on the front and back sides. The process flow shows in Fig. 3.2.

(1) N-type silicon thickness 325 μm

(2) Oxidation for 500 nm

This material is reserved for educational use only, not allowed for commercial use.
Forbidden to modify the content, and cite the document when use.

(3) Photolithography process and Ion implantation of Phosphorus (n^+) on back side

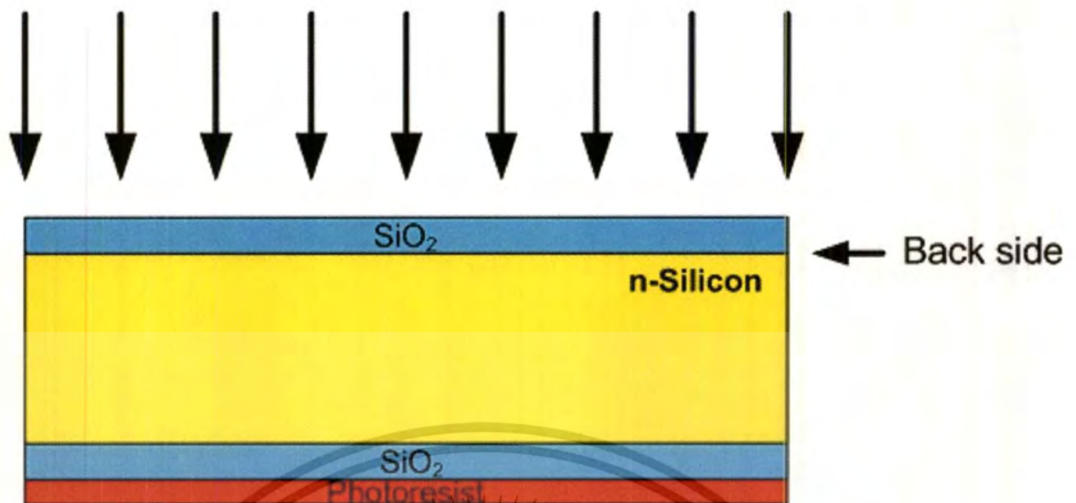

(4) After Phosphorus doping process on back side

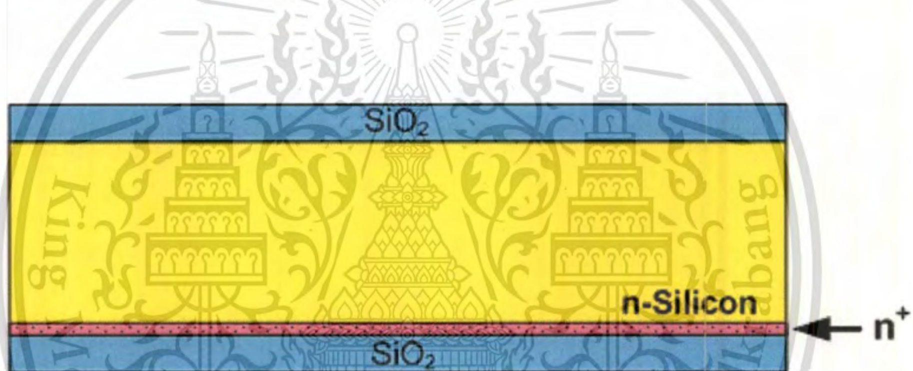

(5) Photolithography process and Ion implantation of Boron (p^+) on front side

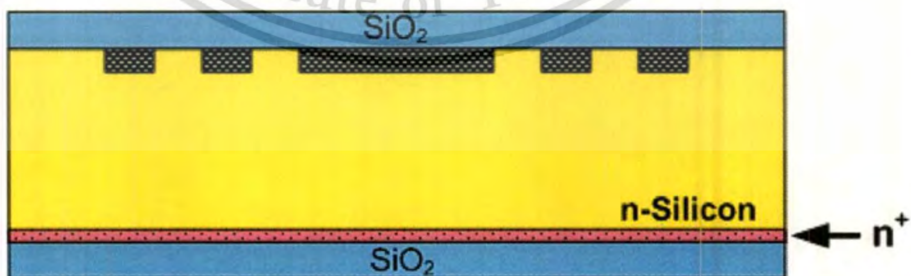

This material is reserved for educational use only, not allowed for commercial use.
Forbidden to modify the content, and cite the document when use.

(6) Plasma enhance chemical vapor deposition (PECVD) oxide for 1.5 μm

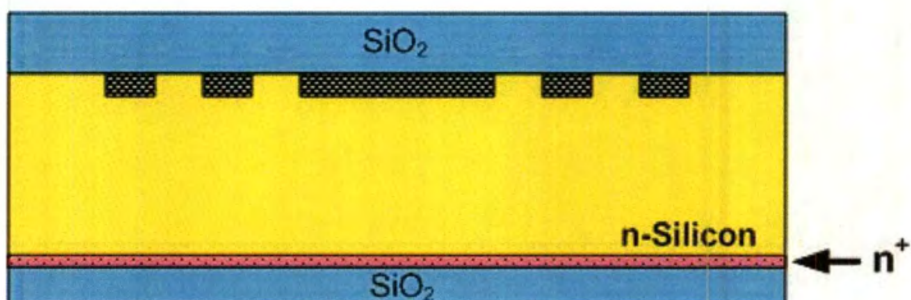

(7) Photolithography and dry etching SiO_2

(8) Deposited Al for 1μm

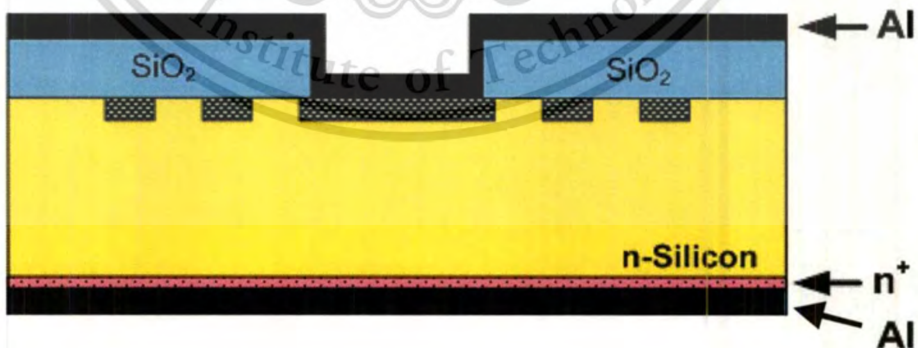

King Mongkut's Institute of Technology Ladkrabang

This material is reserved for educational use only, not allowed for commercial use.
Forbidden to modify the content, and cite the document when use.

(9) Photolithography and Dry etching Al

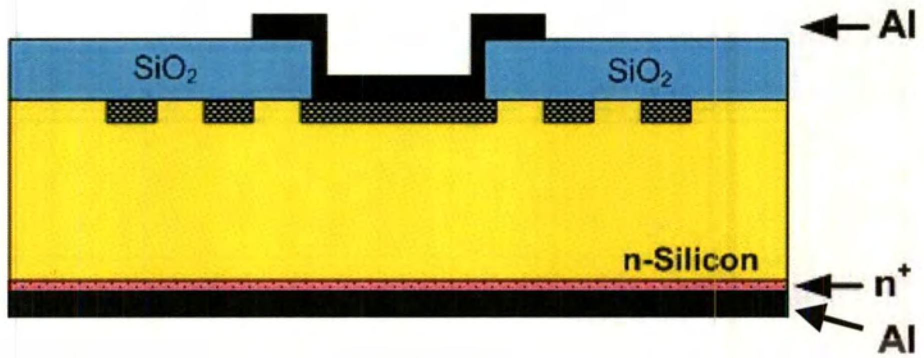

(10) Plasma enhance chemical vapor deposition (PECVD) Nitride for 500 nm on front side

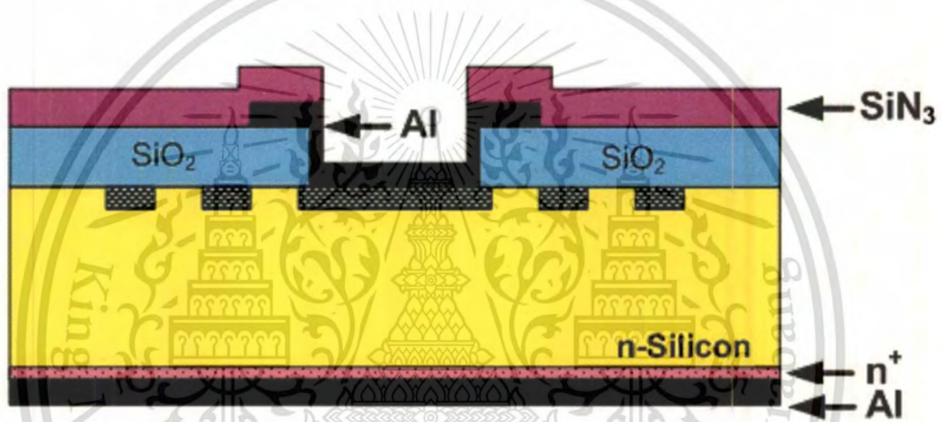

Fig. 3.2 Process flow of p-n diode fabrication base on silicon

This material is reserved for educational use only, not allowed for commercial use.
Forbidden to modify the content, and cite the document when use.

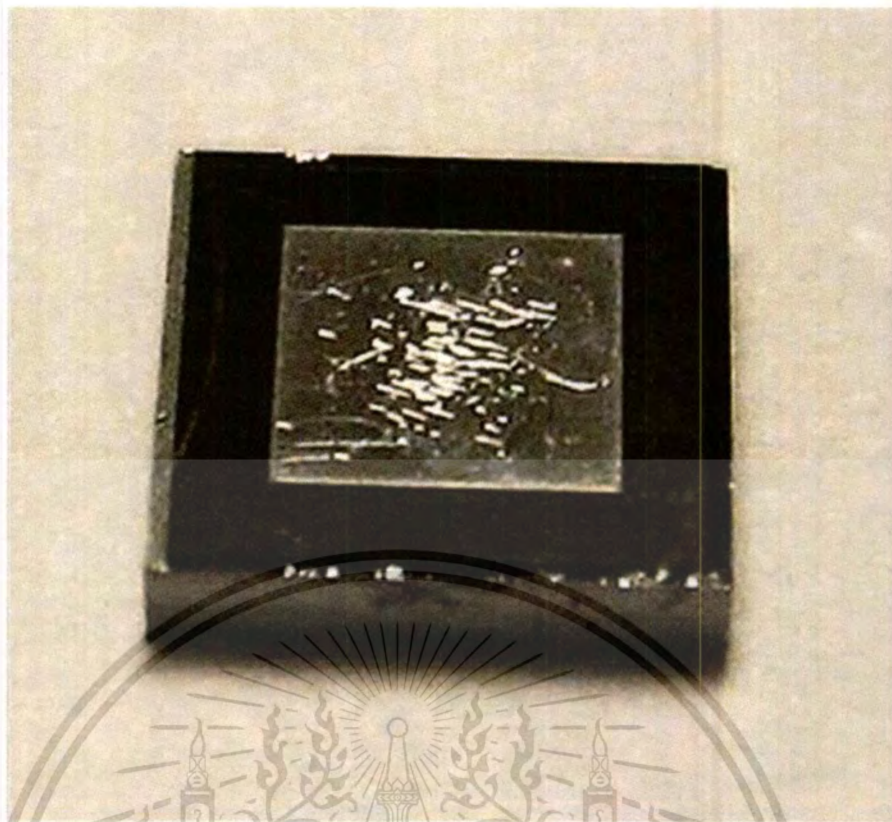

Fig. 3.3 p-n junction diode after fabrication

3.2. Experiment

p-n junction diode after fabrication are irradiation by X-ray various dose. The X-ray irradiation on p-n diode as shown in fig. 3.4.

King Mongkut's Institute of Technology Ladkrabang

This material is reserved for educational use only, not allowed for commercial use.

Forbidden to modify the content, and cite the document when use.

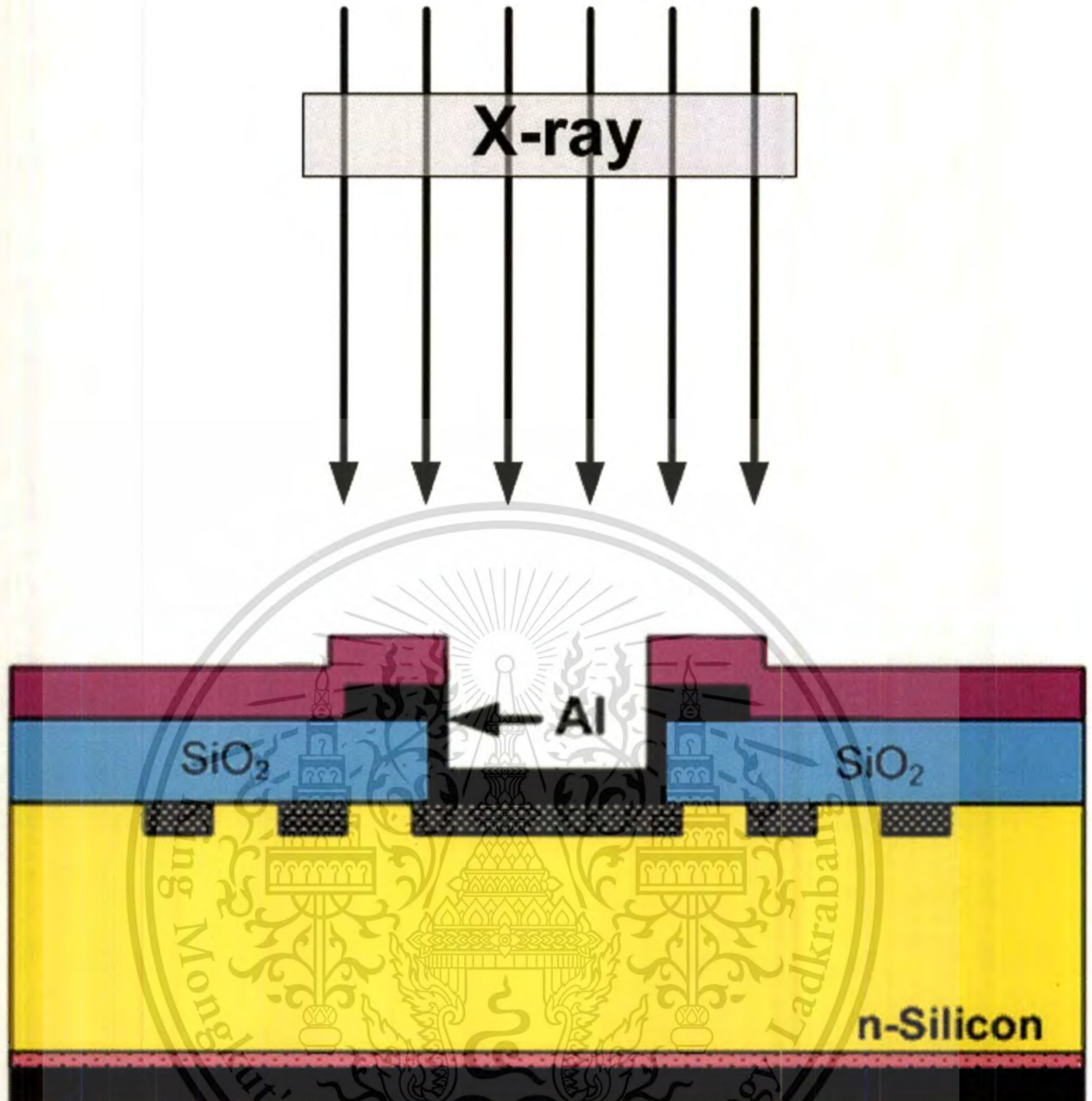

Fig. 3.4 X-ray irradiation on front side of p-n junction diode

The resulting values were compared for both before and after X-ray irradiation at room temperature with various dose. X-ray dose are use in the experiment shown in Table. 3.1.

The semiconductor parameter analyzer, model HP4156B, was used to measure the electrical properties of diode, before and after irradiation. The current-voltage (I-V) characteristics of the p-n diode were measured at room temperature to examine the change

This material is reserved for educational use only, not allowed for commercial use.
Forbidden to modify the content, and cite the document when use.

of the dark current (I_D) by X-ray irradiation. The current-voltage (I-V) characteristics were measured on wafer with biasing step of 25 mV for both reverse (V_R) and forward (V_F) voltages.

Table 3.1 Dose rate of X-ray radiation.

Condition	X-ray energy (keV)	Time (s)	Electrical charge (mA·s)	X-ray quantity (Roentgen)
1	40	5	0.2	7.11×10^4
2	40	55	0.2	7.82×10^5
3	40	205	0.2	2.92×10^6
4	55	5	0.7	4.71×10^5
5	55	55	0.7	5.18×10^6
6	55	205	0.7	1.93×10^7
7	70	5	4.5	4.90×10^6
8	70	55	4.5	5.39×10^7
9	70	205	4.5	2.01×10^8

King Mongkut's Institute of Technology Ladkrabang

This material is reserved for educational use only, not allowed for commercial use.
Forbidden to modify the content, and cite the document when use.

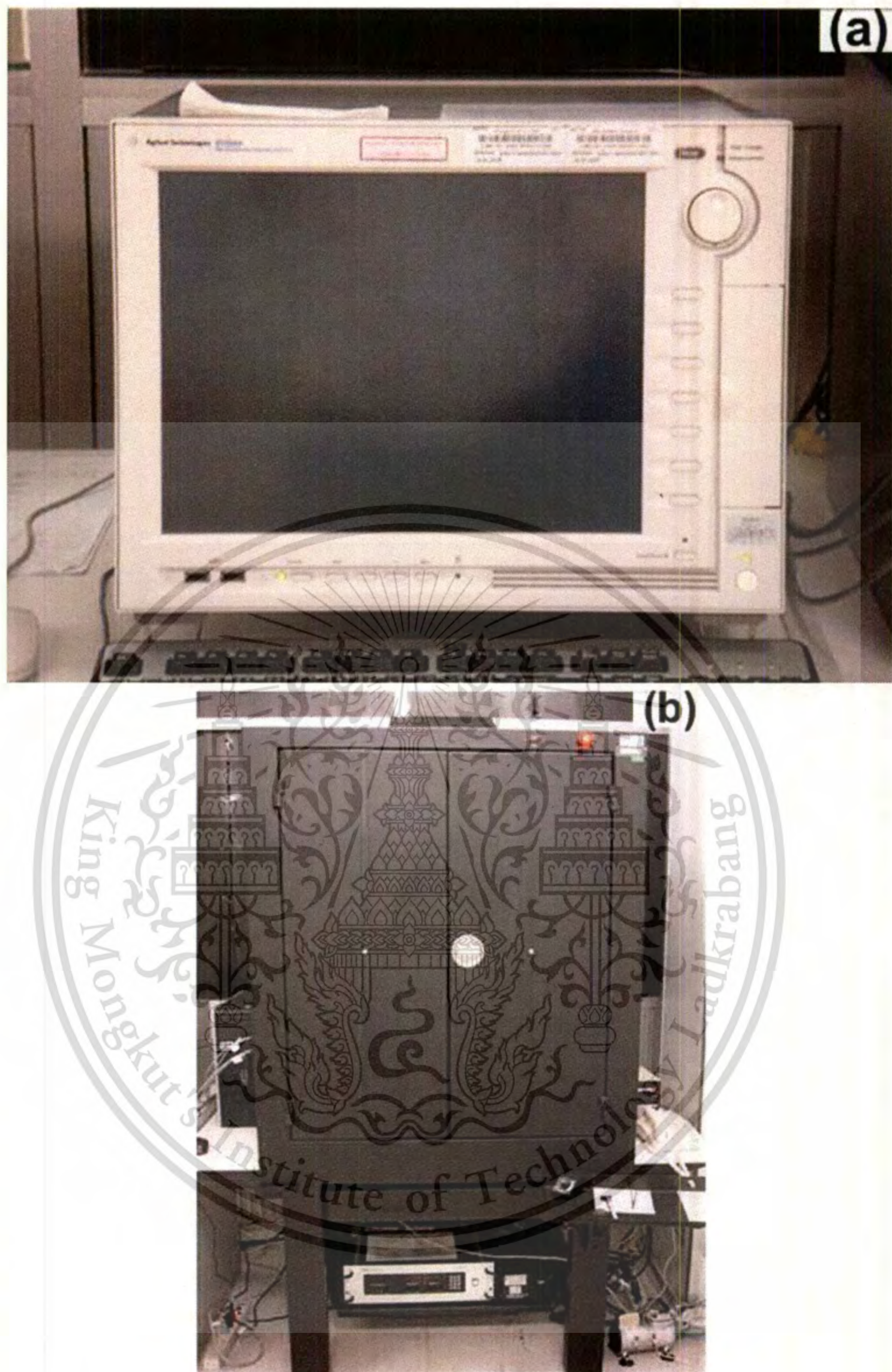

Fig. 3.5 IV probe station HP4156B (a) monitor and control center, (b) the cascada microtech model M150, (c,d) probe station and chunk and (e) probe control

This material is reserved for educational use only, not allowed for commercial use.
Forbidden to modify the content, and cite the document when use.

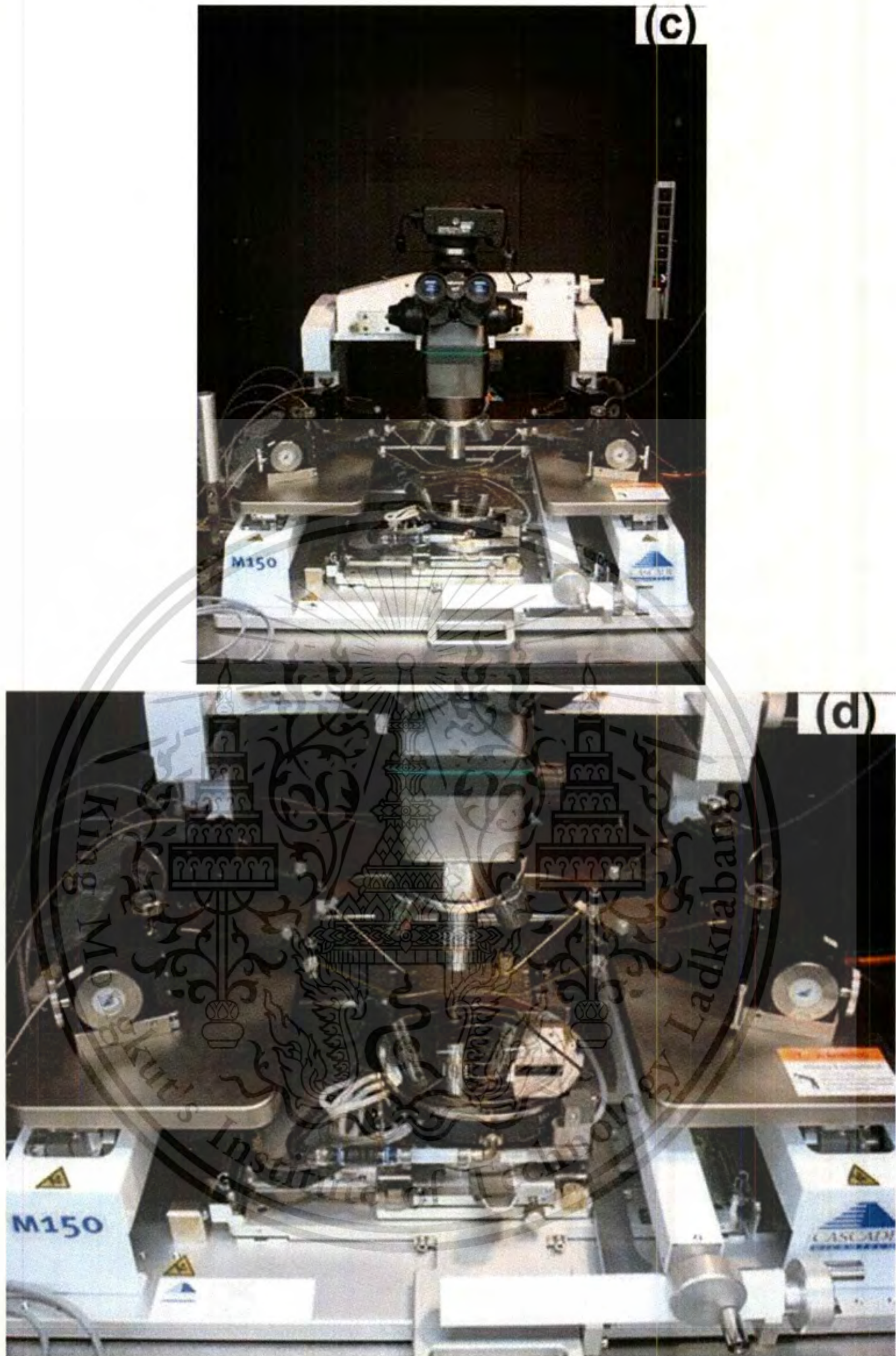

Fig. 3.5 IV probe station HP4156B (a) monitor and control center, (b) the cascada microtech model M150, (c,d) probe station and chunk and (e) probe control. (Cont.)

This material is reserved for educational use only, not allowed for commercial use.
Forbidden to modify the content, and cite the document when use.

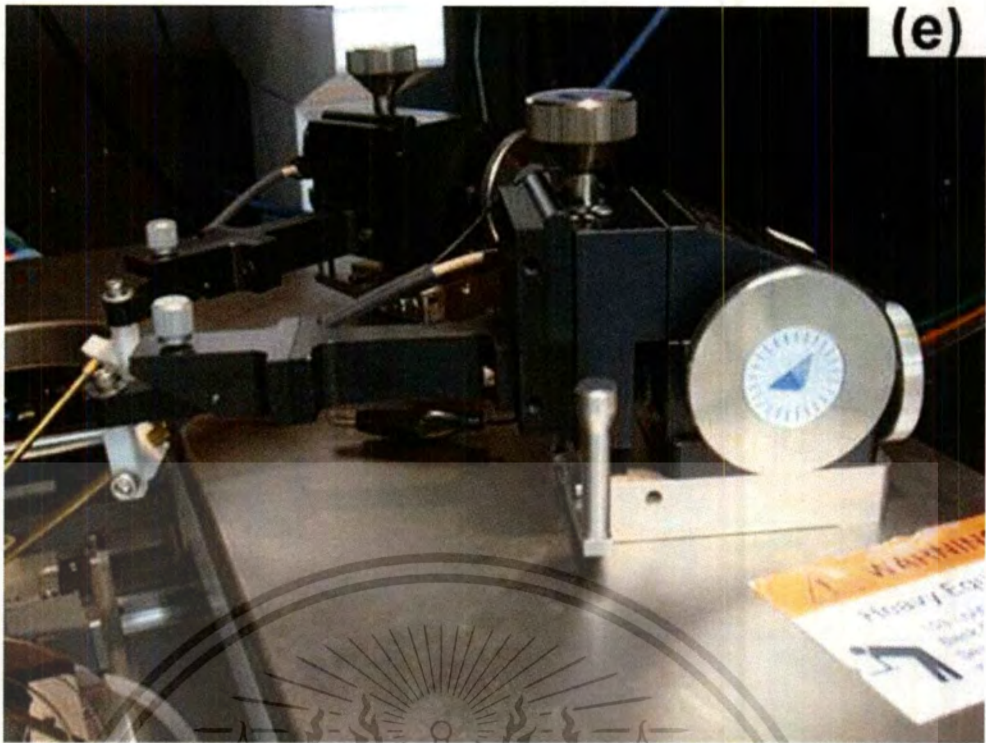

Fig. 3.5 I-V probe station HP4156B (a) monitor and control center, (b) the cascada microtech model M150, (c,d) probe station and chunk and (e) probe control. (Cont.)

The C-arm Siemens Siremobil compact 650 135 X-ray machine is the low dose X-ray shown in fig. 3.6.

King Mongkut's Institute of Technology Ladkrabang

This material is reserved for educational use only, not allowed for commercial use.

Forbidden to modify the content, and cite the document when use.

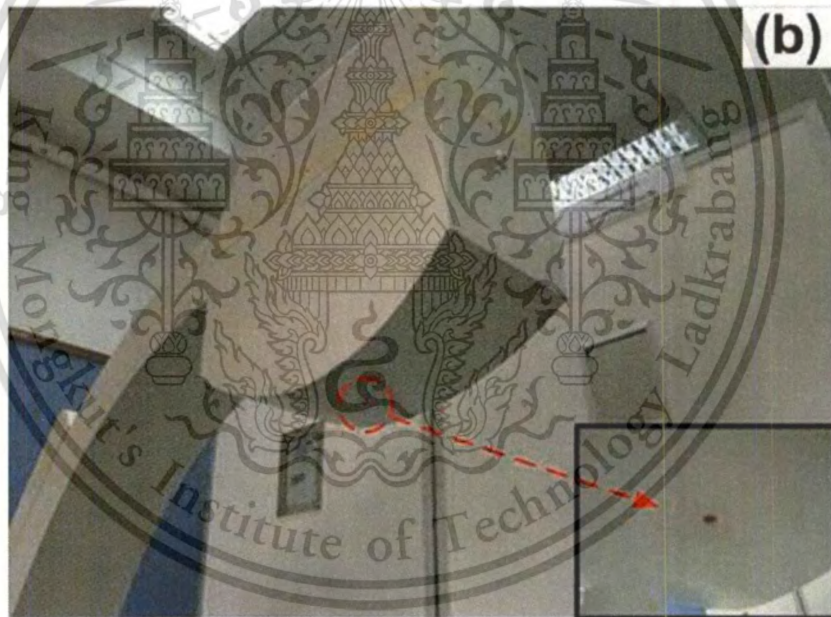

Fig. 3.6 X-ray machine C-arm Siemens Siremobil compact 650 135 (a) C-arm, (b) X-ray point, (c,d) controller and (e) X-ray test device

This material is reserved for educational use only, not allowed for commercial use.
Forbidden to modify the content, and cite the document when use.

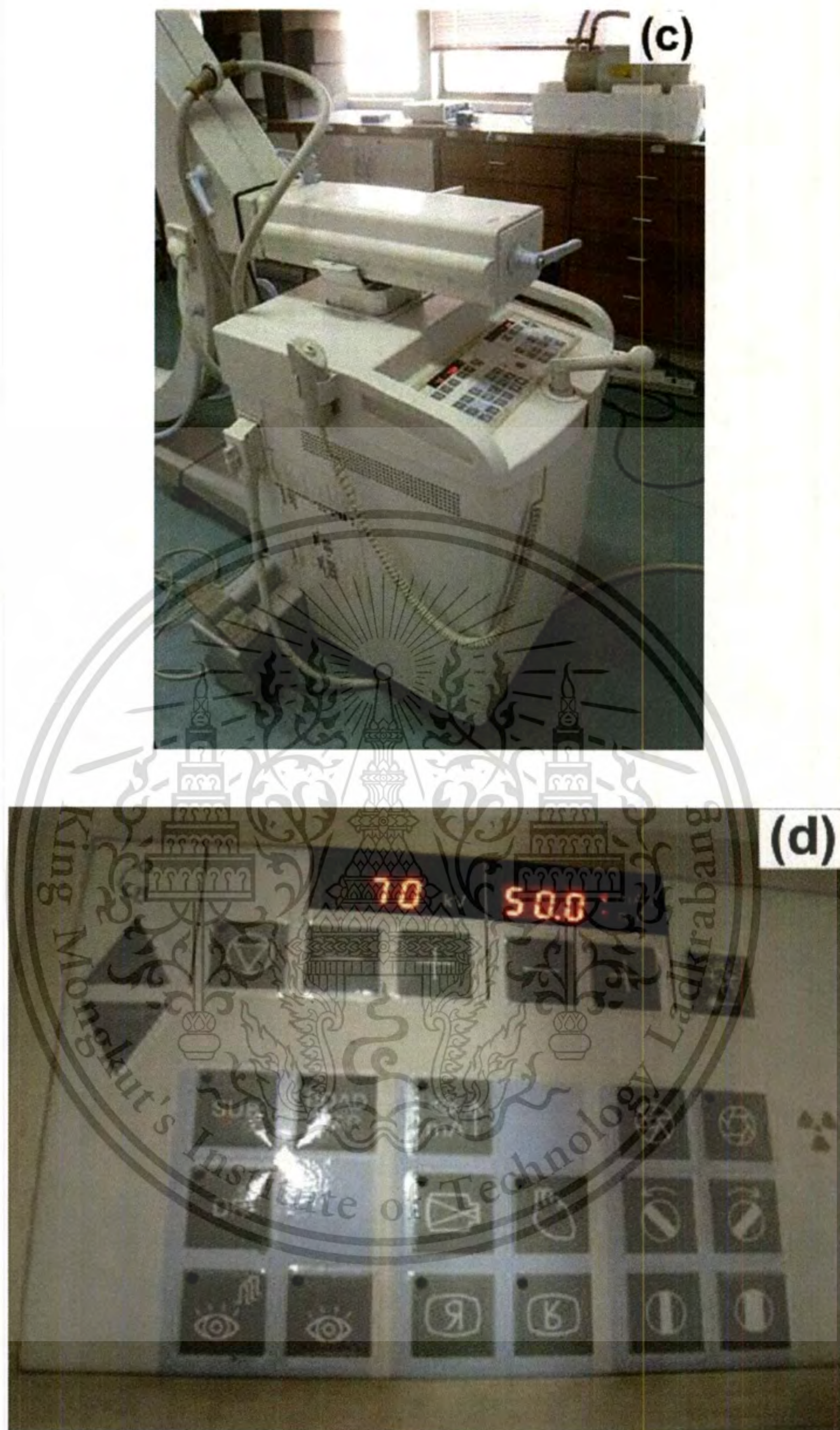

Fig. 3.6 X-ray machine C-arm Siemens Siremobil compact 650 135 (a) C-arm, (b) X-ray point, (c,d) controller and (e) X-ray test device. (Cont.)

King Mongkut's Institute of Technology Ladkrabang

This material is reserved for educational use only, not allowed for commercial use.

Forbidden to modify the content, and cite the document when use.

Fig. 3.6 X-ray machine C-arm Siemens Siremobil compact 650 135 (a) C-arm, (b) X-ray point, (c,d) controller and (e) X-ray test device. (Cont.)

High dose X-ray machine at Chulalongkorn University were irradiated on p-n diode shown in fig. 3.7. This machine can irradiate X-ray energy about 160 keV and limited time to expose per round around 1-2 minute.

Fig. 3.7 X-ray irradiation machine at Chulalongkorn University (a,b) head of X-ray irradiation, (c) X-ray head spec, and (d) controller

This material is reserved for educational use only, not allowed for commercial use.
Forbidden to modify the content, and cite the document when use.

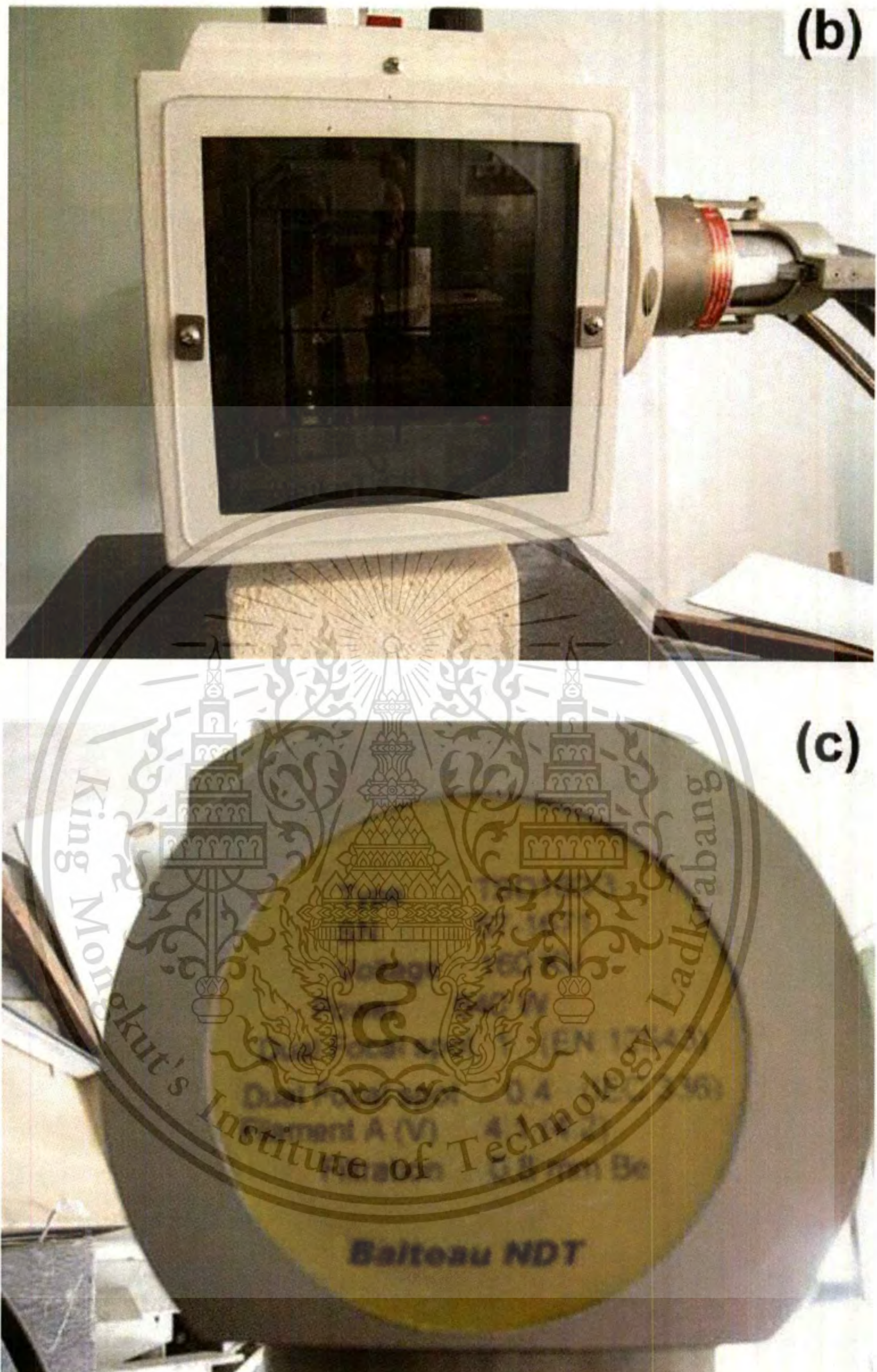

Fig. 3.7 X-ray irradiation machine at Chulalongkorn University (a,b) head of X-ray irradiation, (c) X-ray head spec, and (d) controller. (Cont.)

King Mongkut's Institute of Technology Ladkrabang

This material is reserved for educational use only, not allowed for commercial use.
Forbidden to modify the content, and cite the document when use.

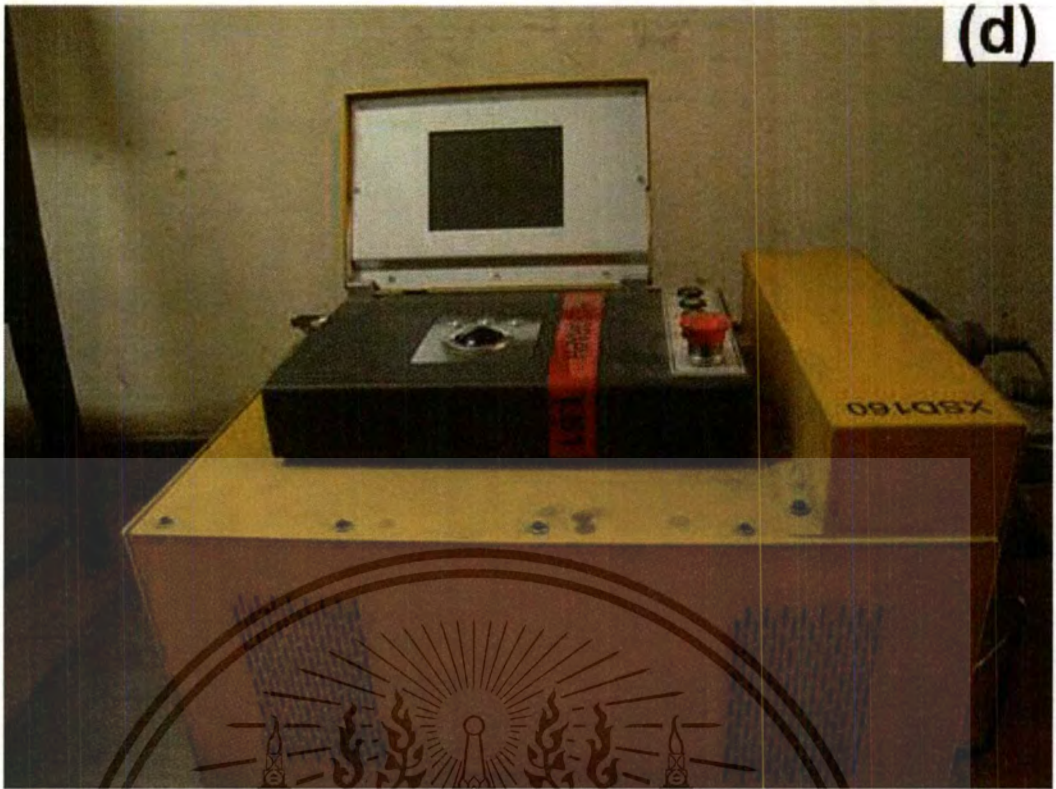

Fig. 3.7 X-ray irradiation machine at Chulalongkorn University (a,b) head of X-ray irradiation, (c) X-ray head spec, and (d) controller. (Cont.)

King Mongkut's Institute of Technology Ladkrabang

This material is reserved for educational use only, not allowed for commercial use.

Forbidden to modify the content, and cite the document when use.

Chapter 4
Results and Discussion

4.1 Study of Electrical properties of p-n diode

The electrical properties of p-n junction diode were studied and analysis in this thesis. The diode parameters were determined from the I-V characteristics and C–V characteristics, which are usually, described using the thermionic emission theory. The ideal diode equation or sometimes called the Shockley diode equation is explaining by equation (4.1). [10] –[12]

$$I = I_0 (e^{qV/\eta kT} - 1) \quad (4.1)$$

Where I_0 is the saturation current, V is the bias voltage, k is the Boltzmann's constant, q is the electronic charge constant and T is the absolute temperature.

Where the saturation current (I_0) equals the diffusion current (I_d).

$$I_0 = I_d = qn_i^2 B[(D_n/L_nN_A)+(D_p/L_pN_D)] \quad (4.2)$$

Where η is the ideality factor of p-n diode, B is the active area and n_i is the intrinsic carrier density. For values of V greater than nkT/q, D_n and D_p are the diffusion coefficient of electrons in the p-side and holes in the n-side, L_n and L_p are the electron and hole diffusion length, the ideality factor from Eq. (4.2) can be written as described by Eq. (4.3).

$$\eta = [q/kT][dV/d\ln I] \quad (4.3)$$

This material is reserved for educational use only, not allowed for commercial use.
Forbidden to modify the content, and cite the document when use.

Also the voltage dependent ideality factor $\eta(V)$ can be written using Eq. (4.3) as

$$\eta(V) = qV/[kTln(I/I_0)] \quad (4.4)$$

From Eq. (4.1), I_0 is the saturation current. The saturation current under the reverse bias is the combination of the diffusion current (I_d), as presented in Eq. (4.4).

The forward and reverse bias I-V characteristic of the P-N diode before and after irradiated by the various X-ray energy and times, which can be explained by Eq. (4.5).

$$I = I_0\{exp[(q/kT)(V-IR_s)]-1\} \quad (4.5)$$

From Eq. (4.5) the effect of the series resistance is usually modeled with series combination of a diode and a resistor R_s. The voltage V_D across the diode can be expressed in terms of the total voltage drop V across the diode and the resistance R_s. Thus, $V_D = V - IR_s$ and the Eq. (4.1) can be expressed as:

$$I = I_0\{exp[q(V-IR_s)/\eta kT]\} \quad (4.6)$$

Where R_s is the series resistance, and the IR_s term is the voltage drop across series resistance of device.

Several methods to extract the series resistance R_s of Schottky diode have been suggested. In our case, we have applied the methods developed by Cheung and Cheung and Lien et al [22].

The Cheung's method is achieved by using the functions:

This material is reserved for educational use only, not allowed for commercial use.
Forbidden to modify the content, and cite the document when use.

$$dV/d(\ln I) = IR_s + \eta kT/q \qquad (4.7)$$

Eq. (4.7) should give a straight line for the data of the downward curvature region of the forward bias I-V characteristics. Thus, the slope and y-axis intercept of a plot of dV/d(ln(*I*)) versus I will give R_s and $\eta kT/q$, respectively.

4.2 Capacitance-voltage characteristics (C–V) of p-n junction diode

In case of reverse bias, the saturation current is presenting in Eq. (4.8), which is the combination of the diffusion current (I_d) and the generation current, which generate in the depletion region.

$$I_0 = I_d + Bqn_iW/\tau_g \qquad (4.8)$$

Where B is the area of p-n junction, n_i is the intrinsic carrier concentration, W is the width of depletion region and τ_g is carrier generation lifetime.

According to our experiment results, the leakage current versus depletion width plot (fig. 4.1) shows increment of the leakage current at higher reverse bias (larger depletion width higher reversed bias voltage), which can be surely explained by Eq. (4.8). Assuming, the diffusion current is biasing independent, the increment of leakage current at higher reverse bias is mostly the result of generation current. This current depends on the width of depletion region, which can be calculated using Eq (4.9).

King Mongkut's Institute of Technology Ladkrabang

This material is reserved for educational use only, not allowed for commercial use.

Forbidden to modify the content, and cite the document when use.

$$W = B\mathcal{E}_{Si}/C \tag{4.9}$$

Where $\mathcal{E}_{Si}$ is the dielectric permittivity of silicon, C is the capacitance, which can be obtained from the capacitance-voltage (C-V) characteristics as shown in Fig. 4.2.

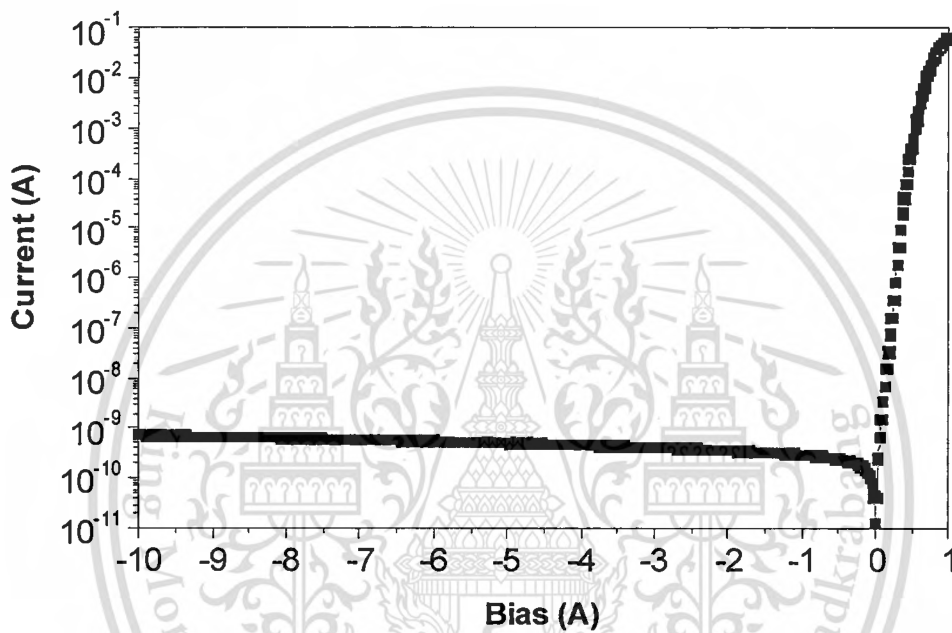

Fig. 4.1 Leakage current versus bias voltage of the p-n junction diode

This material is reserved for educational use only, not allowed for commercial use.
Forbidden to modify the content, and cite the document when use.

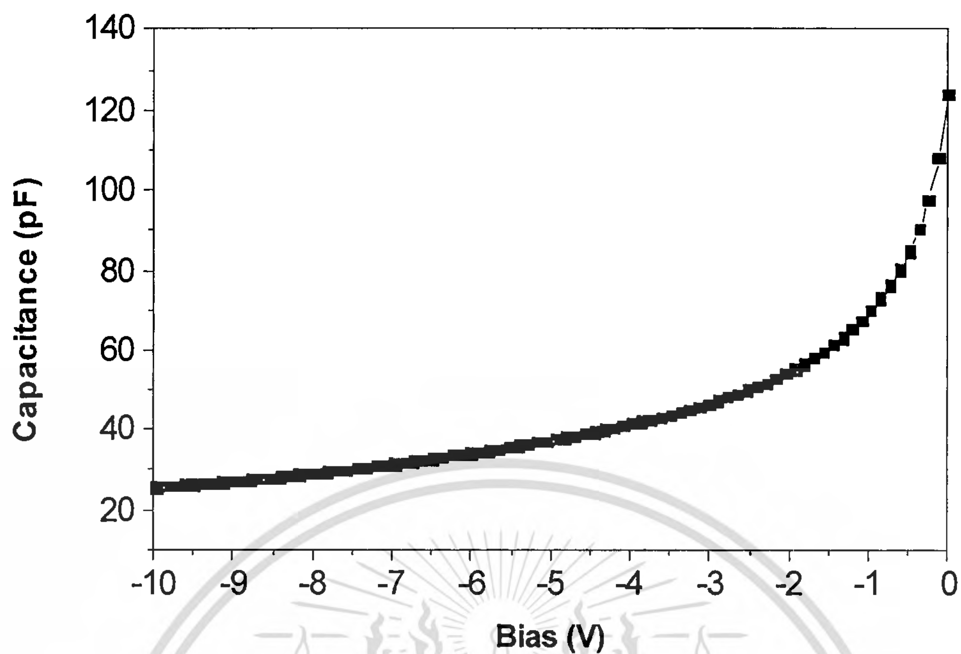

Fig. 4.2 Capacitance-voltage (C-V) characteristics of p-n junction diode

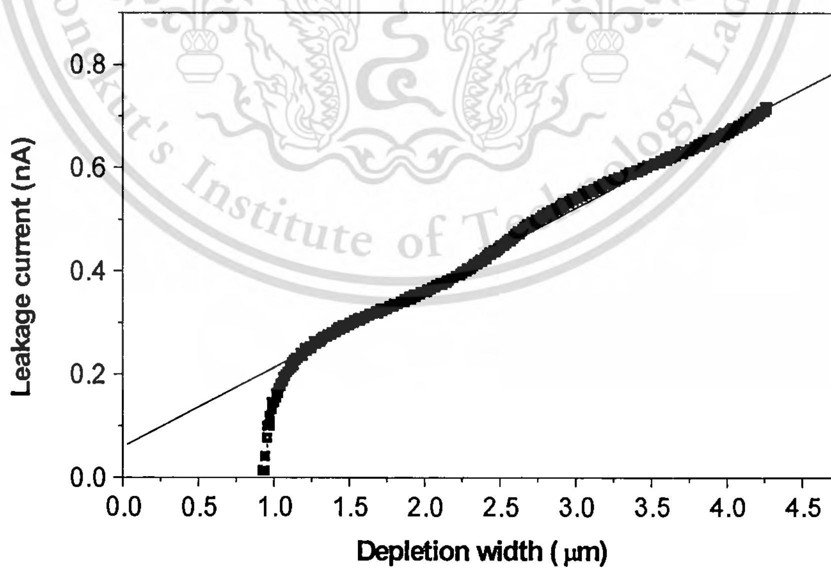

Fig. 4.3 Leakage current versus depletion width of the p-n junction diode

This material is reserved for educational use only, not allowed for commercial use.
Forbidden to modify the content, and cite the document when use.

The diffusion current can be calculated from the relation of leakage current and depletion width as in fig. 4.3. In this case, the diffusion current is 0.08 nA at zero depletion width.

4.3 Current-voltage characteristics (I-V) study of p-n junction diode before and after X-ray irradiated

Then we measured the I–V and C–V characteristics of p—n junctions before and after X-ray irradiated under various conditions. Table 4.1 lists the X-ray irradiation conditions.

Table 4.1 X-ray radiation conditions

Condition	X-ray energy (keV)	Time (s)	Electrical charge (mA·s)	X-ray quantity (Roentgen)
1	40	5	0.2	7.11×10^{4}
2	40	55	0.2	7.82×10^{5}
3	40	205	0.2	2.92×10^{6}
4	55	5	0.7	4.71×10^{5}
5	55	55	0.7	5.18×10^{6}
6	55	205	0.7	1.93×10^{7}
7	70	5	4.5	4.90×10^{6}
8	70	55	4.5	5.39×10^{7}
9	70	205	4.5	2.01×10^{8}

This material is reserved for educational use only, not allowed for commercial use.
Forbidden to modify the content, and cite the document when use.

4.3.1 Forward bias study of p-n junction diode after X-ray irradiation

The forward biased Current–Voltage (I–V) characteristics of diodes can serve as the basis for the extraction of physical parameters such as ideality factor (η), series resistances (R_S), and reverse saturation current (I_0), which determines the zero bias barrier height (Φ_B) provided that the Richardson constant is known. Two stages of graphical parameter extraction from the experimental I–V characteristics are required in this technique. The first is used to determine the ideality factor and series resistance and the second to get the saturation current. [18],[19] Alternatively, [20]-[24] the ideality factor and saturation current are found first followed by a determination of the series resistance. However, there is no perfect solution including this technique. In this technique, a determination of the existence and establishment of the nature and magnitude of a leakage conductance requires an analysis of the reverse biased current–voltage characteristic which complicates the measurement. [18] No published method accommodates a nonlinear series resistance. All published parameter extraction techniques use many step-like graphical solutions and do not lend themselves to automation of the measurement processes, which is crucial for the selection of defective diodes in a mass production environment. [25]

The general relationship between current and voltage for a p–n junction diode is given by Eq. (4.10) [10] – [13] , [26] – [30]

$$I(V,T) = I_0(T)\{\exp[X(T)V] - 1\} \tag{4.10}$$

where I_0 is the saturation current, V is the bias voltage, and X is a coefficient. I_0 and X are generally dependent on temperature T. For small forward-bias voltages, the exponential term in the equation is very large; hence, the subtracted “1” is negligible and the forward-diode current is often approximated as in Eq. (4.11):

This material is reserved for educational use only, not allowed for commercial use.
Forbidden to modify the content, and cite the document when use.

$$I(V,T) = I_0(T)\{exp[X(T)V]\} \quad (4.11)$$

The I-V plot of p-n junction diode under forward bias condition is presenting in fig. 4.4. It is very interesting that the x-ray irradiated samples provide higher forward current with approximately three orders of magnitude compared with non-radiated samples at 1.0 volt of forward bias.

Table 4.2 Basic conduction processes

Conduction mechanism	I	A	N
Diffusion	$I \propto \exp(-E_g/kT)$	$A = q/kT$	$\eta = 1$
Recombination	$I \propto \exp(-E_g/2kT)$	$A = q/\eta kT$	$\eta \leq 2$
Tunneling	$I \propto \exp(-E_T/kT)$	$A = const$	$\eta = const$
Thermionic	$I \propto [\exp(-\Phi_B/kT)]\, kT^{3/2}$	$A = q/kT$	$\eta = 1$

E_g is the energy gap, k is the Boltzmann constant, T is the absolute temperature, η is the ideality factor, E_T is the activation energy, and Φ_B is the barrier energy.

This material is reserved for educational use only, not allowed for commercial use.
Forbidden to modify the content, and cite the document when use.

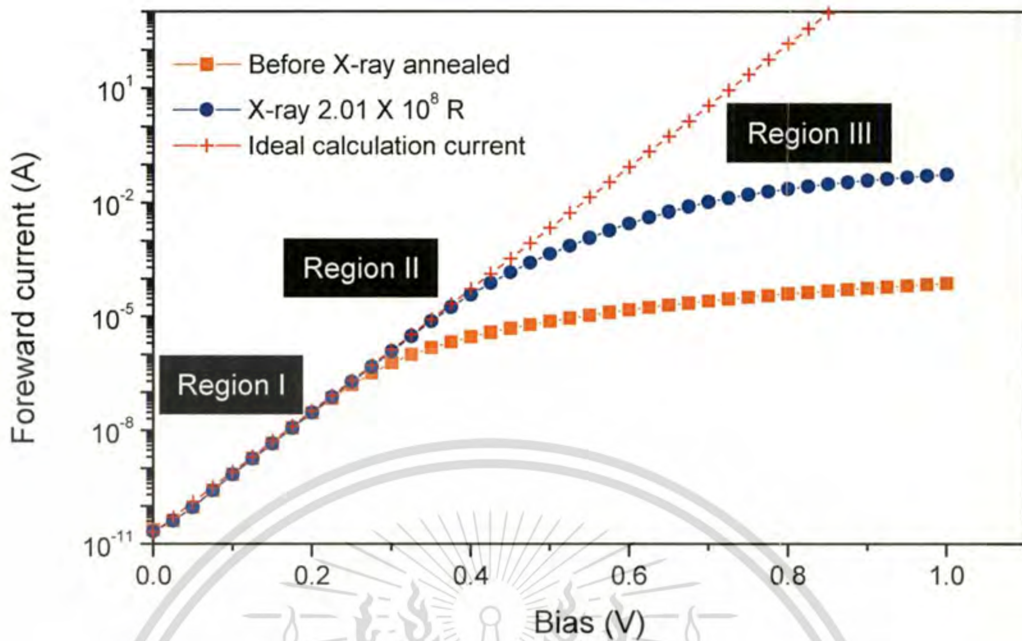

Fig. 4.4 Plots of forward I–V characteristics for a p–n junction diode before and after X-ray irradiation, measured at 303 K

Fig. 4.4 shows I–V plots for a p–n junction diode under forward bias before and after X-ray irradiation. Interestingly, at V = 1.0 V, I is approximately two orders of magnitude higher after X-ray irradiated than before. The plots suggest the existence of three different mechanisms of current transport: (1) In Region I (<0.1 V), I increases linearly with V that is, I ∝ V suggesting that current transport is dominated by tunneling. (2) In Region II (0.1–0.5 V), I increases exponentially with V according to the relationship I ∝ {exp[X(T)V]}; the ideality factor n is determined in this region, and the current transport is dominated by recombination. (3) In Region III (>0.5 V), I follows the power law I ∝ V_m, suggesting that current transport is space-charge-limited.[10] To simplify analysis, we thus divide the further discussion of forward bias into two sections: forward-bias voltages of <0.5 V and ≥0.5 V.

This material is reserved for educational use only, not allowed for commercial use.
Forbidden to modify the content, and cite the document when use.

4.3.1.1 Forward-bias voltages of <0.5 V

At small forward-bias voltages, the p–n junction ideality factor η can be calculated by Eq. (4.12) as follows:[27]

$$ln[I(V,T)] = ln[I_0(T)] + X(T)V \tag{4.12}$$

For $X(T) = q/\eta kT$, this gives

$$ln[I(V,T)] = ln[I_0(T)] + (q/\eta kT)V \tag{4.13}$$

where q is the electronic charge constant, η is the ideality factor and k is the Boltzmann's constant

At forward biases in the range 0.1–0.3 V, I_0 and n can be calculated from Eq. (4.13) and the plot of forward I–V characteristics in fig 4.4.

This material is reserved for educational use only, not allowed for commercial use.
Forbidden to modify the content, and cite the document when use.

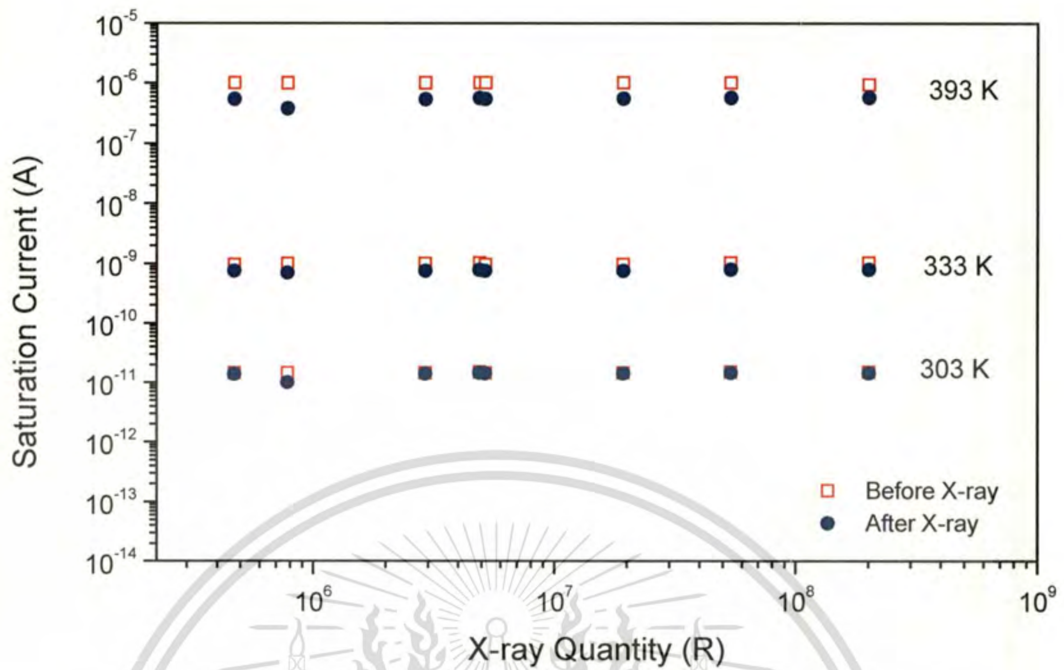

Fig. 4.5 Plots of saturation current vs X-ray quantity for a p–n junction diodes before and after X-ray irradiation under various conditions, measured at different temperatures

Fig. 4.5 shows plots of I_0 for p–n junction diodes before and after X-ray irradiation measured at different temperatures. When measured at room temperature (303 K), I_0 is essentially the same before and after X-ray irradiation; however, when measured at higher temperatures, I_0 is higher before X-ray irradiation than after.

This material is reserved for educational use only, not allowed for commercial use.
Forbidden to modify the content, and cite the document when use.

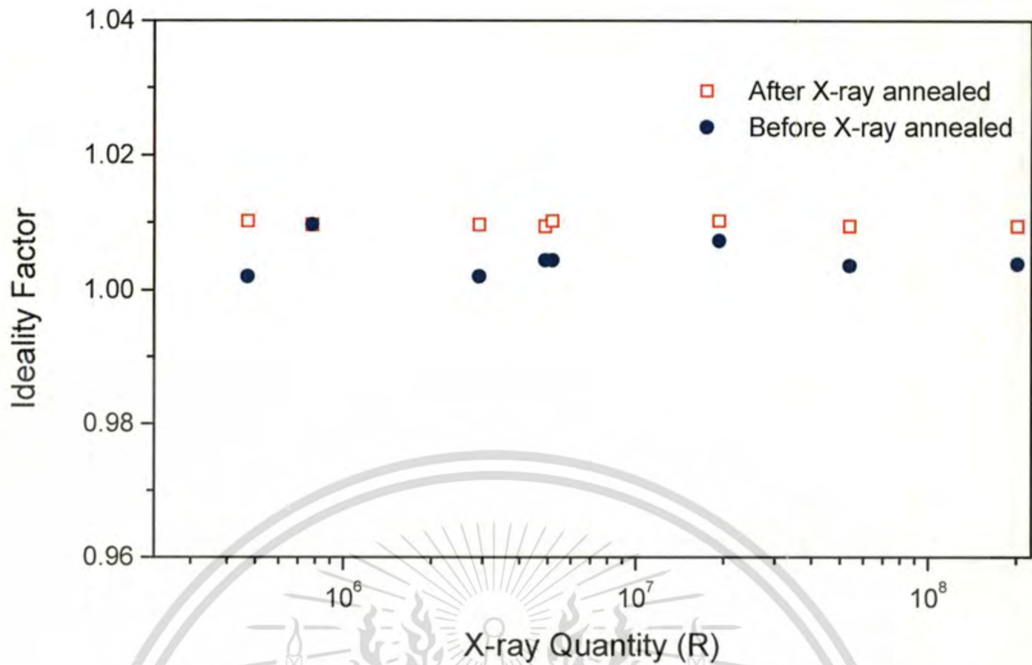

Fig. 4.6 Plots of ideality factor vs X-ray quantity for a p–n junction diode before and after X-ray irradiation, measured at 303 K

Fig. 4.6 shows plots of n for a p–n junction diode before and after X-ray irradiation. The value of n is essentially the same, close to 1, before and after X-ray irradiation, suggesting that the mechanism of current transport is dominated by diffusion.

This material is reserved for educational use only, not allowed for commercial use.
Forbidden to modify the content, and cite the document when use.

4.3.1.2 Activation Energy (E_T) study of p-n junction diode after X-ray irradiation

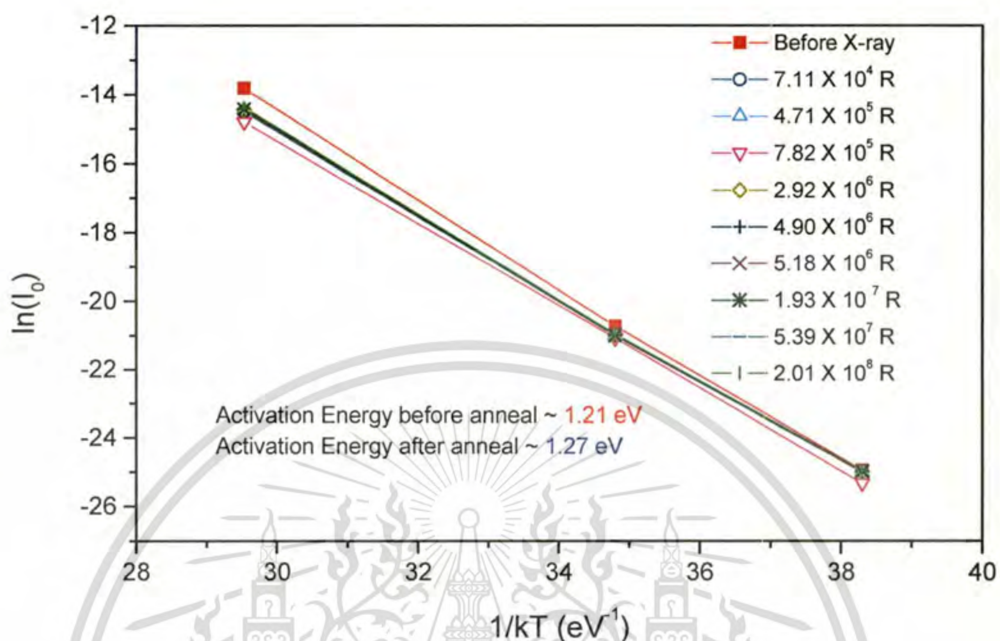

Fig. 4.7 Plots of $\ln(I_0)$ vs 1/kT for a p–n junction diodes before and after X-ray irradiation under various conditions, measured at 303 K

Fig. 4.7 shows plots of $\ln(I_0)$ as a function of 1/kT for p–n junction diodes before and after X-ray irradiation. The slope of an Arrhenius plot, I_0 vs 1/kT yields the activation energy E_T.[32] Activation energy E_T before X-ray irradiation is ~1.21 eV and after X-ray irradiation is ~1.27 eV, which supports the results shown in Fig. 4.5. E_T for a diode is the minimum energy required to trigger temperature-accelerated failure. The measured E_T values thus indicate a tendency for failure to be accelerated by temperature; that is, a lower E_T value favors triggering of failure with temperature. Therefore, the higher E_T value of the X-ray irradiated diodes, compared with the non-X-ray irradiated diodes, means that their electrical properties are less sensitive to changes in temperature. Furthermore, the measured E_T values are close to the energy gap of crystalline silicon, ~1.12 eV. Thus, our results confirm

This material is reserved for educational use only, not allowed for commercial use.
Forbidden to modify the content, and cite the document when use.

that the mechanism of current transport is dominated by diffusion under both X-ray irradiated and non-X-ray irradiated conditions,[30] which also corresponds to the results for the ideality factor in fig. 4.6.

4.3.1.3 Forward-bias voltages of ≥0.5 V

At large forward-bias voltages, I–V characteristics deviate from exponential dependence because of voltage drops across the bulk of the diode. However, as voltage increases even further, resistance eventually decreases and current increases superlinearly.

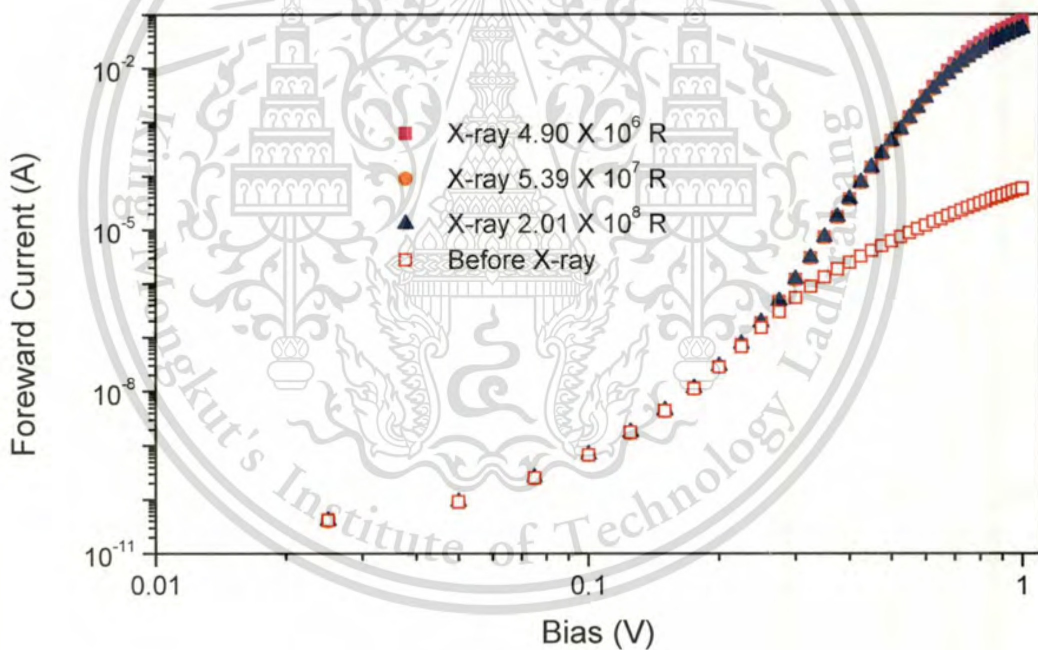

Fig. 4.8 Plots of forward I vs V (log–log scale) for a p—n junction diodes before and after X-ray irradiation under various conditions, measured at 303 K

This material is reserved for educational use only, not allowed for commercial use.
Forbidden to modify the content, and cite the document when use.

Fig. 4.8 shows plots of I–V characteristics for p–n junction diodes before and after X-ray irradiation. On the log–log scale of the plots, I depends linearly on V. This superlinear or power-law dependence is characteristic of space-charge-limited currents.[30]

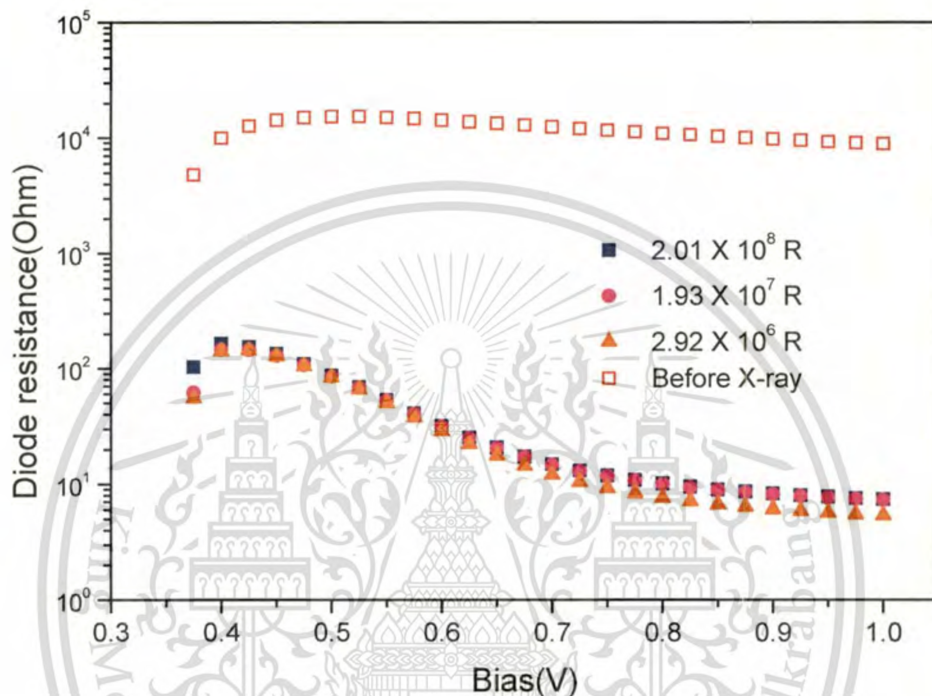

Fig. 4.9 Plots of series resistance vs bias voltage for p-n junction diodes before and after X-ray irradiation under various conditions, measured at 303 K

4.3.1.4 Series Resistance study of p-n junction diode after X-ray irradiation

Fig. 4.9 shows plots of series resistance (R_S) before and after X-ray irradiation. Below the turn-on voltage, R_S decreases with increasing forward bias, and above the turn-on voltage, it remains constant. Under forward bias, at p-n junction, the conduction-band barrier decreases, enhancing electron flow from the n-type to the p-type region and hole

This material is reserved for educational use only, not allowed for commercial use.
Forbidden to modify the content, and cite the document when use.

flow from the p-type to the n-type region. Successive recombination gives rise to the forward-bias current flow. As forward-bias voltage increases, R_S decreases until the conduction-band barrier becomes negligible, beyond which it remains constant.[31] The decrease in the value of resistance after X-ray irradiated indicates that the product of the mobility and/or the free carrier concentration has increased, which may be because of crystallinity improvement due to the vacancies, migration and vacancy–interstitial recombination.[33]

The R_S is the sum of total resistance value of the resistors in series and the resistance in the semiconductor device in the direction of current flow or bulk and contact resistance.[34]-[36] To investigate the origin of the change in R_S with soft X-ray irradiation, under forward bias, we evaluated the substrate resistance, aluminum layer resistance and Schottly Barrier Height (SBH) before and after soft X-ray irradiation. The effect of soft X-ray irradiation to p-n junction will be evaluated under reverse bias condition in the next section.

King Mongkut's Institute of Technology Ladkrabang

This material is reserved for educational use only, not allowed for commercial use.
Forbidden to modify the content, and cite the document when use.

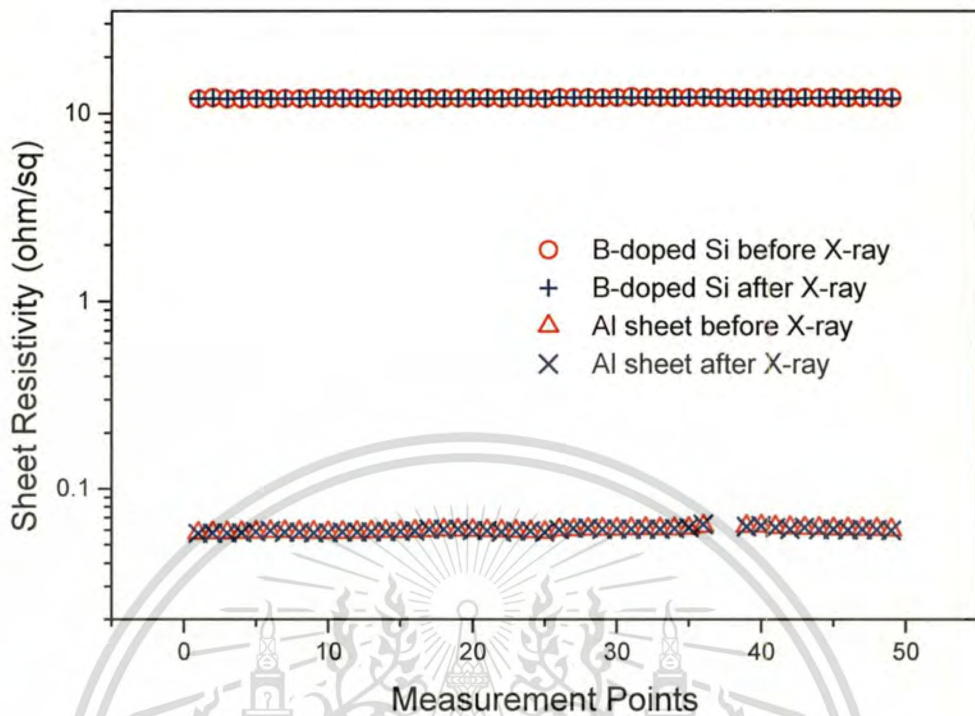

Fig. 4.10 Plots of sheet resistance of Boron doped Si and Aluminum layer before and after X-ray irradiation

The substrate and aluminum sheet resistance are not significantly different before and after X-ray irradiated, as measured by the four-probe method. Then we evaluated the SBH before and after soft X-ray irradiation.

4.3.1.5 SBH study of p-n junction diode after X-ray irradiation

At high forward-bias voltages, V>3kT, current transport in Schottky contact is due to majority carriers. It may be described by thermionic emission over the interface barrier. The experimental data are fitted by the conventional thermionic emission equation, which is given by Eq. (4.10) and I_0 is given by [34]-[39]

This material is reserved for educational use only, not allowed for commercial use.
Forbidden to modify the content, and cite the document when use.

$$I = I_0 \exp(qV/nkT)[1- \exp(-qV/\eta kT)] \tag{4.14}$$

For V>3kT, $I = I_0 \exp(qV/\eta kT)$

$$I_0 = AA^{*}T^2 \exp[(-q\Phi_{B0})/kT] \tag{4.15}$$

where A*,A and Φ_{B0} represent the Richardson constant, the contact area and zero-bias SBH, respectively.

From Eq. (4.15)

$$\Phi_{B0} = (kT/q) \ln(AA^{*}T^2/I_0) \tag{4.16}$$

$$\ln(I_0/T^2) = \ln(AA^{*})-(q\Phi_{B0}/kT) \tag{4.17}$$

Plot of $\ln(I_0/T^2)$ versus q/kT should give a straight line whose slope and intercept will give barrier height.

The nature of the potential barrier between the Fermi level in the metal and the conduction band edge of the semiconductor at the interface is the most important characteristics of the metal–semiconductor interface. Since electrical contacts to semiconductors require metal–semiconductor interfaces and depending upon this potential barrier height, interfaces exhibit a modest resistance to current flow in either direction or a high resistance in one direction and low resistance in the opposite direction.[36]

This material is reserved for educational use only, not allowed for commercial use.
Forbidden to modify the content, and cite the document when use.

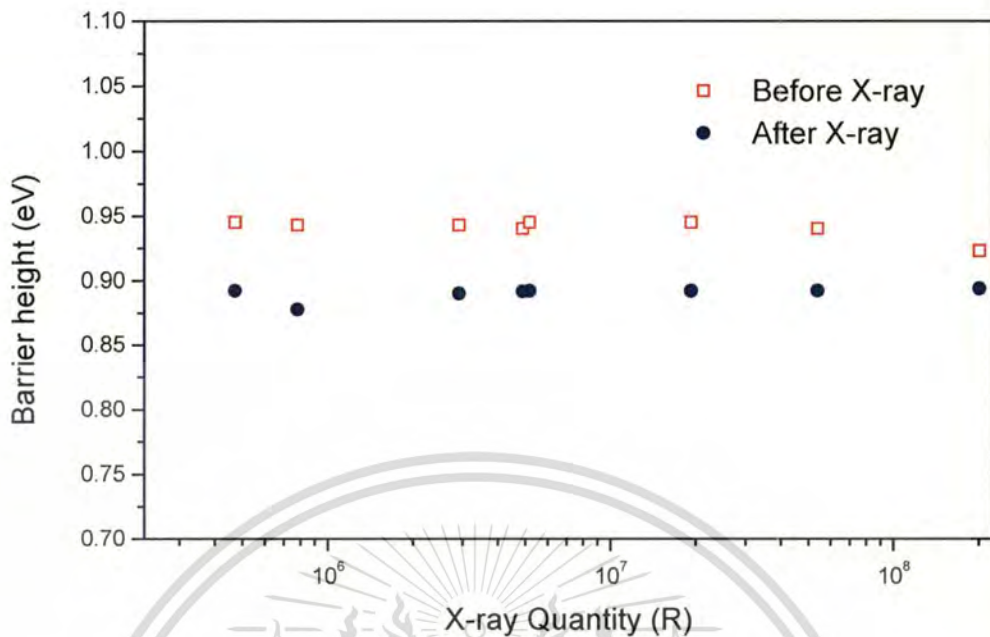

Fig. 4.11 Plots of SHB vs X-ray quantity before and after X-ray irradiation

Fig. 4.11 shows plots of SBH before and after X-ray irradiation. The SBH for prepared sample is about 0.94 eV. The SBH decreases after soft X-ray irradiation becomes 0.89 eV at X-ray quantity 7.11 X 10^4 R and remains insensitive up to the X-ray quantity up to 2.01 X 10^8 R. Thus, our results present that the soft X-ray irradiated device has lower potential barrier height of metal–semiconductor interfaces than non-irradiated sample.

To understand the observed modifications in the Schottky Barrier Diode (SD) properties it is necessary to analyze the possible implications of ion transport through the diode. One of the possibilities of this phenomenon is because of crystallinity improvement due to the vacancies, migration and vacancy–interstitial recombination. When X-ray passes through the contact metal-semiconductor interface, its ion losses energy via nuclear energy loss S_n resulting from elastic collisions of the ion with the target atoms causing their displacement from the regular lattice sites, and electronic energy loss S_e which induces ionization/excitation of electrons inside the solid. The variation of S_n and S_e are function of

This material is reserved for educational use only, not allowed for commercial use.

Forbidden to modify the content, and cite the document when use.

depth inside the sample. If S_e value is larger than S_n , it may cause partial annealing of point defects that produced by S_n. These annealing of point defects lead to a decrease in the interface state density at the MS interface.

So the cumulative effects of S_n and S_e also result in constancy of interface state density. So the cumulative effects of S_n and S_e result in constancy of interface state density. This constancy of interface states leads to resistance of diode parameters with respect to radiation dose. [33] This is also correspondent to the result present in fig. 4.11, the SBH remain no change after X-ray radiation.

4.3.2 Reverse bias

4.3.2.1 Leakage current (I_0) study of study of p-n junction diode after X-ray irradiation

Saturation current I_0 under reverse bias is a combination of diffusion current I_d and generation current I_g in the depletion region, as shown in Eq. (4.18):

$$I_0 = I_d + Bqn_iW/\tau_g, \quad (4.18)$$

where B is the p–n junction area, n_i is the intrinsic carrier concentration, τ_g is the carrier-generation lifetime, and W is the depletion-region width. The latter can be calculated from Eq. (4.19):

$$W = B\varepsilon_S/C, \quad (4.19)$$

where ε_{Si} is the dielectric permittivity of silicon and C is capacitance, which can be obtained from a plot of capacitance–voltage (C–V) characteristics.

This material is reserved for educational use only, not allowed for commercial use.
Forbidden to modify the content, and cite the document when use.

4.3.2.2 Carrier-generation lifetime (τ_g) study of study of p-n junction diode after X-ray irradiation

The equation for carrier-generation lifetime (Eq. (4.20), below) is exactly in the form of Eq. (4.18) reversed slope.

$$\tau_g = Bqn_iW/(I_0 - I_d) \tag{4.20}$$

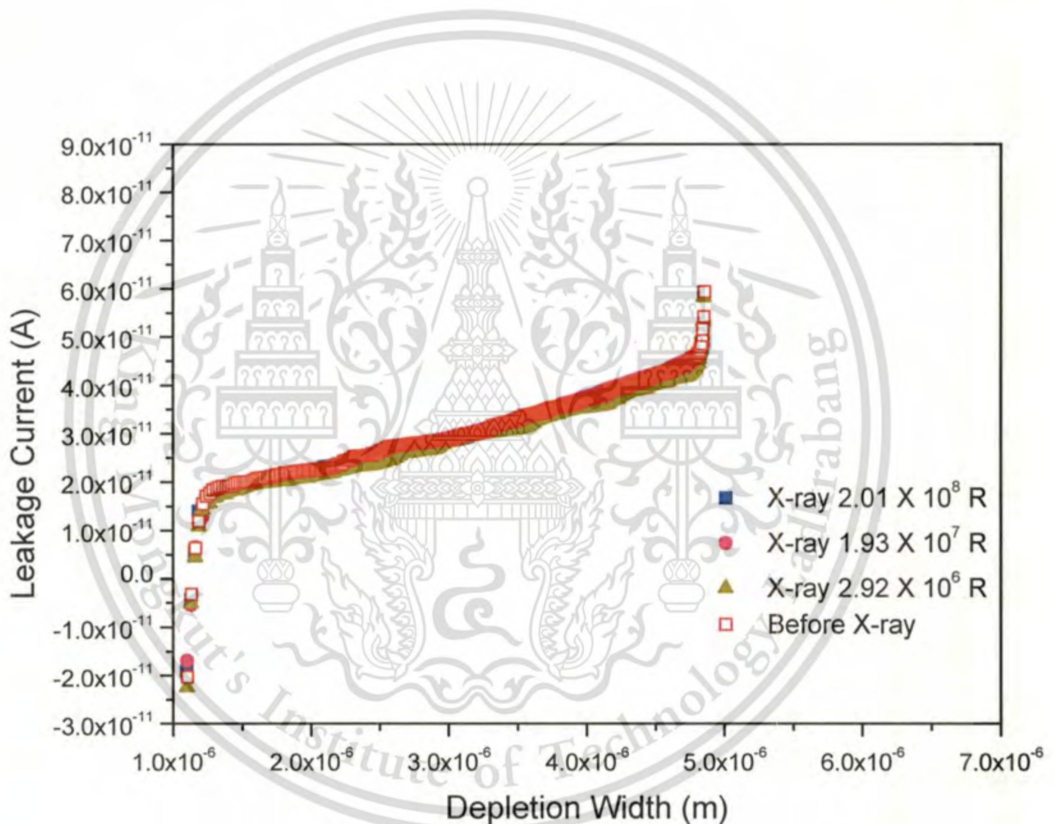

Fig. 4.12 Plots of leakage current vs depletion width for p—n junction diodes before and after X-ray irradiation under various conditions, measured at 303 K

Fig. 4.12 shows plots of leakage current as a function of depletion width for p–n junction diodes before and after X-ray irradiation. Under reverse-bias conditions, changes in depletion width have insignificant impact on diffusion current; thus, Eq. (4.15) shows that leakage current depend on carrier-generation lifetime, which may also be related to device

This material is reserved for educational use only, not allowed for commercial use.
Forbidden to modify the content, and cite the document when use.

defects. Diffusion current can be determined by extrapolation of the plots to zero depletion width, and then generation current can be calculated.

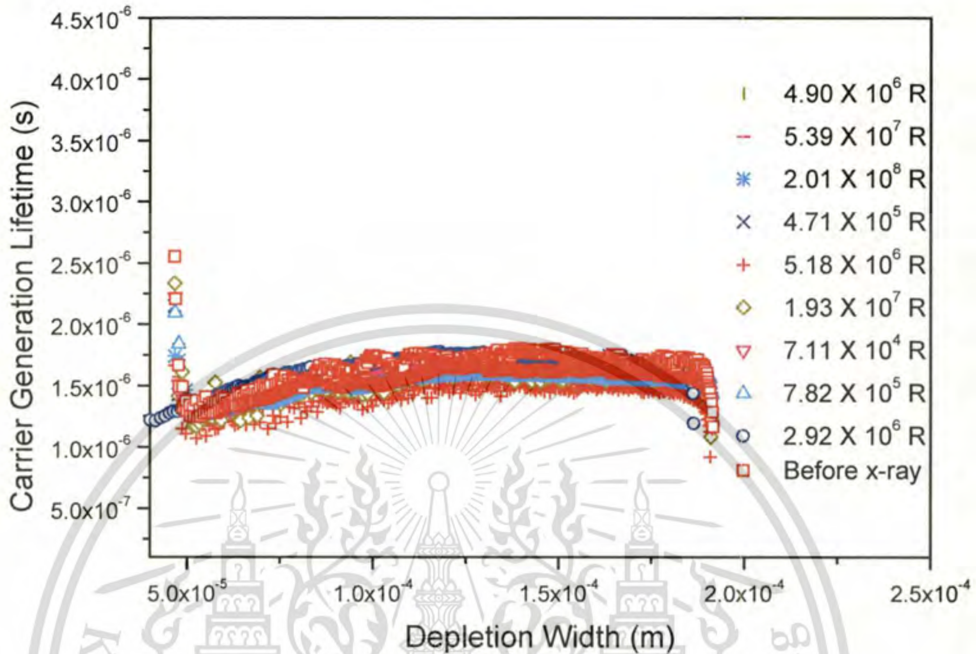

Fig. 4.13 Plots of carrier-generation lifetime vs depletion width for p—n junction diodes before and after X-ray irradiation under various conditions, measured at 303 K

Fig. 4.13 shows plots of carrier-generation lifetime as a function of depletion width for p–n junction diodes before and after X-ray irradiation. Carrier-generation lifetime is essentially the same before and after X-ray irradiation, suggesting that the irradiation process has insignificant impact to diode defects and p-n junction.

4.3.2.3 Reverse-bias activation Energy (E_T) study of p-n junction diode after X-ray irradiation

To confirm this speculation, we analyzed the activation energy of p–n junction diodes, which can be used to study the types of defects in a p—n junction. Accurate values of this activation energy can be obtained from the generation current.[40],[41] Generation current depends on temperature as follows:

This material is reserved for educational use only, not allowed for commercial use.
Forbidden to modify the content, and cite the document when use.

$$I_g = [(QWBT^{1.7} + \xi)/\tau_r] \exp(-E_T/kT) \tag{4.21}$$

where W is the depletion width, Q is a constant, ξ is a small number (<1) related to the temperature dependence of the depletion width, τ_r is the recombination lifetime, and E_T is the activation energy.[40]

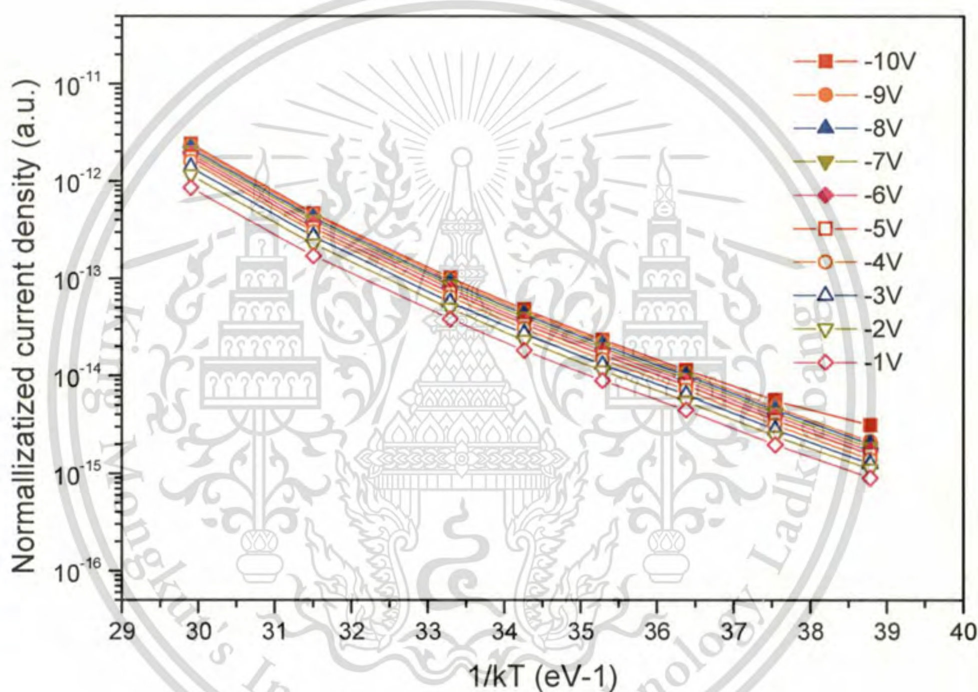

Fig. 4.14 Arrhenius plots of $I_g/T^{1.7}$ vs 1/kT for p–n junction diodes after X-ray irradiation (dose 2.01×10^8R under various reverse biases

Fig. 4.14 shows sample of Arrhenius plots of $I_g/T^{1.7}$ as a function of 1/kT for p–n junction diodes after X-ray irradiation with an X-ray quantity of 2.01×10^8 R under various reverse biases. The slope of a line yields E_T.

The activation energy at difference reverse bias and X-ray irradiation conditions are summarized in fig 4.15.

This material is reserved for educational use only, not allowed for commercial use.
Forbidden to modify the content, and cite the document when use.

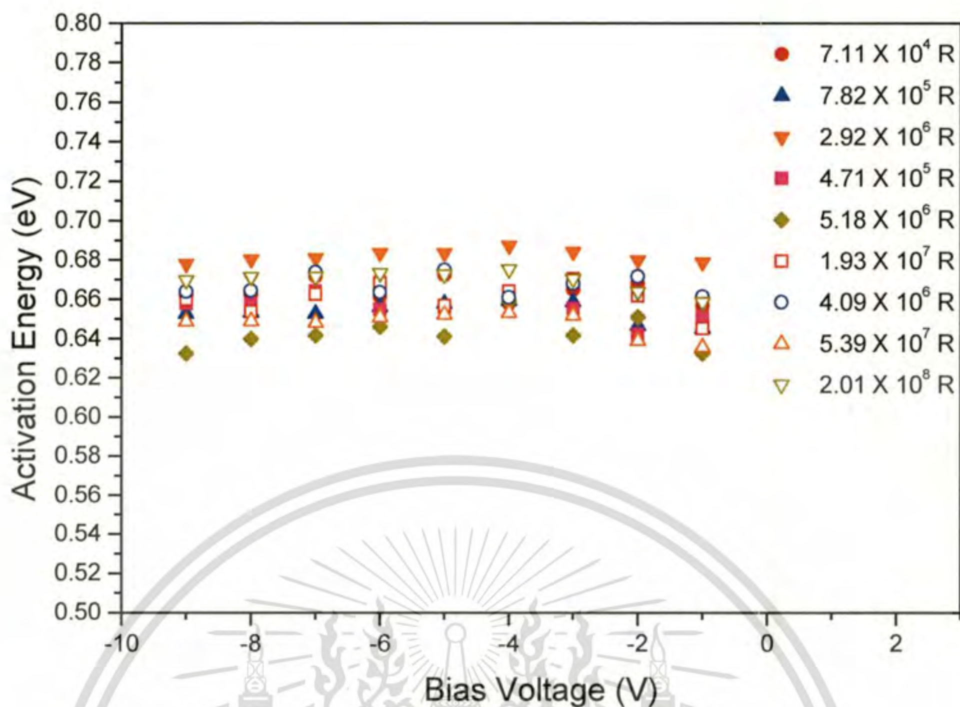

Fig. 4.15 Activation energy of p-n junction diode after X-ray irradiation under various conditions

The E_T for all samples is in the range 0.63–0.68 eV, which is close to the value of $E_g/2$ for crystalline silicon (E_g ~1.12eV), suggesting that soft X-ray irradiation has insignificant impact to E_T and the recombination process in the silicon is likely the dominant mechanism of current transport.

Our analysis of the effects of reverse-bias conditions suggests that soft X-ray irradiation has insignificant impact to p-n junction and diode defects. However, soft X-ray irradiation effect significant improvements in the forward-diode current as a result of changes in the Schottky barrier height. The above results also suggested that the soft X-ray

This material is reserved for educational use only, not allowed for commercial use.
Forbidden to modify the content, and cite the document when use.

irradiation process only has impact to the Metal-Semiconductor contact layer in the device.[42]

We analyzed the I–V and C–V relationships for silicon p–n junction diodes before and after soft X-ray irradiation. Under a forward bias (1.0 V), forward current is about two orders of magnitude higher for all X-ray irradiated samples than for non-X-ray irradiated samples, as measured at 303 K. The saturation current and ideality factor can be maintained and series resistance can be improved using this soft X-ray irradiation process. Under reverse-bias conditions, analysis of leakage current, carrier-generation lifetime, and activation energy indicate that soft X-ray irradiation does not significantly create new defects in a device. Thus, the soft X-ray irradiation process can improve the device series resistance under forward-bias conditions. However, optimum process conditions may need to be specifically developed for each particular device.

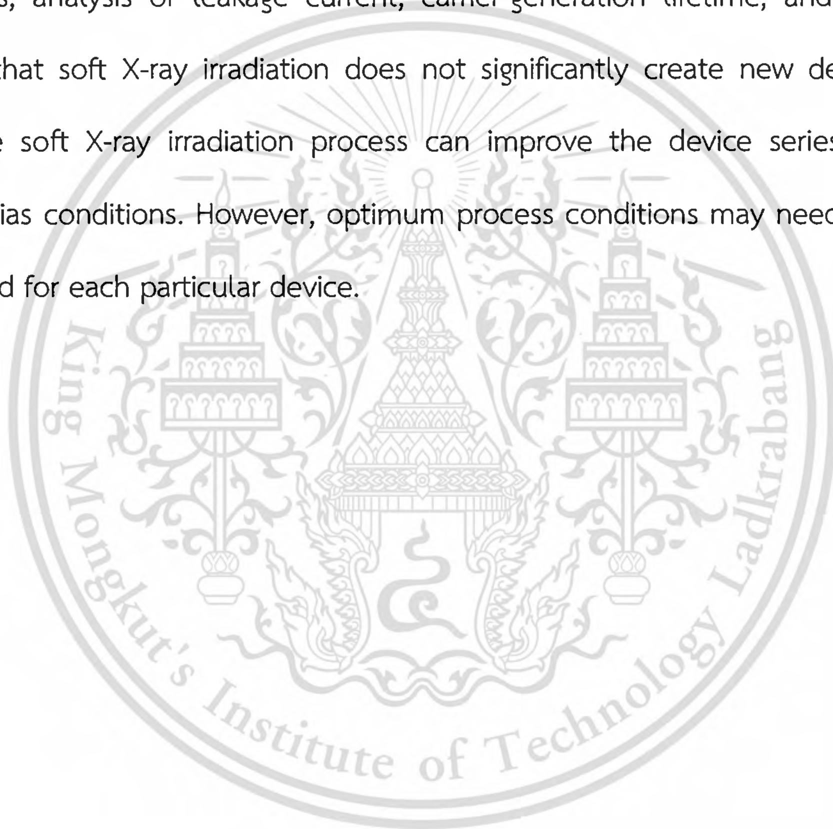

This material is reserved for educational use only, not allowed for commercial use.
Forbidden to modify the content, and cite the document when use.

Chapter 5

Conclusion

This thesis presents the electrical properties of p-n junction diode after irradiated by X-ray various dose. The p-n junction diodes in the thesis were fabrication by using CMOS technology at Thai Microelectronics Center (TMEC). The p-n diodes were simulation by the p-n diode team before fabrication by using TCAD simulation program. The p-n junction diode before and after irradiation were studied the electrical properties such as current-voltage (*I-V*) and capacitance-voltage (*C-V*) characteristics. The *I-V* characteristics were used to calculate parameters as ideality factor (η), series resistances (R_S), and reverse saturation current (I_0), which determines the zero bias barrier height (ΦB) and activation energy (E_T). Also the *C-V* characteristics were used to calculate as depletion width (W), built in voltage (V_{bi}) and carrier lifetime (τ).

Also after p-n junction diodes were fabricated, it was radiated by X-ray under various conditions. The X-ray was exposed directly on top side of the p-n diode.

Current-voltage characteristics of p-n diode are divided into 2 conditions, forward bias and reverse bias. The current in X-ray irradiated p-n junction diode under forward bias has increased approximately 1,000 times compare with standard device. The change of forward current suspected caused by X-ray radiation change the mechanism of p-n junction diode. The change in forward current parameter can explained using series resistance (diode resistance), Schottky barrier height(SBH). The resistance of p-n junction diode at saturation stage before radiation was 10 kΩ and after radiated, it was decreased down to 5 Ω. The SBH for prepared sample is about 0.94 eV but the SBH decreases after soft X-ray irradiation becomes 0.89 eV at X-ray quantity 7.11 X 10^4 R and remains insensitive up to the X-ray quantity up to 2.01 X 10^8 R. The change of SBH may caused by the ion

This material is reserved for educational use only, not allowed for commercial use.

Forbidden to modify the content, and cite the document when use.

losses energy via electronic energy loss (S_e) value is larger than the ion that losses energy via nuclear energy loss (S_n) ,therefore, it may cause partial annealing of point defects that produced by S_n. These annealing of point defects is suspect lead to a decrease in the interface state density at the MS interface which also results as a possible reason of causing the change of diode resistance in X-ray irradiated device.

In the reverse bias condition, the leakage current was change after irradiated by X-ray. The change of leakage current by X-ray irradiation cause from many factor such as (i) X-ray dominate carrier in silicon bulk, and (ii) X-ray induced the defects or trapping center in silicon bulk. X-ray may induced defects or change type defects, therefore, activation energy is the important for confirm trap level of p-n diode after irradiation by X-ray. The activation energy before and after irradiation are in the range of 0.63–0.68 eV. From the promising results of E_T before and after soft X-ray irradiation, it presents that the trapping center of p-n junction diode is not change after irradiated by X-ray. Although, the trapping level confirmed no change after X-ray but this technique cannot confirm the type of defects in silicon bulk. The small change of the Arrhenius plot is also confirming the trapping level in the X-ray irradiated devices. Therefore, Carrier generation lifetime were use to double confirm the effect of X-ray on the leakage current. Carrier generation lifetime is changed from 1.3 μsec before irradiated by X-ray to 1.7 μsec, after soft X-ray irradiated, which is insignificant. The leakage current after X-ray irradiation is also insignificant different compare with before X-ray. The ideality factor that calculates in forward bias condition before and after X-ray irradiation is also present insignificant change, which is near 1.0 in both conditions.

Our analysis of the effects of reverse-bias conditions suggests that soft X-ray irradiation has insignificant impact to p-n junction and diode defects. However, soft X-ray irradiation effect significant improvements in the forward-diode current as a result of

This material is reserved for educational use only, not allowed for commercial use.

Forbidden to modify the content, and cite the document when use.

changes in the Schottky barrier height at the Metal-Semiconductor contact layer in the device.[42] However, optimum process conditions may need to be specifically developed for each particular devices.

From these promising results, the soft X-ray irradiation process can be used to improve electrical properties of p-n junction diode or electronics devices without creating any damage or induced major defects in the p-n junction diode. The benefit of this thesis will change the semiconductor work and increase opportunity of recover defective devices in process which will help to save waste and cost in the future electronics market.

This material is reserved for educational use only, not allowed for commercial use.
Forbidden to modify the content, and cite the document when use.

References

[1] Rahimo M.T., Shammas N.Y.A.; "Freewheeling Diode Failure Modes in IGBT Applications" IEEE Transactions on Industry Applications, vol. 37., Issue 2, 2001, pp. 661-670.

[2] Lutz J., "The Freewhelling diode – No Longer the Weak Component" PCIM 1997, Nürnberg, Proc. Power Electronics, 1997, pp. 259-265.

[3] Benda V.; "Design Considerations for Fast Soft Reverse Recovery Diodes" Power Electronics and Applications, Fifth European Conference, 1993, vol.2, pp. 288-292.

[4] M.Miller., "Differences Between Platinum and Gold-Doped Silicon Power Devices" IEEE Transactions on Electron Devices, Vol. Ed-23, No.12, 1976, pp. 1279-1283.

[5] R. Locher and J. Bendal "Minimize Diode Recovery Losses and EMI in PFC Boost Converters" PCIM, 1993, pp. 18-23.

[6] J.Lutz, "Axial Recombination Center Technology for Freewheeling Diodes", Proceedings of EPE97, Trondheim, 1997, pp. 1.502–1.506.

[7] J.Vobecky, P.Hazdra, J.Homola, "Optimization of Power Diode Characteristics by Means of Ion Irradiation", IEEE Trans. On El. Dev., Vol. 43, No.12, 1996, pp. 2283-2289.

[8] H. Schlangenotto, J. Serafin, F.Sawitzki, H. Maeder, "Improved Recovery of Fast Power Diodes with Self-Adjusting p Emitter Efficiency", IEEE Electron Device Letters, Vol. 10, No. 7, 1989, pp.322-324.

[9] Nando Kaminski, Norbert Galster, Stefan Linder, "1200V Merged PIN Schottky Diode with Soft Recovery and Positive Temperature Coefficient", Lausanne, EPE, 1999.

[10] M. Msimangaa, M. McPhersona, C. Theron, "Fabrication and characterisation of gold-doped silicon Schottky barrier detectors", Radiation Physics and Chemistry, Vol. 71, 2004, pp. 733–734.

This material is reserved for educational use only, not allowed for commercial use.
Forbidden to modify the content, and cite the document when use.

[11] J. Vobecký, P. Hazdra, V. Záhlava, "Helium irradiated high-power P-i-N diode with low ON-state voltage drop" Solid-State Electronics, Vol. 47, No.1, 2003, pp. 45–50.

[12] P. Hazdra, J. Rube and J. Vobecký, "Divacancy profiles in MeV helium irradiated silicon from reverse I–V measurement" Nuclear Instruments and Methods in Physics Research Section B, Vol. 159, 1999, pp. 207-217.

[13] P. Hazdra, J. Vobecky´, H. Dorschnerb, K. Brand, "Axial lifetime control in silicon power diodes by irradiation with protons, alphas, low- and high-energy electrons", Microelectronics Journal, Vol. 35, Issue3, 2004, pp. 249–257.

[14] H.-J. Schulze, F.-J. Niedernostheide, M. Schmitt, U. Kellner-Werdehausen, G. Wachutka, "Influence of Irradiation Induced Defects on the Electrical Performance of Power Devices", Electrochemical Society Proceeding, Vol.20, 2002, pp. 320-335.

[15] R. Siemieniec, F. J. Niedernostheide, H.J. Schulze, W. Sudkamp, U. Kellner-Werdehausen, and J. Lutz, "Irradiation-Tnduced Deep Levels in Silicon for Power Device Tailoring". Journal of the Electrochemical Society, 153 (2), 2006, pp. G108-G118.

[16] M. A. Krivov, S. V. Malyanov, "Effect of roentgen radiation on germanium and germanium p-n junctions" Soviet Physics Journal, Volume 9, Issue 4, 1966, pp. 76-78.

[17] M. A. Krivov, S. V. Malyanov, V. I. Gaman, "The effect of X-rays on silicon and silicon p-n junctions" Soviet Physics Journal, Volume 10, Issue 6, 1967, pp. 106-109

[18] J. H. Werner, "Schottky barrier and pn-junction I/V plots Small signal evaluation", Appl. Phys. A: Solids Surf. 47, 1988, pp. 291-300.

[19] M. Lyakas, R. Zaharia, and M. Eizenberg, "Analysis of nonideal Schottky and p-n junction diodes: Extraction of parameters from I–V plots", J. Appl. Phys. 78, 1995, pp. 5481.

[20] H. Norde, "A Modified Forward I–V Plot for Schottky Diodes with High Series Resistance", J. Appl. Phys. 50, 1979, pp. 5052 - 5053.

This material is reserved for educational use only, not allowed for commercial use.
Forbidden to modify the content, and cite the document when use.

[21] C. D. Lien, F. C. T. So, and M. A. Nicolet, "An improved forward I-V method for non ideal Schottky diodes with high series resistance", IEEE Trans. Electron Devices ED-31, 1984, pp. 1502.

[22] S. K. Cheung and N. W. Cheung, "Extraction of Schottky diode parameters from forward current - voltage characteristics", Appl. Phys. Lett. 49, 85, 1986.

[23] T. C. Lee, S. Fung, C. D. Beiling, and H. L. Au, "A Systematic Approach to the Measurement of Ideality Factor, Series Resistance, and Barrier Height for Schottky Diodes", J. Appl. Phys. 72, 1992, pp. 4739-4742.

[24] D. Gromov and V. Pugachevich, Appl. Phys. A, "Modified method for the calculation of real Schottky-diode parameters", Appl. Solids Surf. 59, 1994, pp. 331-333.

[25] V. Mikhelashvili, G. Eisenstein, V. Garber, S. Fainleib, G. Bahir, D. Ritter, M. Orenstein, and A. Peer, "On the extraction of linear and nonlinear physical parameters in nonideal diodes", J. Appl. Phys. 85, 1999, pp. 6873.

[26] D Biselloa, A Candeloria, A Kaminskia, A Litovchenkoa, E Noahb, L Stefanutti, "X-ray radiation source for total dose radiation studies", Radiation Physics and Chemistry", *Radiation Physics and Chemistry*, 71, 2004, pp. 713–715.

[27] S.M. Sze: Physics of semiconductor devices, John Wiley & Sons, New York, 1981.

[28] Gerold W. Neudeck: The pn junction diode, Addison-Wesley Publishing Company, 1989.

[29] D.K. Schroder, "Carrier Lifetimes in Silicon", IEEE Trans. Electron Devices, Vol. 44, 1997, pp. 160-170.

[30] L.F. Marsal, I. Martin, J. Pallares, A. Orpella, R. Alcubilla, "Annealing effects on the conduction mechanisms of p+-amorphous- Si0.8 C0.2:H/ n-crystalline-Si diodes", J. Appl. Phys. Vol. 94, No. 4, 2003, pp. 15.

This material is reserved for educational use only, not allowed for commercial use.
Forbidden to modify the content, and cite the document when use.

[31] N. Bano, I. Hussain, O. Nur, M. Willander, P. Klason, “Study of Radiative Defects Using Current-Voltage Characteristics in ZnO Rods Catalytically Grown on 4H-p-SiC”, Journal of Nanomaterials Vol. 2010, 2010, Article ID 817201, 5 pagesdoi:10.1155/2010/817201.

[32] A Czerwinski, E Simoen, A Poyai and C Claeys, “Activation energy analysis as a tool for extraction and investigation of p–n junction leakage current”, *J Appl Phys*, 94, 2003, pp. 1218–1221

[33] Sandeep Kumar1, Y S Katharria, Y Batra and D Kanjilal “Influence of swift heavy ion irradiation on electrical characteristics of Au/n-Si (1 0 0) Schottky barrier structure” JOURNAL OF PHYSICS D: APPLIED PHYSICS, 40, 2007, pp. 6892–6897.

[34] M K Hudait, S B Krupanidhi, “Doping dependence of the barrier height and ideality factor of Au/n-GaAs Schottky diodes at low temperatures”, *Physica B*, 307, 2001, pp. 125–137.

[35] E H Rhoderick and R H Williams, *Metal–Semiconductor Contacts*, 2nd edn, Oxford: Clarendon, 1988.

[36] S Kumar, Y S Katharria, Y Batra and D Kanjilal, “Influence of swift heavy ion irradiation on electrical characteristics of Au/n-Si (1 0 0) Schottky barrier structure’, *J Phys D*, 40, 2007, pp. 6892–6897.

[37] S Chand, “Theoretical evidence for random variation of series resistance of elementary diodes in inhomogeneous Schottky contacts”, Physica B, 373, 2006, pp. 284–290.

[38] S Khanna, S Neeleshwara, A Noor, “Current–Voltage-Temperature (I-V-T) Characteristics of CR/4H-SIC Schottky Diodes”, *Journal of Electron Devices*, 9, 2011, pp. 382-389.

[39] D Korucua, T S Mammadova, S Özçelika, “The Role OF Series Resistance on the Forward Bias Current-Voltage (I-V) Characteristics in Sn/p-InP (MS) Contacts”, *Journal of Ovonic Research*, 6, 2008, pp. 159–164.

King Mongkut's Institute of Technology Ladkrabang

This material is reserved for educational use only, not allowed for commercial use.

Forbidden to modify the content, and cite the document when use.

[40] A Poyai, E Simoen, C Claeys, A Czerwinski, *Materials Science and Engineering B*, 73, 2000, pp. 191–196.

[41] A. Poyai: Ph.D. Thesis, Katholieke Universiteit Leuven, Belgium, 2002.

[42] S Chand, S Bala, “Simulation studies of current transport in metal–insulator–semiconductor Schottky barrier diodes”, *Physica B*, 390, 2007, pp. 179–184.

This material is reserved for educational use only, not allowed for commercial use.
Forbidden to modify the content, and cite the document when use.

Appendix

This material is reserved for educational use only, not allowed for commercial use.
Forbidden to modify the content, and cite the document when use.

Appendix A

X-ray Radiation Generator

This material is reserved for educational use only, not allowed for commercial use.
Forbidden to modify the content, and cite the document when use.

X-ray radiation generator at KMUTNB

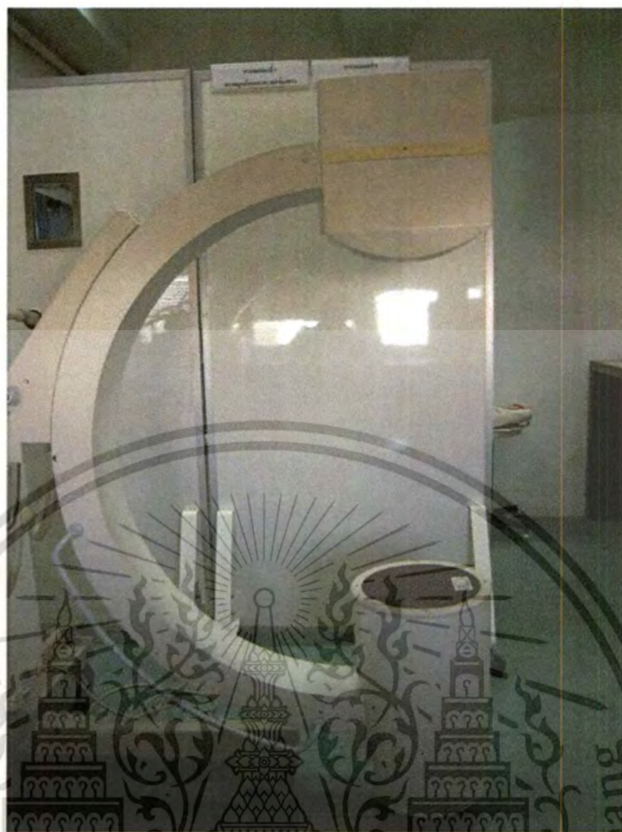

Fig. A1 C-arm of X-ray radiation generator.

Fig. A2 Monitor shows the image of device.

King Mongkut's Institute of Technology Ladkrabang

This material is reserved for educational use only, not allowed for commercial use.

Forbidden to modify the content, and cite the document when use.

Fig. A3 Control part of the X-ray generator.

Fig. A4 Control screen of X-ray generator.

King Mongkut's Institute of Technology Ladkrabang
This material is reserved for educational use only, not allowed for commercial use.
Forbidden to modify the content, and cite the document when use.

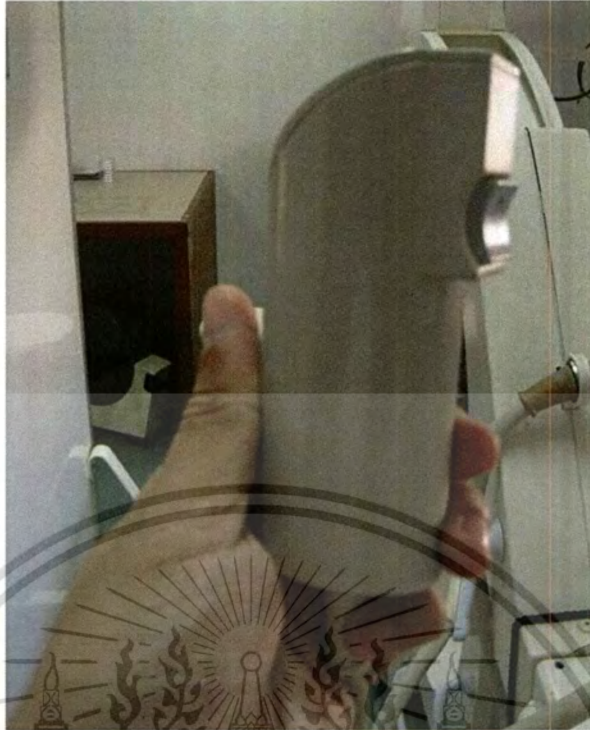

Fig. A5 Hand switch to control the emission of X-rays.

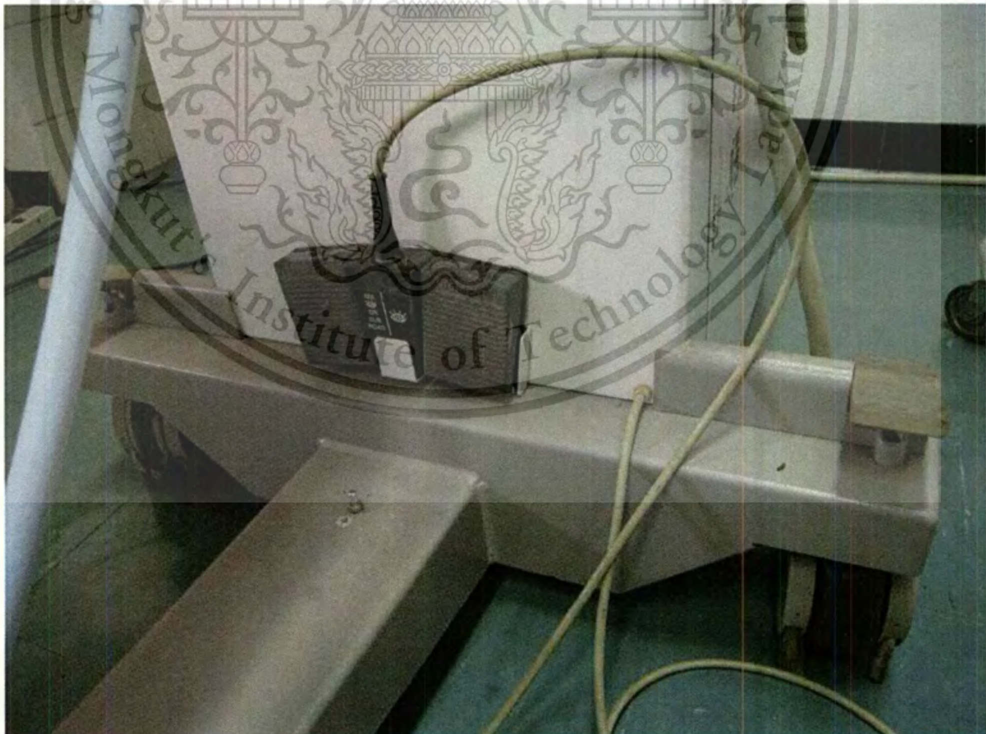

Fig. A6 Foot switch to control the emission of X-rays.

King Mongkut's Institute of Technology Ladkrabang
This material is reserved for educational use only, not allowed for commercial use.
Forbidden to modify the content, and cite the document when use.

X-ray generator at Chulalongkorn University

Fig. A7 X-ray generator at CU.

King Mongkut's Institute of Technology Ladkrabang

This material is reserved for educational use only, not allowed for commercial use.

Forbidden to modify the content, and cite the document when use.

Fig. A8 Point of the device on X-ray generator.

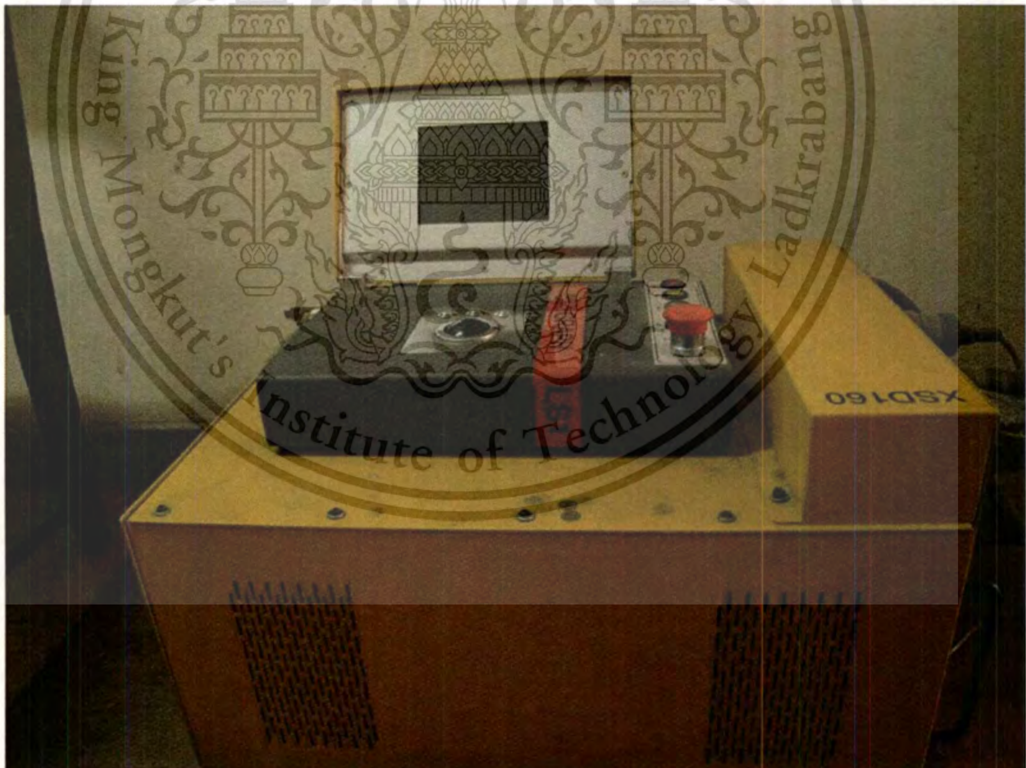

Fig. A9 Control part of X-rays at CU.

King Mongkut's Institute of Technology Ladkrabang

This material is reserved for educational use only, not allowed for commercial use.

Forbidden to modify the content, and cite the document when use.

Fig. A10 Control part of X-rays at CU. (Cont.)

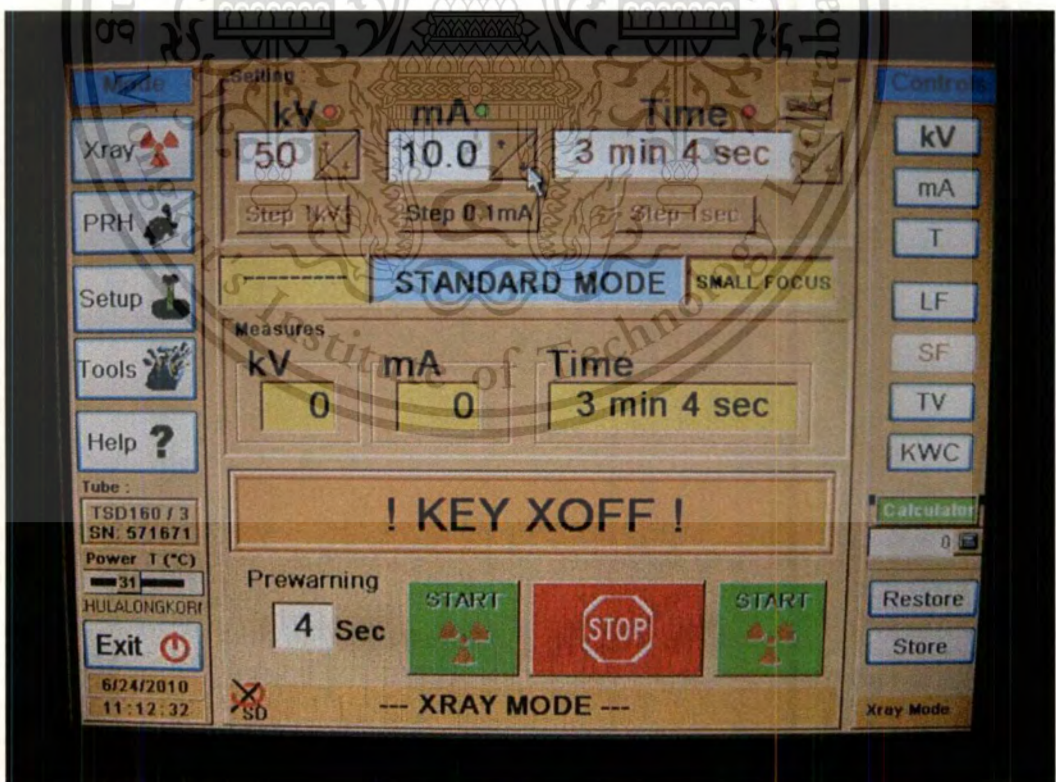

Fig. A11 Screen control of X-rays.

This material is reserved for educational use only, not allowed for commercial use.
Forbidden to modify the content, and cite the document when use.

Appendix B

CMOS Technology for Device Fabrication at TMEC

This material is reserved for educational use only, not allowed for commercial use.
Forbidden to modify the content, and cite the document when use.

CMOS Technology for Device Fabrication at TMEC

Fig. B1 Automotive wet bench.

Fig. B2 SVG TMX 2604 Diffusion Furnace

This material is reserved for educational use only, not allowed for commercial use.
Forbidden to modify the content, and cite the document when use.

Fig. B3 Mask aligner and PR coating machine.

This material is reserved for educational use only, not allowed for commercial use.
Forbidden to modify the content, and cite the document when use.

Fig. B4 Sputter machine.

Fig. B5 Mark II Dry Etcher.

This material is reserved for educational use only, not allowed for commercial use.
Forbidden to modify the content, and cite the document when use.

Appendix C

Paper publications

This material is reserved for educational use only, not allowed for commercial use.
Forbidden to modify the content, and cite the document when use.

Author Profile

Name-Surname	Mr. Poopol Rujanapich
Birth date	21 October 2511
Birthplace	Nakornratchasima
Address	3/25 Moobann Nuttanum3, Soi ChangArgardUtit16, Vibhavadi Rd., Donmuang, Bangkok 10210, Thailand
Education Background	2551 Doctoral Student, Department of Microelectronics, Faculty of Engineering, King Mongkut's Institute of Technology Ladkrabang 2536 Master Degree of Electrical Engineering, Department of Microelectronics, Faculty of Engineering, King Mongkut's Institute of Technology Ladkrabang 2533 Bachelor Degree of Science (Physics), Faculty of Science, Silpakorn University
Expertise	1) Photolithography process 2) Semiconductor device 3) Semiconductor Fabrication 4) Semiconductor measurement 5) Analyze the semiconductor properties

Publications

Journal Publications

[1] **P. Rujanapich**, I. Srithanachai, S. Ueamanapong, A. Poyai, W. Titiroongruang, "X-ray soft annealing process study for p-n junction diode", ***Indian Journal of Pure & Applied Physics.*** Vol.51, August, pp. 587-592 (2013)

This material is reserved for educational use only, not allowed for commercial use.
Forbidden to modify the content, and cite the document when use.

[2] **P. Rujanapich**, I. Srithanachai, S. Ueamanapong, A. Poyai, S. Niemcharoen, W. Titiroongruang, "An Improvement of Forward Current of P-N Diode using Soft X-ray Method", ***Advance science letters***. Vol. 19, Number 2, pp. 690-693 (2012)

[3] I. Srithanachai, S. Ueamanapong, **P. Rujanapich**, A. Poyai, S. Niemcharoen and W. Titiroongruang, "Effect of X-Ray Irradiation on the Current of P-N Diode", ***Materials Science Forum***, Vol. 695, pp. 561-564 (2011).

[4] I. Srithanachai, S. Ueamanapong, **P. Rujanapich**, N. Atiwongsangthong, S. Niemcharoen, A. Poyai, and W. Titiroongruang, "Defects study by activation energy profile for lowering leakage current in P-N junction", ***Materials Science Forum***, Vol. 695, pp. 569-572 (2011).

[5] K. Sato, M. Takahashi, H. Takano, H. Hashimoto, Y. Niikura, T. Matsumoto, **P. Rutchanaphit**, "Generalization of Ramo's Theorem and Its Application to Semiconducting Materials", Jpn. J. Appl. Phys. 34, pp. 2057-2061(1995)

Proceeding Publications

[1] **P. Rujanapich**, A. Poyai, I. Srithanachai, P. Pengpad, C. Hruanan, S. Sophitpan, W. Titiroongruang, "Generation Lifetime Analysis of P-N Junction X-ray Detector", ***Electrical Engineering/Electronics, Computer, Telecommunications and Information Technology Asscociation of Thailand (ECTI-CON-2010)***, THAILAND, pp. 780-783 (2010).

[2] **P. Rujanapich**, A. Poyai, I. Srithanachai, P. Pengpad, C. Hruanan, S. Sophitpan, S. Ueamanapong, W. Titiroongruang, W. Titiroongruang, "Saturation Current Analysis of Low Dose X- ray Irradiated P-N Junction Diodes", ***Joint International Conference on Information & Communication Technology, Electronic and Electrical Engineering (JICTEE 2010),*** LAOS, pp. 231-233 (2010).

[3] I. Srithanachai, **P. Rujanapich**, S. Ueamanapong, W. Titiroongruang, A. Poyai, S. Niemcharoen, and W. Titiroongruang, "Electrical Characteristics Study on the Effect of X-ray Irradiation Various Energy and Exposure Time on P-N Junction", ***Joint International Conference on Information & Communication Technology, Electronic and Electrical Engineering (JICTEE 2010),*** LAOS, pp. 234-237 (2010).

[4] Y. Sundarasaradula, I. Srithanachai, **P. Rujanapich**, S. Ueamanaphong ,P. Pengpad, M. Saenlamool, W. Titiroongruang, P. Tosranon, A. Poyai, S. Niemcharoen, and W. Titiroongruang, "Effect of X-ray Irradiation on the Characteristics of P-N Junction

This material is reserved for educational use only, not allowed for commercial use.

Forbidden to modify the content, and cite the document when use.

Diodes", *The 33th Electrical Engineering Conference (EECON-33),* THAILAND, pp. 1121-1124 (2010).

[5] **P. Rujanapich**, A. Poyai, I. Srithanachai, P. Pengpad, C. Hruanan, S. Sophitpan, S. Ueamanapong, W. Titiroongruang, and W. Titiroongruang, "Activation Energy Analysis OF P-N Junction X-ray Direct Detector", *International Technical Conference on Circuits/Systems, Computers and Communications (ITC-CSCC 2010),* THAILAND, pp. 257-260 (2010).

[6] **P. Rujanapich**, A. Poyai, I. Srithanachai, P. Pengpad, C. Hruanan, S. Sophitpan, and W. Titiroongruang, "Diode analysis of X-ray Detector", *The 4th International Confernece on Sensors (Asiasense 2010)*, THAILAND (2010).

[7] **P. Rujanapich**, A. Poyai, I. Srithanachai, S. Ueamanapong, and W. Titiroongruang, "Defects Engineering for Silicon Power Diode by X-ray Irradiation", *26th International Conference on Defects in Semiconductors 2010 (ICDS'26)*, NEW ZEALAND (2010).

[8] I. Srithanachai, S. Ueamanapong, **P. Rujanapich**, N. Atiwongsangthong, S. Niemcharoen, A. Poyai, and W. Titiroongruang, "Defects Study by Activation Energy Profile for Lowering Leakage Current in P-N Junction", *11th International Symposium on Eco-materials Processing and Design (ISEPD-2011),* Thailand (2011).

[9] I. Srithanachai, S. Ueamanapong, **P. Rujanapich**, A. Poyai, S. Niemcharoen and W. Titiroongruang, "Effect of X-Ray Irradiate to the Current of P-N Diode", *11th International Symposium on Eco-materials Processing and Design (ISEPD-2011),* Thailand (2011).

This material is reserved for educational use only, not allowed for commercial use.
Forbidden to modify the content, and cite the document when use.

NISCAIR

Indian J Pure & Appl Phys
August 2013
Volume 51(08) 531-5927
CODEN: IJOPAU
ISSN : 0019-5596
ijpap@niscair.res.in

Indian Journal of Pure & Applied Physics

www.niscair.res.in

Published by
National Institute of Science Communication And Information Resources, CSIR
New Delhi, INDIA
in association with
Indian National Science Academy, New Delhi, INDIA

King Mongkut's Institute of Technology Ladkrabang

This material is reserved for educational use only, not allowed for commercial use.
Forbidden to modify the content, and cite the document when use.

Indian Journal of Pure & Applied Physics
Vol. 51, August 2013, pp. 587-592

X-ray soft annealing process study for *p-n* junction diode

Poopol Rujanapich[a], Amporn Poyai[b], Itsara Srithanachai[a], Surada Ueamanapong[a] & Wisut Titiroongruang[a]

[a]Department of Electrical Engineering, Faculty of Engineering, King Mongkut's Institute of Technology Ladkrabang, Chalongkrung Road, Ladkrabang, Bangkok 10520, Thailand

[b]Thai Microelectronics Center (TMEC), 51/4 Moo 1, Wang-Takien District, Amphur Muang, Chachoengsao 24000, Thailand

E-mail: poopolr@yahoo.com

Received 28 March 2012; revised 19 March 2013; accepted 18 April 2013

The effect of X-ray soft annealing on the electrical properties of *p–n* junction diodes has been investigated. Under a forward bias of 1.0 V at 303 K, the forward current is approximately two orders of magnitude higher for X-ray annealed than for non-X-ray annealed samples. This effect is further investigated by evaluating the following properties under forward-bias conditions: ideality factor, saturation current, activation energy, series resistance, under reverse-bias conditions, carrier-generation lifetime, and activation energy. Results suggest that X-ray soft annealing improves the electrical properties of *p-n* junction diodes under forward-bias conditions.

Keywords: X-ray annealing, *p-n* junction diode

1 Introduction

Optimization of power-device characteristics such as carrier lifetime is clearly of significant and ongoing importance. Optimization techniques formerly involved the use of gold and platinum impurities, but today, involve the use of irradiation[1-4]. To date, however, the required radiation sources use significant amounts of power, and thus incur high operational costs[4]. With the goal of lowering these operational costs, the electrical properties of *p-n* junction diodes irradiated using low-energy X-ray sources (40-70 keV) have been examined. Not only are such low-energy sources inexpensive to operate[5], but they are also already present in most laboratories and hospitals. As described herein, we compared the current–voltage characteristics of irradiated and non irradiated samples and found that, under a forward bias of 1.0 V at 303 K, forward current is approximately two orders of magnitude higher for irradiated than for non irradiated samples. This result suggests the possibility of using low-energy X-rays as an energy source for X-ray soft annealing *p-n* junction diodes. To investigate the origin of the change in electrical properties with X-ray soft annealing, we evaluated the following parameters before and after X-ray annealing: ideality factor, saturation current, activation energy, series resistance and carrier-generation lifetime.

2 Experimental Details

Silicon substrates (*n*-type, orientation <111>, resistivity 134-140 Ωcm, silicon dioxide thickness 1 μm) were used to fabricate *p-n* junctions. The fabrication process was as follows. The first round of photolithography and etching was performed to open a window (1×1 mm^2) in silicon dioxide. The wafers were then subjected to boron implantation (dose 1×10^{16} cm^{-2} at energy of 120 keV), thermal treatment (1050°C for 60 min), and metallization for creating an aluminium layer (1 μm) on both sides. A second round of photolithography and etching was performed for creating aluminium patterns. The wafers were thermal annealed (400°C for 30 min) and then cut into chips. The chips were assembled on printed circuit boards and wired with the necessary electrical connections to prepare them for testing. Fig. 1 shows the resulting diode structure.

X-rays for irradiation were generated by a laboratory-scale X-ray source. Current-voltage (*I-V*) and capacitance–voltage (*C-V*) characteristics were measured by a semiconductor parameter analyzer (Agilent HP4156B). The same samples were tested before and after X-ray annealed.

3 Results and Discussion

We measured the *I-V* and *C-V* characteristics of *p-n* junctions before X-ray annealing and after X-ray annealing under various conditions. Table 1 lists the X-ray annealing conditions.

This material is reserved for educational use only, not allowed for commercial use.
Forbidden to modify the content, and cite the document when use.

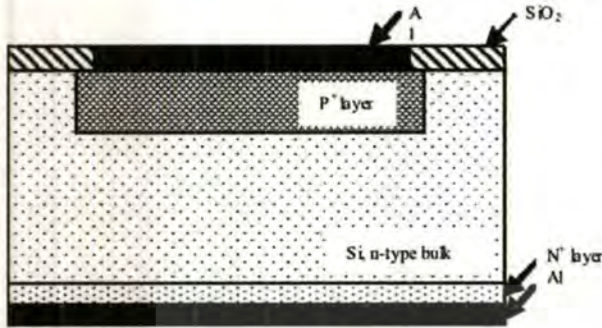

Fig. 1 — Structure of *p-n* junction diodes

Table 1 — X-ray radiation conditions

Condition	X-ray energy (keV)	Time (s)	Electrical charge (mA·s)	X-ray quantity (Roentgen)
1	40	5	0.2	7.11×10^4
2	40	55	0.2	7.82×1^5
3	40	205	0.2	2.92×10^6
4	55	5	0.7	4.71×10^5
5	55	55	0.7	5.18×10^6
6	55	205	0.7	1.93×10^7
7	70	5	4.5	4.90×10^6
8	70	55	4.5	5.39×10^7
9	70	205	4.5	2.01×10^8

3.1 Forward bias

The general relationship between current and voltage for a *p-n* junction diode[1-9] is given by Eq. (1):

$$I(V,T) = I_0(T)\,\{\exp[X(T)V] - 1\} \qquad \ldots(1)$$

where I_0 is the saturation current, V is the bias voltage, and X is a coefficient. I_0 and X are, generally, dependent on temperature T. For small forward-bias voltages, the exponential term in the equation is very large; hence, the subtracted *1* is negligible and the forward-diode current is often approximated as in Eq. (2):

$$I(V,T) = I_0(T)\,\{\exp[X(T)V]\} \qquad \ldots(2)$$

Figure 2 shows *I-V* plots for a *p-n* junction diode under forward bias before and after X-ray annealing. Interestingly, at V = 1.0 V, I is approximately two orders of magnitude higher after X-ray annealing than before X-ray annealing. The plots suggest the existence of three different mechanisms of current transport: (1) In Region I (<0.1 V), I increases linearly with V that is, $I \propto V$ suggesting that current transport is dominated by tunneling. (2) In Region II (0.1-0.5 V), I increases exponentially with V according to the

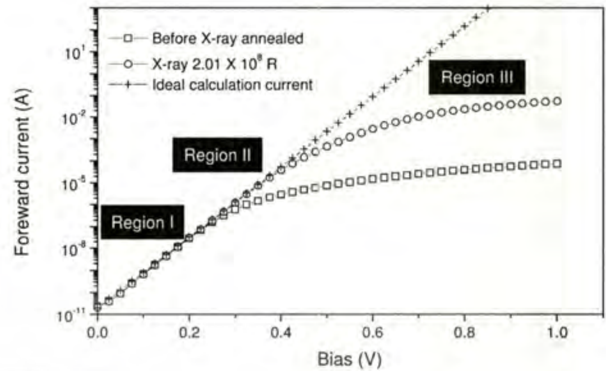

Fig. 2 — Plots of forward *I–V* characteristics for a *p-n* junction diode before and after X-ray annealing, measured at 303 K

relationship $I \propto \{\exp[X(T)V]\}$; the ideality factor n is determined in this region, and the current transport is dominated by recombination. (3) In Region III (>0.5 V), I follows the power law $I \propto V_m$, suggesting that current transport is space-charge-limited[10]. To simplify analysis, we thus divide the further discussion of forward bias into two sections: forward-bias voltages of <0.5 V and ≥0.5 V.

3.1.1 Forward-bias voltages of <0.5 V

At small forward-bias voltages, the *p-n* junction ideality factor n can be calculated[6] by Eq. (2) as follows:

$$\ln[I(V,T)] = \ln[I_0(T)] + X(T)V \qquad \ldots(3)$$

For $X(T) = q/nkT$, this gives:

$$\ln[I(V,T)] = \ln[I_0(T)] + (q/nkT)V \qquad \ldots(4)$$

where q is the electronic charge constant, n is the ideality factor and k is the Boltzmann's constant.

At forward biases in the range 0.1-0.3 V, I_0 and n can be calculated from Eq. (4) and the plot of forward *I-V* characteristicsis shown in Fig. 2.

Figure 3 shows plots of I_0 for *p-n* junction diodes before and after X-ray annealing measured at different temperatures. When measured at room temperature (303 K), I_0 is essentially the same before and after X-ray annealing; however, when measured at higher temperatures, I_0 is higher before X-ray annealing than after X-ray annealing.

Figure 4 shows plots of n for a *p–n* junction diode before and after X-ray annealing. The value of n is essentially the same, close to 1, before X-ray annealing and after X-ray annealing, suggesting that the mechanism of current transport is dominated by diffusion.

This material is reserved for educational use only, not allowed for commercial use.
Forbidden to modify the content, and cite the document when use.

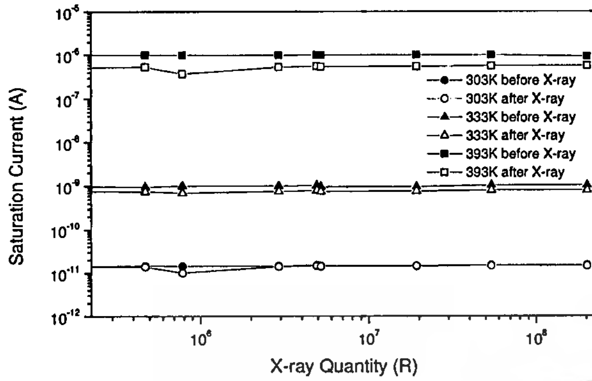

Fig. 3 — Plots of saturation current versus X-ray quantity for a *p-n* junction diodes before and after X-ray annealing under various conditions, measured at different temperatures

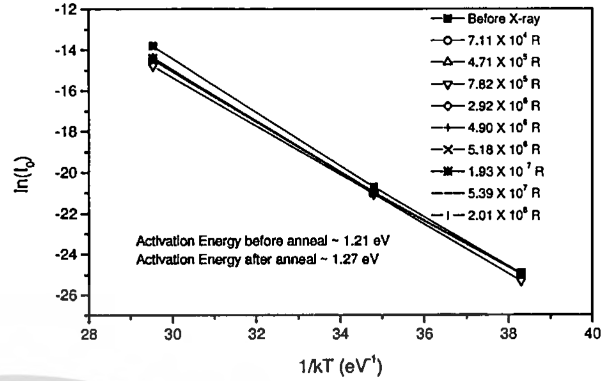

Fig. 5 — Plots of $\ln(I_0)$ versus $1/kT$ for a *p-n* junction diodes before and after X-ray annealing under various conditions, measured at 303 K

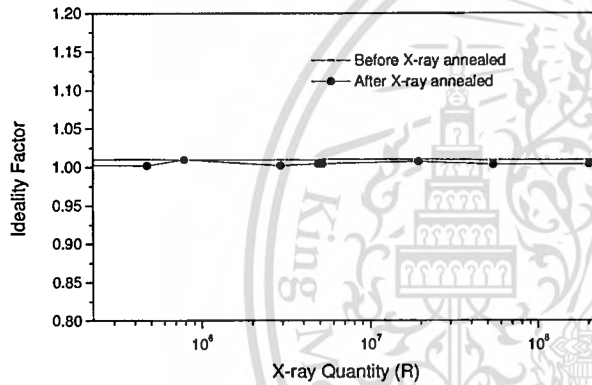

Fig. 4 — Plots of ideality factor versus X-ray quantity for a *p–n* junction diode before and after X-ray annealing, measured at 303 K

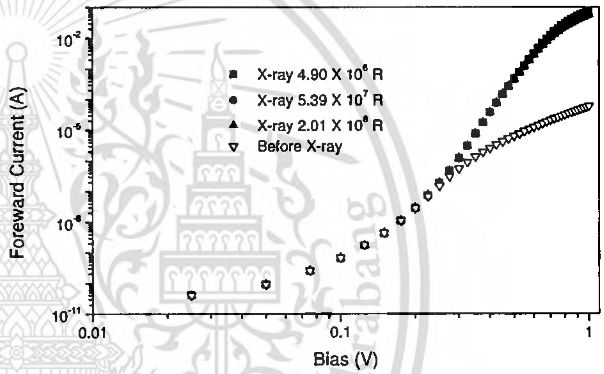

Fig. 6 — Plots of forward *I* versus *V* (log-log scale) for a *p-n* junction diodes before and after X-ray annealing under various conditions, measured at 303 K

Figure 5 shows plots of $\ln(I_0)$ as a function of $1/kT$ for *p–n* junction diodes before and after X-ray annealing. The slope of an Arrhenius plot, I_0 versus $1/kT$ yields the activation energy[11] E_T. Activation energy E_T before X-ray annealing is ~1.21 eV and after X-ray annealing is ~1.27 eV, which supports the results shown in Figure 3. E_T for a diode is the minimum energy required to trigger temperature-accelerated failure. The measured E_T values thus indicate a tendency for failure to be accelerated by temperature; that is, a lower E_T value favours triggering of failure with temperature. Therefore, the higher E_T value of the X-ray annealed diodes, compared with the non-X-ray annealed diodes, means that their electrical properties are less sensitive to changes in temperature. Furthermore, the measured E_T values are close to the energy gap of crystalline silicon, ~1.12 eV. Thus, our results confirm that the mechanism of current transport is dominated by diffusion under both X-ray annealed and non-X-ray annealed conditions[9], which also corresponds to the results for the ideality factor in Figure 4.

3.1.2 Forward-bias voltages of ≥0.5 V

At large forward-bias voltages, *I-V* characteristics deviate from exponential dependence because of voltage drops across the bulk of the diode. However, as voltage increases even further, resistance eventually decreases and current increases super linearly.

Figure 6 shows plots of *I-V* characteristics for *p-n* junction diodes before and after X-ray annealing. On the log-log scale of the plots, *I* depends linearly on *V*. This superlinear or power-law dependence is characteristic of space-charge-limited currents[9].

Figure 7 shows plots of series resistance (R_S) before and after X-ray annealing. Below the turn-on voltage, R_S decreases with increasing forward bias, and above the turn-on voltage, it remains constant. Under

This material is reserved for educational use only, not allowed for commercial use.
Forbidden to modify the content, and cite the document when use.

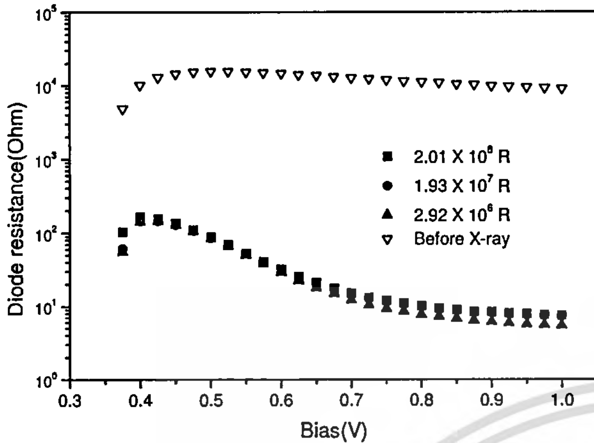

Fig. 7 — Plots of series resistance versus bias voltage for *p-n* junction diodes before and after X-ray annealing under various conditions, measured at 303 K

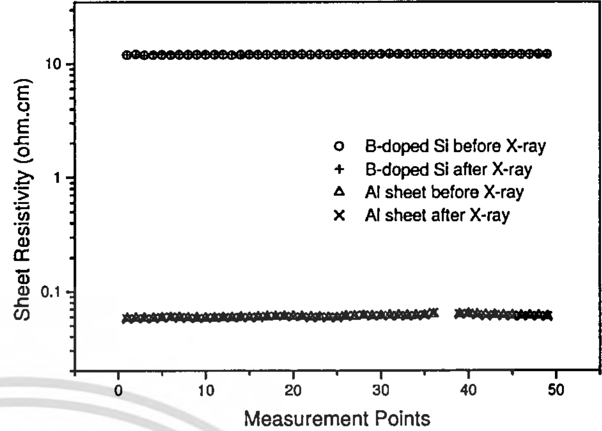

Fig. 8 — Plots of sheet resistance of boron doped Si and aluminium layer before and after X-ray annealing

forward bias, at *p-n* junction, the conduction-band barrier decreases, enhancing electron flow from the *n*-type to the *p*-type region and hole flow from the *p*-type to the *n*-type region. Successive recombination gives rise to the forward-bias current flow. As forward-bias voltage increases, R_S decreases until the conduction-band barrier becomes negligible, beyond which it remains constant[10].

The R_S is the sum of total resistance value of the resistors in series and the resistance in the semiconductor device in the direction of current flow or bulk and contact resistance[12,14]. To investigate the origin of the change in R_S with X-ray soft annealing, under forward bias, we evaluated the substrate resistance, aluminium layer resistance and Schottky Barrier Height (SBH) before and after X-ray soft annealed as shown in Fig. 8. The effect of X-ray soft annealing to *p-n* junction will be evaluated under reverse bias condition.

The substrate and aluminium sheet resistance are not significantly different before and after X-ray annealed, as measured by the four-probe method. Then, we evaluated the SBH before and after X-ray soft annealed.

At high forward-bias voltages, $V>3kT$, current transport in Schottky contact is due to majority carriers. It may be described by thermionic emission over the interface barrier. The experimental data are fitted by the conventional thermionic emission equation[12-17], which is given by Eq. (1) and I_0 is given by

$$I_0 = AA^*T^2 \exp[(-q\Phi_{B0})/kT] \quad ...(5)$$

where A^*, A and Φ_{B0} represent the Richardson constant, the contact area and zero-bias SBH, respectively. Plot of $\ln(I_0/T^2)$ versus q/kT should give a straight line whose slope and intercept will give barrier height.

The nature of the potential barrier between the Fermi level in the metal and the conduction band edge of the semiconductor at the interface is the most important characteristics of the metal-semiconductor interface. Since electrical contacts to semiconductors require metal–semiconductor interfaces and depending upon this potential barrier height, interfaces exhibit a modest resistance to current flow in either direction or a high resistance in one direction and low resistance in the opposite direction[14].

Figure 9 shows plots of SBH before and after X-ray annealing. The SBH for prepared sample is about 0.94 eV. The SBH decreases after X-ray soft annealed becomes 0.89 eV at X-ray quantity 7.11×10^4 R and remains insensitive up to the X-ray quantity up to 2.01×10^8 R. Thus, our results present that the X-ray soft annealed device has lower potential barrier height of metal–semiconductor interfaces than non-X-ray soft annealed sample. These results are also suggested to be the possible reason for causing decrease in R_S in X-ray soft annealed devices.

3.1.3 Reverse bias

Saturation current I_0 under reverse bias is a combination of diffusion current I_d and generation current I_g in the depletion region, as shown in Eq. (6):

$$I_0 = I_d + Bqn_iW/\tau_g \quad ...(6)$$

This material is reserved for educational use only, not allowed for commercial use.
Forbidden to modify the content, and cite the document when use.

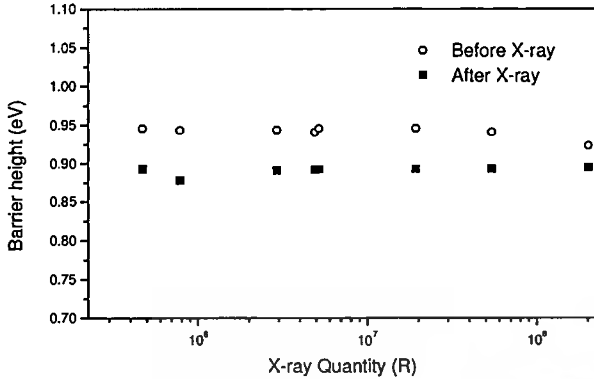

Fig. 9 — Plots of SHB versus X-ray quantity before and after X-ray annealing

where B is the p-n junction area, n_i is the intrinsic carrier concentration, τ_g is the carrier-generation lifetime, and W is the depletion-region width. The latter can be calculated from Eq. (7):

$$W = B\varepsilon_{Si}/C \quad ...(7)$$

where ε_{Si} is the dielectric permittivity of silicon and C is capacitance, which can be obtained from a plot of capacitance-voltage (C-V) characteristics.

The equation for carrier-generation lifetime (Eq. (8), below) is exactly in the form of Eq. (6) reversed slope.

$$\tau_g = Bqn_iW/(I_0 - I_d) \quad ...(8)$$

Figure 10 shows plots of leakage current as a function of depletion width for p-n junction diodes before and after X-ray annealing. Under reverse-bias conditions, changes in depletion width have insignificant impact on diffusion current; thus, Eq. (6) shows that leakage current depends on carrier-generation lifetime, which may also be related to device defects. Diffusion current can be determined by extrapolation of the plots to zero depletion width, and then generation current can be calculated.

Figure 11 shows plots of carrier-generation lifetime as a function of depletion width for p-n junction diodes before and after X-ray annealing. Carrier-generation lifetime is essentially the same before and after X-ray annealing, suggesting that annealing has insignificant impact to diode defects and p-n junction.

To confirm this speculation, we analyzed the activation energy of p-n junction diodes, which can be used to study the types of defects in a p-n junction. Accurate values of this activation energy can be obtained from the generation current[18,19]. Generation current depends on temperature as follows:

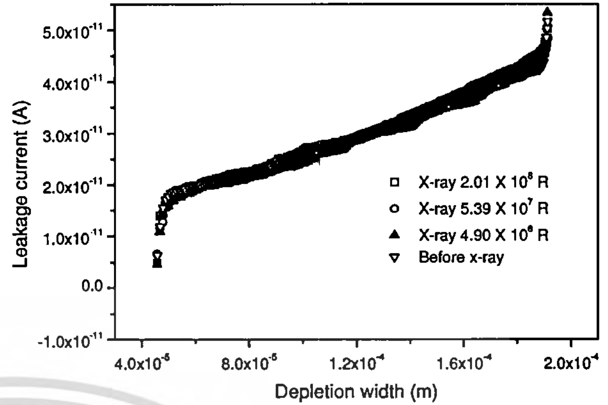

Fig. 10 — Plots of leakage current versus depletion width for p-n junction diodes before and after X-ray annealing under various conditions, measured at 303 K

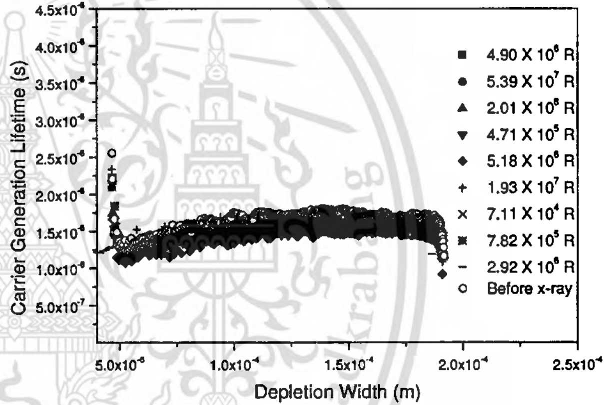

Fig. 11 — Plots of carrier-generation lifetime versus depletion width for p-n junction diodes before and after X-ray annealing under various conditions, measured at 303 K

$$I_g = [(QWBT^{1.7} + \xi)/\tau_r]\exp(-E_T/kT), \quad ...(9)$$

where W is the depletion width, Q is a constant, ξ is a small number (<1) related to the temperature dependence of the depletion width, τ_r is the recombination lifetime and E_T is the activation energy[18].

Figure 12 shows sample of Arrhenius plots of $I_g/T^{1.7}$ as a function of $1/kT$ for p-n junction diodes after X-ray annealing with an X-ray quantity of 2.01×10^8 R under various reverse biases. The slope of a line yields E_T.

The activation energy at difference reverse bias and X-ray annealing conditions are summarized in Fig. 13.

The E_T for all samples is in the range 0.63-0.68 eV, which is close to the value of $E_g/2$ for crystalline silicon (E_g ~1.12 eV), suggesting that X-ray soft

This material is reserved for educational use only, not allowed for commercial use.
Forbidden to modify the content, and cite the document when use.

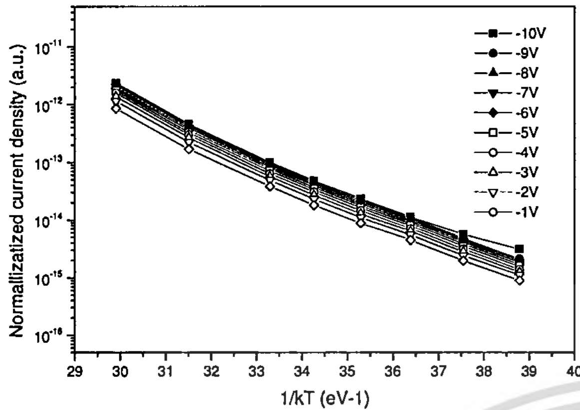

Fig. 12 — Arrhenius plots of $I_g/T^{1.7}$ versus $1/kT$ for *p-n* junction diodes after X-ray annealing (dose 2.01 X 10^8R under various reverse biases

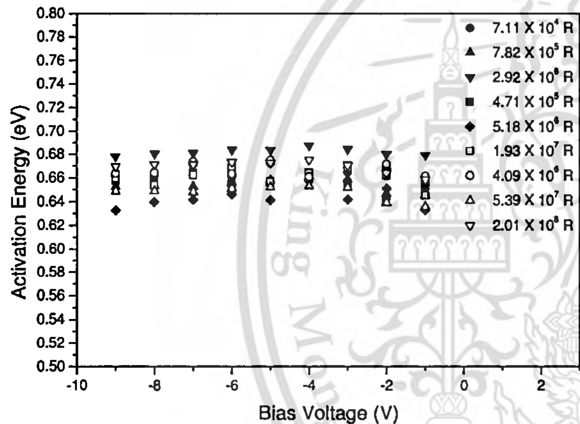

Fig. 13 — Activation energy of *p-n* junction diode after X-ray annealing under various conditions

annealing has insignificant impact to E_T and the recombination process in the silicon is likely the dominant mechanism of current transport.

Our analysis of the effects of reverse-bias conditions suggests that X-ray soft annealing has insignificant impact to *p-n* junction and diode defects. However, X-ray soft annealing effect leads to significant improvements in the forward-diode current as a result of changes in the Schottky barrier height. The above results also suggested that the X-ray soft annealing process only has impact to the Metal-Semiconductor contact layer in the device[20].

4 Conclusions

We analyzed the *I-V* and *C-V* relationships for silicon *p-n* junction diodes before and after X-ray soft annealing. Under a forward bias (1.0 V), forward current is about two orders of magnitude higher for all X-ray annealed samples than for non-X-ray annealed samples, as measured at 303 K. The saturation current and ideality factor can be maintained and series resistance can be improved using this X-ray soft annealing process. Under reverse-bias conditions, analysis of leakage current, carrier-generation lifetime, and activation energy indicate that X-ray soft annealing does not significantly create new defects in a device. Thus, the X-ray soft annealing process can improve the device series resistance under forward-bias conditions. However, optimum process conditions may need to be specifically developed for each particular device.

Acknowledgement

We thank the Thai Microelectronic Center (TMEC) for samples and measurement facilities and the Science faculty of King Mongkut's University of Technology, North Bangkok for X-ray exposure equipment.

References

1 Msimanga M, McPherson M, & Theron C, *Radiat Phys Chem*, 71 (2004) 733.
2 Vobecký J, Hazdra P, & Záhlava V, *Solid-State Electron*, 47 (2003) 45.
3 Hazdra P, Vobecký J, Dorschnerb H, & Brand K, *Microelectron J*, 35 (2004) 249.
4 Hazdra P, Rube J, & Vobecký J, *Nucl Instrum. Methods Phys, Res Sect B*, 159 (1999) 207.
5 Biselloa D, Candeloria A, Kaminskia A, Litovchenkoa A, Noahb E, Stefanutti L, *Radiat Phys & Chem*, 71 (2004) 713.
6 Sze S M, *Phys of semiconductor devices*, Wiley John & Sons, New York, 1981.
7 Neudeck G W, *The pn junction diode*, Neudeck G W. & Pierret Robert F, Addison-Wesley Publishing Company, 1989) 2nd *Modular series on solid state devices.*
8 Schroder D K, *IEEE Trans Electron Devices*, 44 (1997) 160.
9 Marsal L F, Martin I, Pallares J, Orpella A, & Alcubilla R, *J Appl Phys*, 94 4 (2003) 15.
10 Bano N, Hussain I, Nur O, Willander M, & Klason P, *J Nanomater*, 2010 (2010), Article ID 817201, 5 pagesdoi:10.1155/2010/817201.
11 Czerwinski A, Simoen E, A Poyai & Claeys C, *J Appl Phys*, 94 (2003) 1218
12 Hudait M K, Krupanidhi S B, *Physica B*, 307 (2001) 125
13 Rhoderick E H & Williams R H, *Metal–Semiconductor Contacts* (2nd edn, Oxford: Clarendon, 1988).
14 Kumar S, Katharria Y S, Batra Y & Kanjilal D, *J Phys D*, 40 (2007) 6892.
15 Chand S, *Physica B*, 373 (2006) 284.
16 Khanna S, Neeleshwara S, Noor A, *J of Electron Devices*, 9 (2011) 382.
17 Korucua D, T Mammadova S, Özçelika S, *J of Ovonic Research*, 6 (2008) 159 – 164
18 Poyai A, Simoen E, Claeys C, Czerwinski A, *Materials Science and Engineering B*, 73 (2000) 191
19 Poyai A, *Ph.D. Thesis*, Katholieke Universiteit Leuven, Belgium (2002).
20 Chand S, Bala S, *Physica B*, 390 (2007) 179.

This material is reserved for educational use only, not allowed for commercial use.
Forbidden to modify the content, and cite the document when use.

VOLUME 19 • NUMBER 2 FEBRUARY 2013

www.aspbs.com/science

Advanced SCIENCE LETTERS

A Journal Dedicated to All Aspects of Scientific Research

Editor-in-Chief: Hari Singh Nalwa, USA

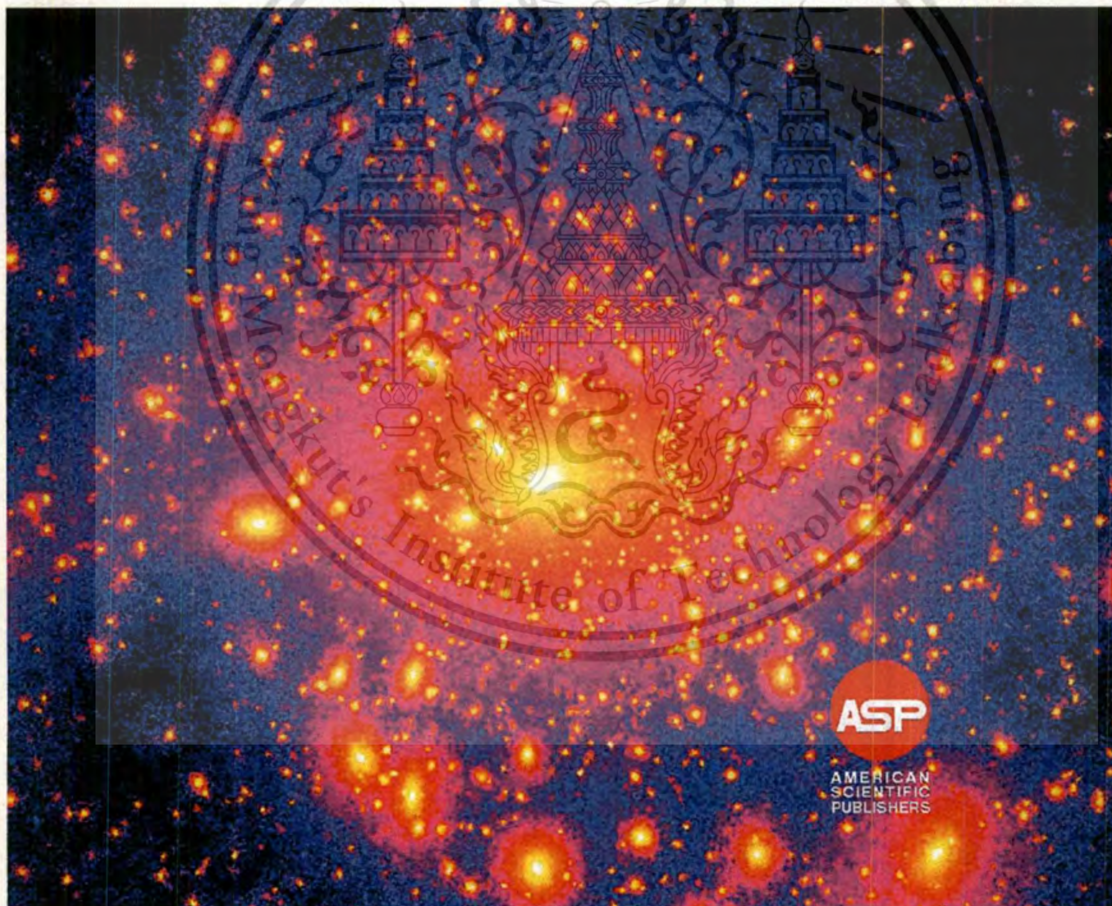

This material is reserved for educational use only, not allowed for commercial use.

Forbidden to modify the content, and cite the document when use.

An Improvement of Forward Current of P-N Diode using Soft X-ray Method

oopol Rujanapich[1], Itsara Srithanachai[1*], Surada Ueamanapong[1], Amporn Poyai[2], Surasak Niemcharoen[1], Wisut Titiroongruang[1]

[1]Department of Electronics, Faculty of Engineering, King Mongkut's Institute of Technology Ladkrabang Bangkok 10520, Thailand

[2]Thai Microelectronics Center (TMEC), 51/4 Moo 1, Wang-Takien District, Amphur Muang, Chachoengsao 24000, Thailand

We present the experimental investigation of platinum doped P-N junction diodes that they were fabricated by using a CMOS technology. The effect of soft X-ray annealing technique on the device is investigated and the device performance improvement observed. The current-voltage (I-V) characteristics of the diodes were measured at room temperature. The forward current before and after irradiation can be explained relatively to the carrier recombination lifetime (τr). After irradiation, at 55 and 70 keV for 55 and 205 seconds, the small change in leakage current is noted. However, the forward current is increased by several orders of magnitude. The carrier recombination lifetime was the main effects of the change in forward current. The recombination lifetimes after irradiation are decreased from 0.55 μs to 0.45 μs and 0.55 μs to 0.48 μs, which show that the device performances are increased after X-ray irradiation. Soft X-ray annealing is a new technique for improve the device performance.

Keywords: Defects, Radiation, Soft X-ray, P-N Diode.

INTRODUCTION

N junction structures are widely used in many areas of plications for such as communication[1], power devices[2], oto-detectors[3], and oxygen sensor[4]. However, the formance of the P-N diodes is relatively low. To ther improve these properties, many researchers have rked to increase the performance of P-N junction des. Generally, a good diode should have a low kage current and a high forward current. Low formance characteristics of the diodes can be caused many parameters[5], where one of them is the high rgy ion implantation process. It is well-known that h energy ion implantation is essential for device rication. On the other hand, the ion implantation can use damages having dramatic effects on the diffusion of oants, especially in the case of CMOS technology[6-8], in ich the ion implantation process can damage the stalline structure in silicon bulk.

However, it has been observed that the residual mage can be repaired by a thermal annealing process[9]. rthermore, the forward current is also of particular erest for improvement, because the requirements to use high responsiveness diodes have been increased.

nail Address: srithanachai@gmail.com

Although, the diodes may be in high demand, it is also inadequate for high frequency work requirements. However, there are many techniques for improving the diode characteristics, where the platinum (Pt) doped silicon is one such technique to increase the responsiveness of diode[10-12]. This technique can be used to change the recombination lifetime, and as a result, the forward currents are also increased. In principle, platinum introduces deep energy levels into the forbidden gap of silicon, and is widely used to reduce the carrier lifetime in fast-switching diodes. The platinum atoms are hybrid solute in silicon which can occupy both interstitial and substitutional sites. Diffusion proceeds via a small fraction of platinum solutes being in the interstitial configuration whereas the majority of the platinum atoms are stationary in substitutional sites[13-14]. Although, Pt doped silicon can increase forward current, it will not produce a substantial increase. Moreover, the Pt diffusion technique may affect the lattice defects in silicon bulk. For a long time, thermal annealing is the technique for treatment of crystalline defect in semiconductor devices. However, it had been observed frequently that, in the case of the high energy ion implantation, the residual damages were difficult to remove by thermal annealing[15-18]. Therefore, a soft X-ray annealing is the new technique and recommended for removing the defects and improving the performance of device base on silicon. Soft X-ray annealing has the optimum energy for removing

This material is reserved for educational use only. It is allowed for personal use.
Forbidden to modify the content, and cite the document when use.

ects or clusters in semiconductor devices. Therefore, defects occurred by platinum diffusion can be noved by using the soft X-ray annealing technique. The of this work is that the forward current characteristics Pt doped silicon devices by soft X-ray annealing nnique is experimentally investigate. Finally, the nple formulas for device interpretation are included, the discussion is made.

EXPERIMENT

Experimentally, the shallow P-N junction diode flow cess with CMOS technology was facilitated by Thai croelectronics Center (TMEC). The P-N junction des were fabricated by using the 325 3M thick 60-90 cm (100) n-type silicon substrate. The diode process dule consisted of (i) deposition of silicon dioxide on substrate, (ii) dry-etching of active area, (iii) plantation of boron at energy of 120 keV and dose of 0^{16} atoms/cm^{-2} on the front side wafers (the plantation been followed by a thermal annealing at 50 °C for 60 min, resulting in a junction depth of about m), (iv) E-beam evaporation of Pt on the back side (v) rmal annealing for 6 hours, (vi) 1 μm thick Al position on the front and back sides. The final device is wn in Fig. 1.

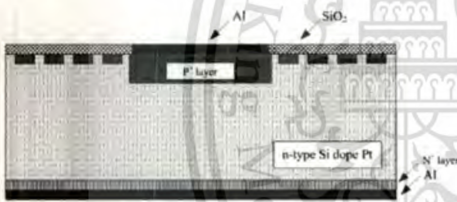

.1. Structure of the Pt dope in P-N diode devices used he study. The bottom picture is zooming on the cross tion in the marked region.

After the wafer dicing, the 4 mm^2 diode electrical perties were measured. The semiconductor parameter lysis model called HP4156B was used to measure the de electrical properties. The results obtained in both fore and after X-ray irradiation were compared at room nperature with various energy exposures of 55 and 70 V and exposure time of 55 and 205 seconds[19,20]. The tic I-V characteristics of the different energies and posure times were measured, which was performed at fer level in dark environment with a voltage range of - to 1 V at the step of 25 mV.

RUSULT AND DISCUSSIONS

Fig. 2 shows the experimental result of the P-N ction diodes for forward and reverse-bias racteristics, where the diode parameters were ermined from the I-V characteristics, which are sically described by the thermionic emission theory, ere the ideal diode equation or sometimes called the ockley diode equation is

$$I = I_0 \exp^{(qV/nkT)} - 1 \quad (1)$$

Here the saturation current (I_0) equals the diffusion current (I_d).

$$I_0 = I_d = q_i^2 A\left(\frac{D_n}{L_n N_A} + \frac{D_p}{L_p N_D}\right) \quad (2)$$

I is the current, q is the electron charge, V is the applied voltage, T is the absolute temperature, k is the Boltzmann constant, n is the ideality factor of P-N diode, A is the active area, n_i is the intrinsic carrier density, and I_0 is the saturation current. For values of V greater than nkT/q, D_n and D_p are the diffusion coefficient of electrons in the p-side and holes in the n-side, L_n and L_p are the electron and hole diffusion length, the ideality factor from Eq. (1) can be written as described in by

$$n = \left(\frac{q}{kT}\right)\left(\frac{dV}{d\ln I}\right) \quad (3)$$

Also the voltage dependent ideality factor $n(V)$ can be written using Eq. (3) as

$$n(V) = \frac{qV}{(kT\ln(I/I_0))} \quad (4)$$

When analyzing the relationship between current-voltage by considering G-R effect can be define as

$$I = \left[\frac{Aqn_iW_A}{2\tau_r \exp^{(qV/2kT)}} + \tau_g\right]\left[\exp^{(qV/kT} - 1\right] \quad (5)$$

In reverse bias, where $2\tau r exp(qV/2kT) << \tau_g$ and $exp(qV/kT) << 1$, the relationship between current and voltage, in area bulk reverse current or area bulk generation current (I_g), is given by

$$I_g = Aqn_iW / \tau_g \quad (6)$$

In forward bias, the forward current or recombination current is given by

$$I_r = \frac{Aqn_iW_A}{2\tau_r \exp^{(qV/2kT)}} \quad (7)$$

Normally, carrier recombination lifetime (τ_r) can be calculated from the area diffusion current density (J_{dA}). Starting from Eq. (2), assuming that the current in the lowly doped region dominates J_{dA}, $N_D >> N_A$ and $L_n = (D_n\tau_r)^{1/2}$, then τ_r can be calculated from

This material is reserved for educational use only, not allowed for commercial use.
Forbidden to modify the content, and cite the document when use.

$$\tau_r = \left(\frac{qn_i^2}{J_{dA} N_A} \sqrt{D_n} \right)^2 \qquad (8)$$

can be obtained through the Einstein relationship

$$D_n = \mu_n \frac{kT}{q} \qquad (9)$$

$$\mu_n \left(N_A, T \right) = \mu_n + \frac{\mu_{on}}{1 + \left(\frac{N_A}{N_{cn}} \right)^{\upsilon}} \qquad (10)$$

$$\mu_{mn} = 88 \left(\frac{T}{300} \right)^{-0.57} \qquad (11)$$

$$\mu_{on} = 1.25x10^3 \left(\frac{T}{300} \right)^{-2.33} \qquad (12)$$

$$\upsilon = 0.88 \left(\frac{T}{300} \right)^{-0.146} \qquad (13)$$

$$N_{cn} = 1.26x10^{17} \left(\frac{T}{300} \right)^{2.4} \qquad (14)$$

Where τ_g is the carrier generation lifetime, W_A is the a depletion width, J_{dA} is the area diffusion current sity, D_n is the diffusion coefficient of electron in the p-e, μ_n is the electron mobility, N_{cn} is the number of ner.

In order to investigate the effect of Pt doping hnique on the electrical characteristics of P-N junction de, the I-V characterization have been measured. Fig. shows the current-voltage (I-V) characteristics of doped and Pt doped P-N junction diodes. From this ure, shows the reverse biased current after increasing dopant, while the increasing forward current has shown most significant change as shown in Fig. 3.

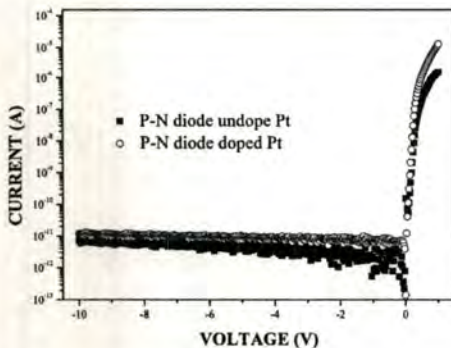

.2. The forward and reverse bias current vs voltage racteristics of the P-N diode undope and Pt dope.

In principle, the changes in forward current were caused by the change in carrier recombination lifetime.

Although, the diode forward current is increased substantially after doping Pt, which may be less significance (only about 2 times the undoped case).

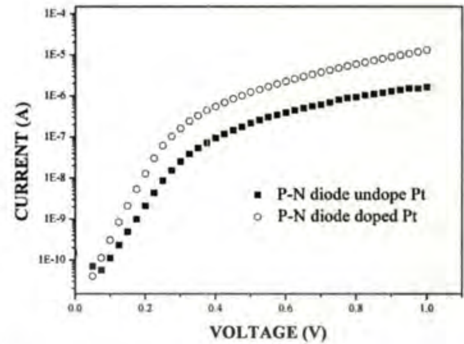

Fig.3. Semi-log forward I-V characteristics of the P-N diode undope and Pt-doped.

Therefore, this paper claimed a new technique to improve the electrical properties of diodes, in which the soft X-ray annealing is a new technique for increasing the performance of diodes.

Moreover, it can be used to remove the defects or trap levels inside the bulk of silicon, which there is no more investigation using X-ray advantage to improve the diode performance.

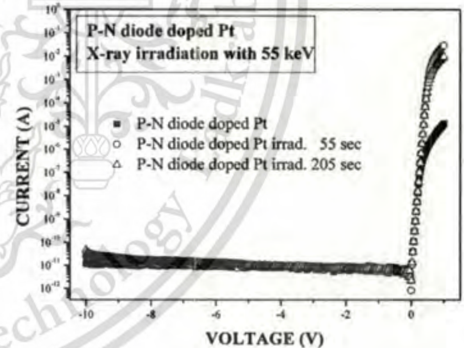

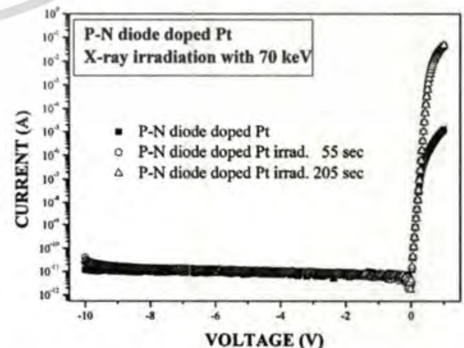

Fig.4. Semi-log I-V characteristics of the Pt dope P-N diode before and after irradiation various energy and times.

Fig. 4 shows the typical results of I-V characteristics

This material is reserved for educational use only, not allowed for commercial use.
Forbidden to modify the content, and cite the document when use.

r X-ray irradiation at different energy and exposure es. From these figures, it was found that, after the diation process, the leakage current did not change. . 5 shows the forward current characteristics after X- irradiation at different energy and exposure times, ich was found that after irradiation the forward current reased significantly, the gain was about 3 to 4 order of gnitude compared with Pt doped only case.

Finally, the carrier recombination lifetime was also estigated. Because it was the main factor that could lain the forward current characteristics, which can be culated by using Eq. (8). The values of recombination time before and after X-ray irradiations, when the X- irradiation energies were at 55 and 70 keV, the ombination lifetimes are 0.55 and 0.52, 0.45 μs and 8 μs, respectively.

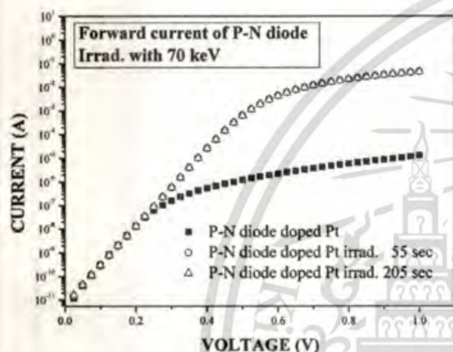

.5. Semi-log forward current characteristics of Pt dope N diode irradiation by X-ray various energy and times.

The recombination lifetime was decreased after diation due to the increasing in causing the forward rent.

CONCLUSIONS

The current-voltage characteristics of diodes have en investigated and discussed. Pt-doped can improve P-N junction diode's performance. The forward rents are increased by about 2 times. The diodes were diated with X-ray at various energy and durations. rward current after irradiation were increased by 3 to 4 ers of magnitude. The increase of forward current was sed by the reduction of carrier recombination lifetime. m the results, Pt-doped and soft X-ray annealing hniques can be used to improve the responsiveness of des. These researches can develop the advantage of t X-ray annealing for industrial and better research in future, which can be considered to have very little ory that explains the advantages of soft X-ray method.

Acknowledgments: The authors would like to thank King Mongkut's University of Technology North Bangkok for providing the X-ray exposure equipment for this experiment, Thai Microelectronics Center (TMEC) for fabrication P-N junction diode, National Electronics and Computer Technology Center, Thailand and Thailand Graduate Institute of Science and Technology (TGIST). Finally, we would like to give our appreciation for the manuscript writing improvement to Mr. Putapon pengpad, Thai Microelectronics Center (TMEC), Chachoengsao 24000, Thailand.

References and Notes

1. Y. Matsumoto, A. Nakazono, T. Kitahara, and Y. Koike, Sensors and Actuators A. 97-98, 318-322 (2002).
2. M. D. Miller, IEEE Trans. Electron Dev. 23, 1279-1283 (1976).
3. D. V. Kuksenkov, H. Temkin, A. Osinsky, R. Gaska, and M. A. Khan, J. Appl. Phys. 97, 759-762 (1997).
4. K. Wallgren, S. Sotiropoulos, Sensors and Actuators B. 60, 174–183 (1999).
5. A. Poyai, Editor, Defect assessment in advanced semiconductor materials and devices, IMEC, Belgium (2002).
6. J. S. Williams, Ion implantation of semiconductor. Mater. Sci. Eng. A. 253, 8–15 (1998).
7. T. E. Felter, L. Hrubesh, A. Kubota, L. Davila, and M. Caturla, Nucl. Instr. Meth. Phys. Res. B. 207, 72–79 (2003).
8. S. Moffatt, P. L. F. Hemment, S. Whelan, D. G. Armour, Mat. Sci. Semicon. Proc. 3, 291-296 (2000).
9. N. Maeda, K. Nozawa, Y. Hirayama, and N. Kobayashi, J. Crystal Growth. 189/190, 359-363 (1998).
10. B. J. Baliga, E. Sun, IEEE Trans. Electron Dev. 24, 685-688 (1977).
11. M. Valdinoci, L. Colalongo, A. Pellegrini, and M. Rudan, IEEE Trans. Electron. Dev. 43, 2269-2275 (1996).
12. M. D. Miller, H. Schade, and C. J. Nuese, J. Appl. Phys. 47, 2569-2578 (1976).
13. Y. K. Kwon, T. Ishikaw, and H. Kuwano, J. Appl. Phys. 61, 1055-1058 (1987).
14. S. D. Brotherton, P. Bradley, and J. Bicknell, J. Appl. Phys. 50, 3396 (1979).
15. K. K. Bourdelle, Y. Chen, R. A. Ashton, L. M. Rubin, A. Agarwal, and W. A. Morris, IEEE Trans. Electron Devices. 48, 2043 (2001).
16. H. Sayama, M. Takai, Y. Yuba, S. Namba, K. Tsukamoto, and Y. Akasaka, Appl. Phys. Lett. 61, 1682-1684 (1992).
17. J. Y. Cheng, D. J. Eaglesham, D. C. Jacobson, P. A. Stolk, J. L. Benton, and J. M. Poate, J. Appl. Phys. 80, 2105-2112 (1996).
18. W. C. Hsu, M. C. Chen, and M. S. Liang, J. Electrochem. Soc. 147, 3111-3116 (2000).
19. I. Srithanachai, S. Ueamanapong, A. Poyai, S. Niemcharoen, and P. P. Yupapin, Opt. Laser Technol. 44, 635-639 (2012).
20. J. Prabket, I. Srithanachai, S. Ueamanapong, A. Poyai, W. Titiroongruang, S. Niemcharoen, and P. P. Yupapin, Sci. Res. Essays. 7, 1230-1236 (2012).

This material is reserved for educational use only, not allowed for commercial use.
Forbidden to modify the content, and cite the document when use.

This material is reserved for educational use only, not allowed for commercial use.
Forbidden to modify the content, and cite the document when use.

ACTIVATION ENERGY ANALYSIS OF P-N JUNCTION X-RAY DIRECT DETECTOR

Poopol Rujanapich[1], Amporn Poyai[2], Itsara Srithanachai[1], Putapon Pengpad[2], Charndet Hruanan[2], Suwat Sophitpan[2], Surada Ueamanapong[2], Worraruthai Titiroongruang[3], Wisut Titiroongruang[1]

[1]Department of Electrical Engineering, Faculty of Engineering, King Mongkut's Institute of Technology Ladkrabang, Chalongkrung Road, Ladkrabang, Bangkok 10520, Thailand.
[2]Thai Microelectronics Center (TMEC), 51/4 Moo 1, Wang-Takien District, Amphur Muang, Chachoengsao 24000, Thailand.
[3] Faculty of Dentistry, Chulalongkorn University, Pathumwan, Bangkok 10330, Thailand

ABSTRACT

Operation lifetime of the X-ray detector is the major factor that defines cost of detector or the actual operation cost of the detector. The purpose of this paper is to study the possibility of operation lifetime extension of the silicon direct x-ray detector by enabling the activation energy, E_T, which is calculated from Current-Voltage and Capacity-Voltage characteristics. In this paper, the study of the device's activation energy before and after device exposed to the X-ray for 4, 54 and 204 second at 40, 55 as well as 70 keV were conducted. The 1 mm^2 p-n junctions were fabricated by boron implantation process into phosphorus doped silicon wafer. The results show that the leakage current activation energy changes after exposed to the X-ray which indicated that the types of defect have been changed. The changes of these activation energies can be higher or lower than the result before X-ray exposure, which depends on type of defects. Further studies of the changes of leakage current activation energy after X-ray irradiation are required for deeper root causes analysis. However, the results in this paper presented that the defects that caused by X-ray irradiation are manageable.

Index Terms— X-ray detector, p-n junction, leakage current, activation energy

1. INTRODUCTION

The X-ray detector is widely use for medical analysis. However, its utilization has limit not only by safety concerns but also by its cost. The X-ray detector itself is expensive, which results high cost of operation. The cost of operation can be reduced by extending the detector operation lifetime, which will increases its cost benefit for longer operation and increase opportunities for people to access to this machine.

In this paper, we concentrate on study the possibility to extend X-ray detector operation lifetime by analyst the leakage current activation energy of p-n junction before and after exposed to the X-ray at different conditions of energies and times. This parameter is used as a monitoring method for the device performance as well as device degradation since it can be referred to types, affect and value of defects or lattice disorders in the p-n junction effective area.

2. EXPERIMENTAL

The <111> orientation 120-134 ohm.cm resistance silicon substrates with 1μm thickness of silicon dioxide were used to fabricated p-n junctions. The wafers were sent into photolithography and etch processes to open 1 mm^2 of silicon dioxide window. After that wafers were sent into boron implantation process with dose of $1X10^{16}$ ion/cm^2 at energy of 120 keV condition and continue with 1050 °C thermal process for 600 minutes. Then the wafers were sent into metallization process to create 1μm thickness of aluminum layer at both sides. The 2nd photolithography and etch processes were conducted to create aluminum patterns then anneal at 400°C for 30 minutes. Wafers were sent into sawing process after that chips were assemble on PCB before finished with the connectorization process. At this point the chip is ready to connect to test circuit outside.

A laboratory x-ray source was used to generate X-ray in these experiments. The Current-Voltage (I-V) characteristic and Capacity-Voltage (C-V) characteristic were measured by HP4156B. The same samples were test before and after exposed to the X-ray with the exposure energy condition of 40, 55 and 70 keV and exposure time of 4,54 and 204 seconds.

This material is reserved for educational use only, not allowed for commercial use.
Forbidden to modify the content, and cite the document when use.

3. RESULTS AND DISCUSSION

The general relation of Current-Voltage of p-n junction diode is presented in equation (1). [1-3]

$$I = I_0 [\exp(qV/kT)-1] \quad (1)$$

Where I_0 is the saturation current, V is the bias voltage, k is the Boltzmann's constant, q is the electronic charge constant and T is the absolute temperature.

In case of reverse bias, the saturation current is presenting in equation (2), which is the combination of the diffusion current (I_d) and the generation current (I_g) that generate in the depletion region.

$$I_0 = I_d + Aqn_iW/\tau_g \quad (2)$$

Where A is the area of p-n junction, n_i is the intrinsic carrier concentration, W is the width of depletion region and τ_g is carrier generation lifetime.

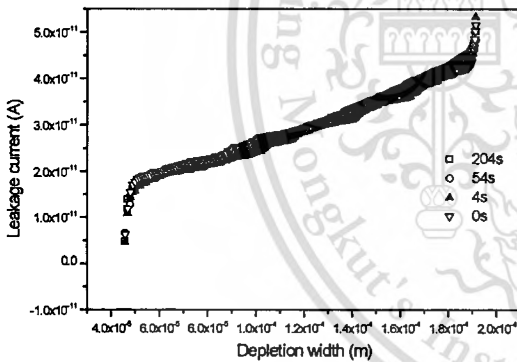

Figure 1. The leakage current versus depletion width of p-n junction before and after 70 keV of X-ray irradiation at various exposure time conditions.

According to the experimental results, the leakage current versus depletion width for p-n junction before and after X-ray irradiation with energy of 70 keV for difference exposure times are shown in Figure 1. The depletion width was calculated from the C-V Characteristics [4]. The leakage current increased at larger depletion width (higher reverse bias). Assuming, the diffusion current is biasing independent, the diffusion current can be found from the extrapolation to zero depletion width. Then the generation current can be calculated from Eq. (2). The results are shown in Fig.2 The generation current change after X-ray irradiation. However, the change of depletion width has insignificantly impact to the leakage current at reverse bias condition as reported in [4]. Therefore, generation current, is mainly depends on the carrier generation lifetime, which may relate to defects in its device.

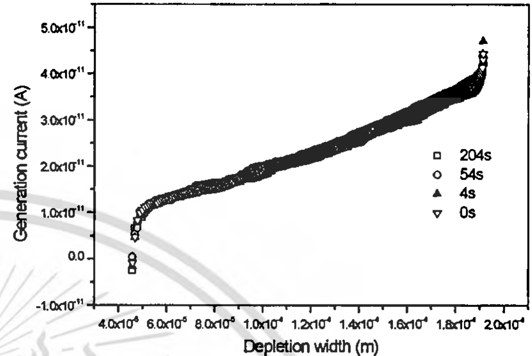

Figure 2. The generation current versus depletion width of p-n junction before and after 70 keV of X-ray irradiation at various exposure time conditions.

The analysis of leakage current activation energy in p-n junction diode can be used to study types of defects in p-n junction. Accurate activation energy value can be found from the generation current [5]. The generation current as function of temperature can be described by

$$I_g = [(QWAT^{1.7+\xi})/\tau_r] \exp(-E_T/kT) \quad (3)$$

Where W is depletion width, A is the junction area, Q is a constant value and ξ is a small number (<1) related to the temperature dependence of the depletion width, recombination lifetime τ_r and activation energy E_T, k is the Boltzmann constant and T is the absolute temperature. [5]

Figure 3 show an Arrhenius plot, $I_g/T^{1.7}$ vs 1/kT of generation current after X-ray irradiation with 70 keV for 204 seconds at difference reverse bias. The slope of the plot yields the activation energy E_T. The activation energy at difference reverse bias for difference X-ray exposure energy and time are summarized in Fig. 4.

This material is reserved for educational use only, not allowed for commercial use.
Forbidden to modify the content, and cite the document when use.

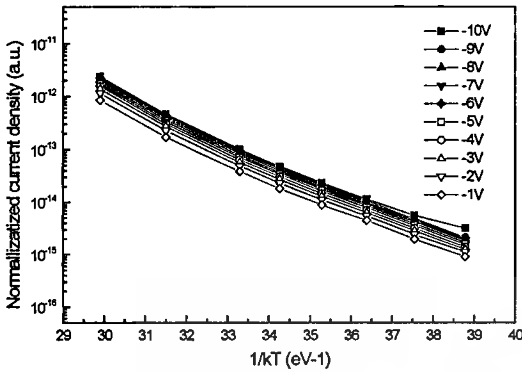

Figure 3. Arrhenius plot, $I_g/T^{1.7}$ vs 1/kT of generation current after X-ray irradiation with 70 keV for 204 seconds at difference reverse bias.

From figure 4, the maximum activation energy of all three samples before exposed to the X-ray is in the range of 0.63 to 0.68 eV. The activation energy reduces after 54 seconds of X-ray exposure in all studied exposure energy conditions but the results of activation energies after exposed to the X-ray for 4 and 204 seconds are not obviously different compare with the result before expose to the X-ray. The results of activation energy after 204 seconds of X-ray irradiation are highest in 40 and 70 keV condition but it is not the case of 55 keV condition. This indicates that the defects were changed after the X-ray irradiation. In order to manage these defects for X-ray direct detector, more studies are needed.

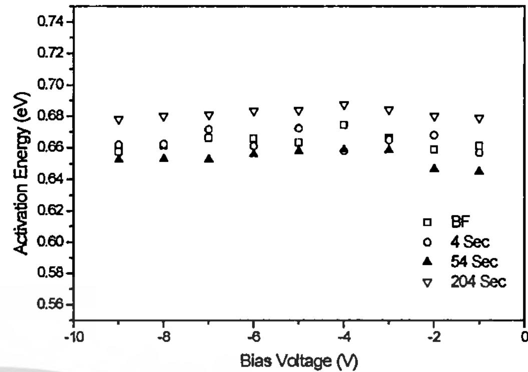

(a)

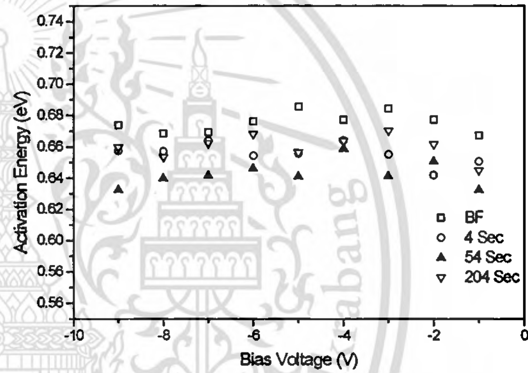

(b)

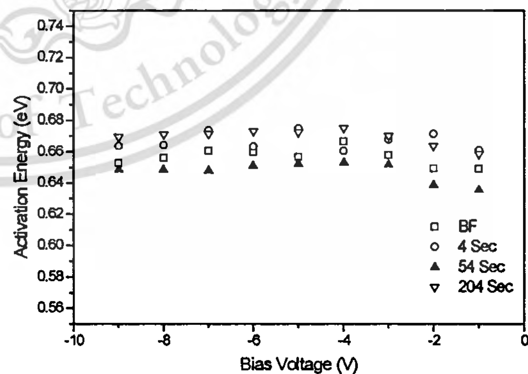

(c)

Figure 4. Activation energy of p-n junction diode before and after 4, 54 and 204 seconds of X-ray irradiation at 40 keV, 55 keV and 70 keV

This material is reserved for educational use only, not allowed for commercial use.
Forbidden to modify the content, and cite the document when use.

4. CONCLUSION

This paper is clearly presented that in certain condition the X-ray is obviously affecting the activation energy of device after exposed to the X-ray. In other hand, the X-ray crated additional defects in device after exposed. The detail study of these defects is requiring for determine the types and amount of these defects, which will lead to the development of device defects controlling process in future. The final objective of this research is to develop the process of defect level control in device that can be used for extend operation lifetime of the direct type of X-ray detector.

5. ACKNOWLEDGEMENT

The Authors are grateful to the members of TMEC team for providing the wafers and Faculty of Science, King Mongkut's University of Technology North Bangkok for providing the X-ray exposure equipments for this experiment.

6. REFERENCES

[1] S.M. Sze, "Physics of semiconductor devices", John Wiley & Sons, New York, 1981.
[2] Gerold W. Neudeck, "The pn junction diode", 2nd Modular series on solid state devices, Eds Gerold W. Neudeck and Robert F. Pierret, Addison-Wesley Publishing Company, 1989.
[3] D.K. Schroder, "Carrier lifetimes in silicon", IEEE Trans. Electron Devices, Vol. 44 (1), pp. 160-170, 1997.
[4] Poopol Rujanapich, Amporn Poyai, Itsara Srithanachai, Putapon Pengpad, Charndet Hruanan, Suwat Sophitpan, Wisut Titiroongruang, "Generation lifetime analysis of p-n junction X-ray detector", ECTI-CON 2010, 2010.
[5] Amporn Poyai, "Defect Assessment in Advanced Semiconductor Materials and Devices", Ph.D. Thesis, Katholieke Universiteit Leuven, 2002. page 52.

Amporn Poyai was born in Pathum-thani, Thailand. He received the B.S. ('91) degree in physics from Silpakorn University, M.Eng. ('94) in electrical engineering from King Mongkut's Institute of Technology Ladkrabang (KMITL), both in Thailand. He obtained M.E. ('98) and Ph.D. ('02) in electrical engineering from Katholieke Universiteit Leuven (KU Leuven), Belgium. His doctoral research was in the field of device physics, low temperature electronics, radiation physics, submicron silicon technologies and defect engineering. In these fields, he has authored or co-authored over 60 publications in Journal and Conference papers, and over 15 presentations at international conferences. In 1994, he joined NECTEC (Thailand), where he has been involved in the nation microelectronics project. From 1997 to 2002, he had got scholarship from Thai government supported through the National Science and Technology Development Agency (NSTDA) of Thailand to join IMEC (Belgium) for his master and doctoral research. Since 2002, he is a researcher of Thai Microelectronic Center (TMEC).

Poopol Rujanapich was born in Nakornratchasima, Thailand. He received the B.S. ('90) degree in physics from Silpakorn University, and M.Eng. ('94) in electrical engineering from King Mongkut's Institute of Technology Ladkrabang(KMITL), both in Thailand. His master degree research was in the field of power device process development. He has 10 years of experiences in wafer fabrication process in Thailand as well as in Singapore. His other 5 years of experiences are in the electronics manufacturing in Thailand. He is now a doctoral student in electrical engineering, Faculty of Engineering, King Mongkut's Institute of Technology Ladkrabang (KMITL).

Institute of Technology

This material is reserved for educational use only, not allowed for commercial use.
Forbidden to modify the content, and cite the document when use.

ECTI-CON 2010

Chaiang Mai, Thailand

19-21 May 2010

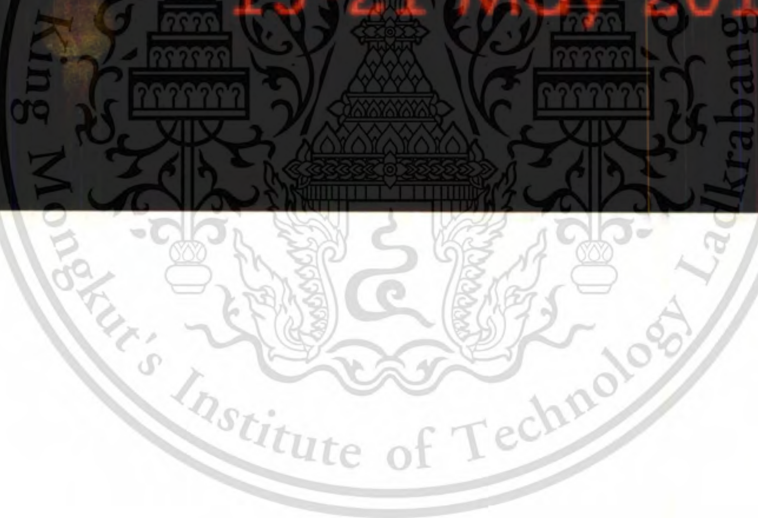

King Mongkut's Institute of Technology Ladkrabang

This material is reserved for educational use only, not allowed for commercial use.

Forbidden to modify the content, and cite the document when use.

GENERATION LIFETIME ANALYSIS OF p-n JUNCTION X-RAY DETECTOR

Poopol Rujanapich[1], Amporn Poyai[2], Itsara Srithanachai[1], Putapon Pengpad[2], Charndet Hruanan[2], Suwat Sophitpan[2], Wisut Titiroongruang[1]

[1]Department of Electrical Engineering, Faculty of Engineering, King Mongkut's Institute of Technology Ladkrabang, Chalongkrung Road, Ladkrabang, Bangkok 10520, Thailand.
[2]Thai Microelectronics Center (TMEC), 51/4 Moo 1, Wang-Takien District, Amphur Muang, Chachoengsao 24000, Thailand.

Abstract— **Operation lifetime of the X-ray detector is the major factor that defines cost of detector or the actual operation cost of the detector. The purpose of this paper is to study the possibility of operation lifetime extension of the silicon x-ray detector. The study of the device's carrier generation lifetime before and after device exposed to the X-ray for 4 and 150 second at 40, 55 as well as 70 keV were conducted in this paper. The 1 mm² p-n junctions were fabricated by boron implantation process into phosphorus doped silicon wafer. A commercial x-ray source for dentist was used to generate x-ray in these experiments. The carrier generation lifetime was calculated from current-voltage (I-V) and capacitance-voltage (C-V) characteristics. The results show that the carrier generation lifetime increased after 4 second of x-ray irradiation at all three energy conditions but decreased back close to the original value after continue exposed devices for another 150 second. However, the lowest point of the generation lifetime after 4 second of x-ray irradiation is depending on the level of energy used. The results also presented that the defects that caused by x-ray irradiation are manageable.**

Index Terms— **X-ray detector, p-n junction, leakage current, generation lifetime**

I. INTRODUCTION

The X-ray detector is widely use for medical analysis. However, its utilization has limit not only by safety concerns but also by its cost. The X-ray detector itself is expensive, which results high cost of operation. The cost of operation can be reduced by extending the detector operation lifetime, which will increases its cost benefit for longer operation and increase opportunities for people to access to this machine. In this paper, we concentrate on study the possibility to extend X-ray detector operation lifetime by analyst the carrier generation lifetime of p-n junction before and after exposed to the X-ray at different conditions of energy and time. This parameter is used as a monitoring method for the device degradation since it can be refer to amount of defects or lattice disorders in the p-n junction effective area which lead to a breakdown condition of the device.

II. EXPERIMENTAL

The <111> orientation 120-134 ohm.cm resistance silicon substrates with 1μm thickness of silicondioxide were used to fabricated p-n junctions. The wafers were sent into photolithography and etch processes to open 1 mm² of silicondioxide window. After that wafers were sent into boron implantation process with dose of $1X10^{16}$ ion/cm² at energy of 120 keV condition and continue with 1050 °C thermal process for 600 minutes. Then the wafers were sent into metallization process to create 1μm thickness of aluminum layer at both sides. The 2nd photolithography and etch processes were conducted to create aluminum patterns then anneal at 400°C for 30 minutes. Wafers were sent into sawing process after that chips were assemble on PCB before finished with the connectorization process. At this point the chip is ready to connect to test circuit outside.

The Current-Voltage (I-V) and Capacity-Voltage (C-V) characteristic were measured by HP4156B. The same samples were test before and after exposed to the X-ray with the exposure energy condition of 40, 55 and 70 keV and exposure time of 4 and 150 seconds.

III. RESULTS AND DISCUSSION

Current-Voltage of p-n junction diode use for X-ray detector is presented in Figure 1., which can be explained by equation (1). [1-3]

$$I = I_0\left[\exp\left(\frac{qV}{kT}\right)-1\right] \qquad (1)$$

Where I_0 is the saturation current, V is the bias voltage, k is the Boltzmann's constant, q is the electronic charge constant and T is the absolute temperature.

This material is reserved for educational use only, not allowed for commercial use.

Forbidden to modify the content, and cite the document when use.

In case of reverse bias, the saturation current is presenting in equation (2), which is the combination of the diffusion current (I_d) and the generation current, which generate in the depletion region.

$$I_0 = I_d + Aqn_iW/\tau_g \qquad (2)$$

Where A is the area of p-n junction, n_i is the intrinsic carrier concentration, W is the width of depletion region and τ_g is carrier generation lifetime.

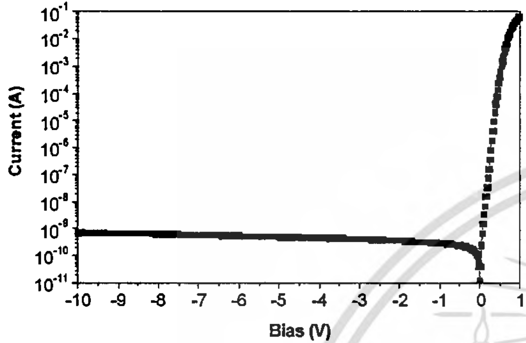

Figure 1. Leakage current versus reverse bias of the p-n junction diode

According to our experiment results, the leakage current versus reverse bias (Figure 1) shows increment of the leakage current at higher reverse bias (larger depletion width higher reversed bias voltage), which can be surely explained by equation (2). Assuming, the diffusion current is biasing independent, the increment of leakage current at higher reverse bias is mostly the result of generation current. This current depends on the width of depletion region, which can be calculated using equation (3).

$$W = A\varepsilon_{Si}/C \qquad (3)$$

Where ε_{Si} is the dielectric permittivity of silicon, C is the capacitance, which can be obtained from the capacitance-voltage (C-V) characteristics as shown in Figure 2.

The diffusion current can be calculated from the relation of leakage current and depletion width as in Figure 3. In this case, the diffusion current is 0.08 nA at zero depletion width. The carrier generation time can be calculated from the slop in Figure 3., which is the average of 8 μs in this graph. The carrier generation lifetime can also be calculated using equation (4) which is exactly in the form of the equation (2) reversed slope.

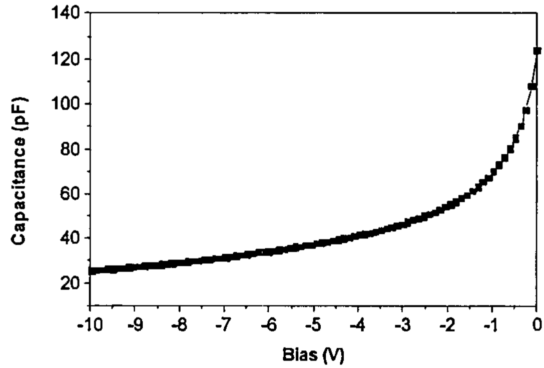

Figure 2. Capacitance-voltage (C-V) characteristics of p-n junction diode.

$$\tau_g = Aqn_iW/(I_0 - I_d) \qquad (4)$$

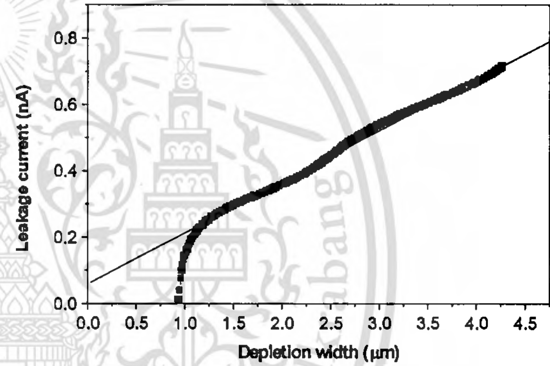

Figure 3. The leakage current versus the depletion width of p-n junction diode.

Table I. The diffusion current for difference conditions X-ray irradiation

Exposed time (s)	Id @40keV (nA)	Id @55keV (nA)	Id @70keV (nA)
non	0.08	0.08	0.04
4	0.09	0.1	0.06
4+150	0.07	0.06	0.03

This material is reserved for educational use only, not allowed for commercial use.
Forbidden to modify the content, and cite the document when use.

Figure 4. show the relation of leakage current and depletion width before and after X-ray irradiation with different expose energy and time. The diffusion current which is obtained from Figure 4., are summarized in Table I. The diffusion current increase after X-ray irradiation with 4 seconds and reduce back close to the original with 4+150 seconds in all the study energy. This may relate to the X-ray induced defects for either temporary or permanently one which possibly depend on energy levels of the X-ray irradiation. Different types of defects could be induced simultaneously in combination and may either suppress or enhance the generation current which lead to unorthodox behavior of the experimental results. However further accurate studies have to be applied to clearly explain this results.

Also from Figure 4., the leakage current versus depletion width before and after 4 and 150 seconds of X-ray irradiation at 40 keV and 55 keV is not significantly difference. It clearly shows the impact of X-ray irradiation at higher reverse bias in case of expose energy of 70 keV. The leakage current reduced after 4 seconds of X-ray irradiation with the energy of 70 keV and the leakage current increased close to the original value after continue exposed to the X-ray for another 150 seconds. These effects may relate to the defects. These defects can be studied from the generation lifetime.

The curve of generation lifetime, which are calculated from equation (4) versus the depletion width for difference X-ray irradiation energy and time are shown in Figure 5. From Figure5., the carrier generation lifetime was increased after device is exposed to the X-ray for 4 seconds in all energy conditions. However, it reduced back to the original value after continue expose to the X-ray for another 150 seconds. The maximum increasing of 1 μs of generation lifetime for the X-ray exposed energy of 40 and 55 keV with 4 seconds has been found. In case of X-ray exposed energy of 70keV with 4 seconds the value of 7μs has been obtained. Also in Figure 5., higher X-ray exposure energy will results higher carrier generation lifetime. The peak of each graphs are also present at different depletion width. The higher X-ray exposure energy has lowest generation lifetime at the wider depletion width.

This indicates that the longer operation lifetime will be achieved for lower dose operation. This can also be mentioned that the defects possibly be annealed by the X-ray. And for prolonging X-ray detector lifetime, longer exposure after typical sensing operation may be concerned. However, in this case, cost per operation hour of X-ray tube and X-ray detector is a trade off and have to be optimized.

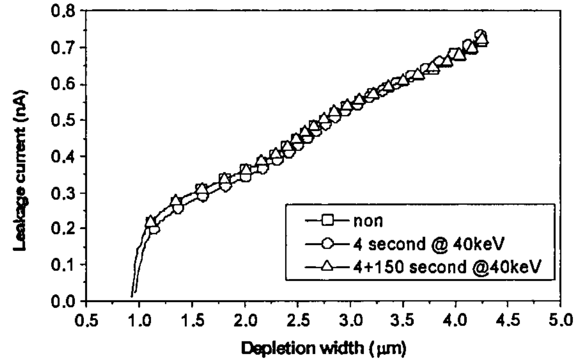

a)

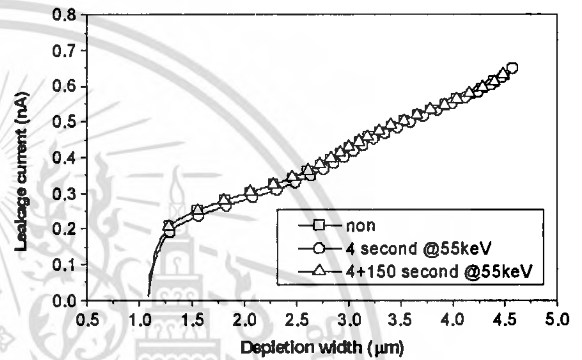

b)

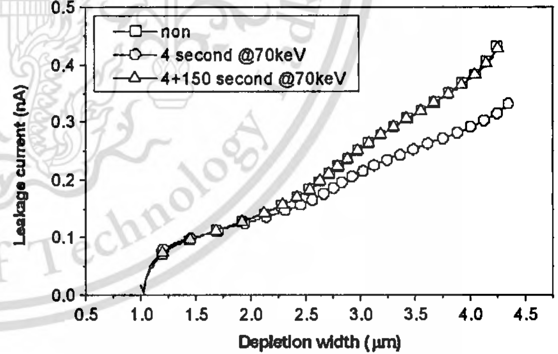

c)

Figure 4. Leakage current versus depletion width before and after 4 and 150 seconds of X-ray irradiation at a) 40 keV, b) 55 keV and c) 70 keV.

This material is reserved for educational use only, not allowed for commercial use.
Forbidden to modify the content, and cite the document when use.

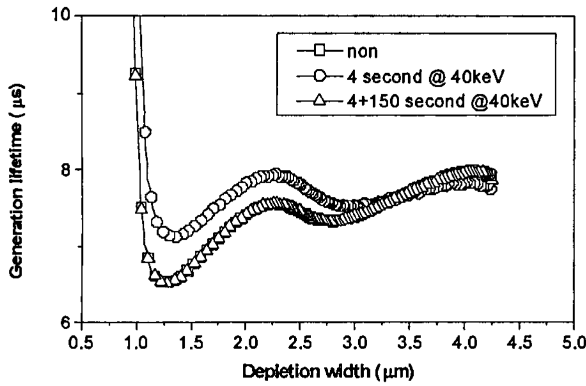

a)

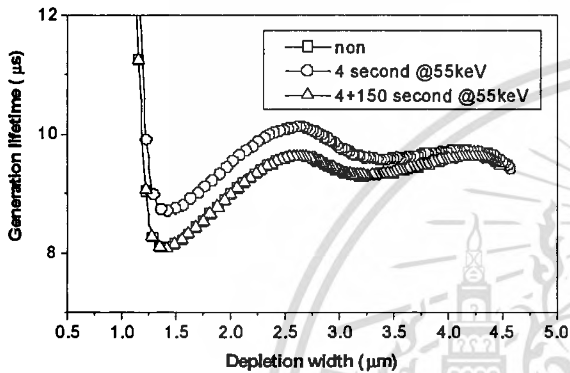

b)

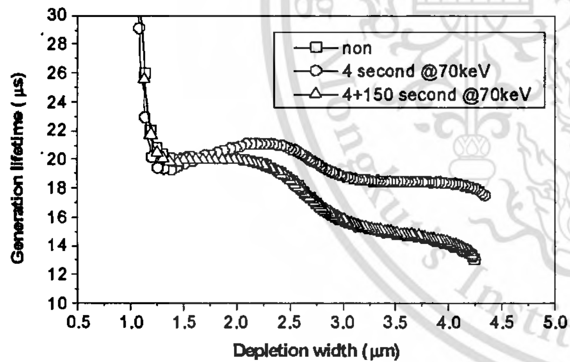

c)

Figure 5. Carrier generation lifetime versus depletion width before and after 4 and 150 seconds of X-ray irradiation at a) 40 keV, b) 55 keV and c) 70 keV.

IV. CONCLUSION

The reduction of leakage current at 4 seconds of X-ray irradiation is the result of the change of the carrier generation lifetime. The value of leakage current is close to the original value after exposed device to the X-ray for another 150 seconds because of the change of defect level in the p-n junction. Therefore, the defect level control in device can be used for extend operation lifetime of the X-ray detector.

ACKNOWLEDGEMENT

The Authors are grateful to the members of TMEC team for providing the wafers.

REFERENCES

1] S.M. Sze, "*Physics of semiconductor devices*", John Wiley & Sons, New York, 1981.

[2] Gerold W. Neudeck, "*The pn junction diode*", 2nd Modular series on solid state devices, Eds Gerold W. Neudeck and Robert F. Pierret, Addison-Wesley Publishing Company, 1989.

[3] D.K. Schroder, "Carrier lifetimes in silicon", IEEE Trans. Electron Devices, Vol. 44 (1), pp. 160-170, 1997.

Amporn Poyai was born in Pathum-thani, Thailand. He received the B.S. ('91) degree in physics from Silpakorn University, M.Eng. ('94) in electrical engineering from King Mongkut's Institute of Technology Ladkrabang (KMITL), both in Thailand. He obtained M.E. ('98) and Ph.D. ('02) in electrical engineering from Katholieke Universiteit Leuven (KU Leuven), Belgium. His doctoral research was in the field of device physics, low temperature electronics, radiation physics, submicron silicon technologies and defect engineering. In these fields, he has authored or co-authored over 60 publications in Journal and Conference papers, and over 15 presentations at international conferences. In 1994, he joined NECTEC (Thailand), where he has been involved in the nation microelectronics project. From 1997 to 2002, he had got scholarship from Thai government supported through the National Science and Technology Development Agency (NSTDA) of Thailand to join IMEC (Belgium) for his master and doctoral research. Since 2002, he is a researcher of Thai Microelectronic Center (TMEC).

Poopol Rujanapich was born in Nakornratchasima, Thailand. He received the B.S. ('90) degree in physics from Silpakorn University, and M.Eng. ('94) in electrical engineering from King Mongkut's Institute of Technology Ladkrabang(KMITL), both in Thailand. His master degree research was in the field of power device process development. He has 10 years of experiences in wafer fabrication process in Thailand as well as in Singapore. His other 4 years of experiences are in the electronics manufacturing in Thailand. He is now a doctoral student in electrical engineering, Faculty of Engineering, King Mongkut's Institute of Technology Ladkrabang (KMITL).

This material is reserved for educational use only, not allowed for commercial use.
Forbidden to modify the content, and cite the document when use.